University of Liège

Laboratory of Bioenergetics

From photon to biomass in green microalgae

fluorimetric and oxymetric studies on the regulation of photosynthetic electron transport

2015

Thomas de Marchin

Promoter : Dr. Fabrice Franck

Co-promoter : Dr. Bart Ghysels

Laboratory of bioenergetics
University of Liège
Belgium

From photon to biomass in green microalgae :
fluorimetric and oxymetric studies on the regulation of photosynthetic electron transport

de Marchin Thomas

A thesis submitted in fulfilment of the requirements for the degree of Doctor in Philosophy in Science

2015-2016

Promoter : Dr. Fabrice Franck
Co-promoter : Dr. Bart Ghysels

Thesis Comitee
Prof. J. Dommes (President)
Prof. R. Bassi (Universita degli studi di Verona)
Prof. R. Valcke (Universiteit Hasselt)
Dr. B. Bailleul (Institut de biologie physico-chimique, Paris)
Dr. F. Franck
Dr. B. Ghysels
Dr. P. Cardol

Abstract

Analyzing the photosynthetic performances of microalgae has become an important topic in view of the ecological importance of these microorganisms and of the growing field of their biotechnological applications. In this thesis, we developed methods which allow effective use of fluorescence and oxygen experimental signals for a more complete analysis of the functioning of the photosynthetic apparatus of green microalgae under different conditions. We applied these methods to analyze the adaptations of the photosynthetic apparatus under selected conditions, especially regarding CO_2 supply.

In the first part of this work, we applied a fluorescence-based method for determining the PSII antenna size based on the kinetics of the fast chlorophyll *a* fluorescence transient in presence of DCMU (or DCMU Fluorescence Rise). We then performed a detailed analysis of the different phases of this transient which are associated with different types of PSII formerly described as PSIIα and PSIIβ (PSII heterogeneity). Our results on PSII heterogeneity during a transition from state 2 to state 1 in *Chlamydomonas reinhardtii* showed for the first time *in vivo* that this transition correlates with a conversion of PSIIβ to PSIIα. We also discuss the possible relationships between PSIIα and PSIIβ and the PSII mega-, super- and core- complexes described by biochemical studies.

In photoautotophic atmospheric conditions, microalgae often have to deal with limited CO_2 availability. The unicellular green algae *Chlamydomonas reinhardtii* can adapt to low CO_2 concentration with the inorganic carbon concentration mechanism (CCM). This has been extensively studied in the past. However, other functional adaptations of the photosynthetic apparatus to CO_2 limitation have been much less studied. In the second part of this work, we used combined fluorescence-based electron transport and oxygen measurements to evaluate the responses to low and high CO_2 in *Chlamydomonas reinhardtii* grown in photobioreactors at different light intensities. We developed a method to rationalize the relationship between the apparent quantum yields of oxygen evolution and of electron transport at PSII while taking into account the variations in the proportion of energy absorbed by PSII. We used this relationship as a tool to evidence a significant O_2-dependent alternative electron transport in low CO_2 acclimated cells. We showed that this alternative electron transport can represent up to 60% of the total electron transport in low CO_2 cells even upon removal of the CO_2 limitation by bicarbonate addition. In contrast, no significant alternative electron transport was detected in high CO_2 cells. We suggest that the alternative electron transport to O_2 observed in low CO_2 cells represents an adaptation that could help to meet the higher ATP demand for the concentration of CO_2 by the CCM. In contrast, in high CO_2 conditions,

the absence of the CCM would reduce the need for ATP and thus the need for electron transport to O_2. Using mutants and inhibitors, we studied the involvement of known O_2-dependent electron sinks such as the mitochondrial cytochrome and alternative oxidase pathways and also of chlororespiration in this light-dependent O_2 uptake and we found no evidence for the involvement of any of these processes. The alternative electron transport was even higher in a mitochondrial mutant devoid of complexes I and III and we suggest that this alternative electron transport could compensate for the absence of mitochondrial ATP synthesis in this mutant. By elimination, our results suggest that the alternative electron transport to O_2 evidenced here could be driven by a Mehler-type reaction although we did not find direct evidences for increased Mehler-type activity in low CO_2 cells.

Additionally from fluorescence measurements performed directly in the cultures, we concluded that low CO_2 cells had a lowest PSII photosynthetic efficiency and developed strong qE NPQ. Our results indicate that *Chlamydomonas reinhardtii* is capable to induce an ample thermal dissipation of excitation energy and the extent of this process is influenced essentially by the CO_2 availability. In contrast with results obtained in previous studies, low temperature fluorescence spectra showed that in high light, high CO_2 cells were characterised by a higher proportion of light energy absorbed by PSI compared to low CO_2 cells. This was accompanied by a decrease of PSII antenna size as shown by DCMU-FR measurements. These findings are discussed in relation with the conflicting theories concerning the role of state transitions in the regulation of the cyclic electron transport around PSI. Our results support the idea that CEF is regulated by the redox state of the chloroplast rather than by state transitions.

Over the last decades, microalgae have been increasingly studied because of their potential applications in industry. Despite a growing interest in microalgae mass cultures, the majority of studies on microalgae have been carried out at a laboratory scale and only few studies have addressed the question of photosynthetic adaptations in mass cultures. It is well known that CO_2 addition increases the growth rate of microalgae and for this reason, some mass microalgae cultures are CO_2 supplemented. Among the studies on microalgae mass culture, as far as we know, none directly compared high CO_2 (CO_2 supplemented air) and low CO_2 (air) conditions. In the last part of our work, two outdoor open thin-layer cascade systems operated as batch cultures with the alga *Scenedesmus obliquus* were used to compare the productivity and photosynthetic adaptations in control and CO_2 supplemented cultures in relation with the outdoor light irradiance. We found that the culture productivity was limited by CO_2 availability beyond a threshold of daily irradiance. In the CO_2 supplemented culture, we obtained a productivity of up to 25 g dw.m^{-2}.day^{-1} and found a photosynthetic efficiency of 2.6%.

Fluorescence and oxygen evolution measurements showed that ETR and oxygen evolution light saturation curves, as well as alternative electron transport were similar in algal samples from both cultures when the CO_2 limitation was removed. In contrast, we found that CO_2 limitation conducted to a decreased PSII photochemical efficiency and an increased light-induced heat-dissipation in the control culture compared to the CO_2 supplemented culture. These features may contribute to the lower productivity observed in absence of CO_2 supplementation in outdoor mass cultures of *Scenedesmus obliquus*.

Remerciements

Voici donc le passage le plus attendu de ma thèse, celui qui aura probablement le plus de succès...

Comment décrire une thèse? Laissez moi vous conter ma petite expérience. Tout commence en réalité à la fin du mémoire. On se rend compte qu'on se plaît assez bien au laboratoire, le sujet est sympa, les collègues aussi. Ce serait chouette de continuer! Une étape de stress intense commence alors avec la préparation de la défense de son projet de thèse pour tenter d'obtenir une bourse FRIA. Deux mois de préparation pour cinq minutes de présentation... La concurrence est rude, il faut être le meilleur! Vient alors le jour J. Je passe ma matinée à relire mes cours de biochimie (on ne sait jamais, le jury pourrait me demander quelle est la composition du buffer de migration lors d'un western blot). Et puis en fait non, voici venir la question qui tue « Monsieur, pourquoi une électrode polarographique s'appelle t-elle une électrode polarographique? »... Je passe ensuite le reste de la journée à me demander pourquoi je n'ai pas étudié le manuel de l'électrode de Clark avant de passer devant la commission. Le lendemain, il est temps de faire jouer son réseau d'informateurs et ouf, c'est bon, c'est parti pour quatre ans! Rendez-vous alors au marché de Noël pour fêter cela avec les amis et collègues. Lors de cette soirée mémorable dont tous les doctorants de mon année se souviendront (ou pas...), nous retiendrons notamment le fameux *Bart à papa*. Commence alors la première année de thèse, année de découverte durant laquelle on lit beaucoup, beaucoup d'articles... On réaménage *un peu* le labo, on construit la chambre de culture (quand on travaille à la bota, il faut être polyvalent!), on retrouve des trésors dans les tiroirs. On pense qu'on a le temps mais en fait... Non! Le premier congrès à Vérone arrive très vite. Quel stress mais surtout quel challenge! D'autres suivront: Paris, Wageningen, Israël, Saint-Louis (n'oublions pas notre rencontre furtive avec Zidane), Bruxelles (tout de suite moins exotique 😁) et Bielefeld, la ville qui n'existe pas.

Il s'en est passé des choses durant ces quatre ans! Bart a eu deux petites filles. Il a aussi cassé 2-3 vélos. J'ai bu environ 3000 cafés (ça fait peur...). J'ai du faire réparer ma voiture environ dix fois avant qu'elle ne rende l'âme lors de la dernière semaine de rédaction. Mais surtout, j'ai écrit ce chef d'œuvre de poésie. Ça n'a pas été simple mais quelle fierté d'y arriver!

Je me dois de remercier,

En premier lieu Mr. Franck, auprès de qui j'ai trouvé l'enthousiasme, la culture et l'intelligence indispensable à la maturation de cette thèse. Chef, merci de m'avoir accepté dans votre laboratoire, merci pour la liberté que vous m'avez accordée durant cette thèse. Nos discussions sur les principes fondamentaux de la photosynthèse vont me manquer...

Bart, mon co-promoteur, dont la confiance et l'amitié sont le plus beau cadeau que l'on puisse faire. À surveiller de près, sous peine de retrouver sa pipette noyée dans une explosion de soupe verte collante. Merci de m'avoir

épaulé durant toutes ces années et... Sorry pour tous les cafés que je t'ai volés ☺.

Évidemment, toute la tribu, plus ou moins permanente, du labo. Anthony, courage pour ta thèse et appelle moi quand tu voudras te débarrasser de *Haematococcus*, j'ai un plan. Steph, qui a sans cesse repoussé les avances du réparateur de hottes. Elles auraient peut-être fonctionné si tu avais fait quelques efforts. Thomas, j'espère pouvoir un jour me parfumer à la... Oups, c'est un secret. N'oublions pas Françoise, qui fait un quart-temps dans notre laboratoire. Enfin, tous ceux que j'ai côtoyés dans notre labo: Philippe, Tung, Amélie, Grégory et Jonathan.

Tout le labo de génétique des microorganismes. Tout d'abord Claire qui m'a accueilli lorsque j'ai (vainement) tenté de produire un mutant. Pierre avec qui j'ai beaucoup discuté et voyagé. Damien, on s'est quand même bien marrés aux congrès (« Ha bon, vous travaillez au Mac Do ? - Non, le manque d'eau ». Gros moment de solitude). Véro, qui nous manque tant. Ainsi que tous ceux que j'y ai croisés, Michèle, Nadine, Benjamin, Nico, Barbara, Rémi,... Au plaisir!

Je ne remercierai jamais assez mes parents sans qui rien n'aurait été possible... Ma mère, qui a eu la bonté de me laisser démonter une bonne partie des appareils électroniques de la maison durant mon enfance. Mon père, qui m'a toujours donné envie d'entreprendre et d'aller de l'avant. Je vous remercie pour l'éducation que vous m'avez donnée (Comment? On me dit qu'ils ont fait quelques erreurs...). Mes trois *petites* sœurs. Sophie, je te souhaite beaucoup de bonheur avec Ralph. Alice et Pauline, maman a le cœur fragile, vous allez la tuer 😁. Manounou, ma grand-mère, qui ne rechignait devant aucune recette pour bien me nourrir sur le temps de midi. Je pense que tu es prête pour Top-chef. Enfin, Bon papa, qui tente chaque année de nous faire gagner au WinForLife, hélas sans succès ☺.

Merci à tous mes amis, les Saints-Barthélemiens, les Bios ainsi que tous ceux que je n'ai pas cités mais que je n'oublie pas.

Enfin, je termine par la plus belle, ma fiancée Floriane à qui je dédie cette thèse. Voilà maintenant douze ans que tu partages ma vie. Que de chemin parcouru dernièrement! Notre maison, nos fiançailles, ton magasin. Merci d'avoir supporté ma mauvaise foi et mon stress durant les dernières semaines. Il faut dire qu'on a pas chômé ces dernières semaines (enfin, façon de parler). Pas facile de finaliser une thèse et de lancer un magasin en même temps... Mais quelle réussite, il est splendide!

Et ils vécurent heureux et eurent beaucoup... Et non, désolé maman, ce n'est pas pour tout de suite 😁.

Sur ce, voici quelques photos souvenirs que j'avais envie de partager afin de se remémorer tous ces bons moments.

Anthony et moi devant un support que nous avons fabriqué pour la chambre de culture (photo non libre de droits).

Le chef et Bart devant un vendeur de légumes à Vérone en Italie à l'occasion de la réunion annuelle du projet européen Sunbiopath en 2011.

Bart et moi devant le mur des lamentations à Jérusalem en Israël à l'occasion de la réunion annuelle du projet européen Sunbiopath en 2012.

Véro, prête à déguster des fraises sans goût dans une serre en plein désert... En Israël bien entendu! (2012).

Bart et moi devant la grande mosquée à Jérusalem en Israël à l'occasion de la réunion annuelle du projet européen Sunbiopath en 2012. Notez le parfait assortiment de Bart à la coupole.

Damien, Steph et moi à Times Square à l'occasion du 16ème congrès international sur la photosynthèse en 2013.

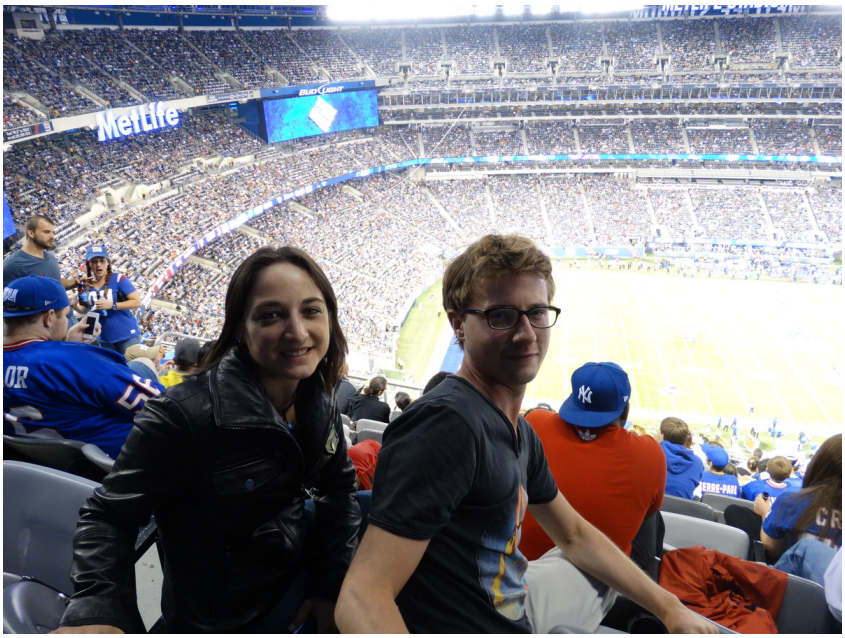

Steph et moi à un match de football américain à New-york à l'occasion du 16ème congrès international sur la photosynthèse en 2013. Le football américain, c'est déjà lent mais alors le baseball...

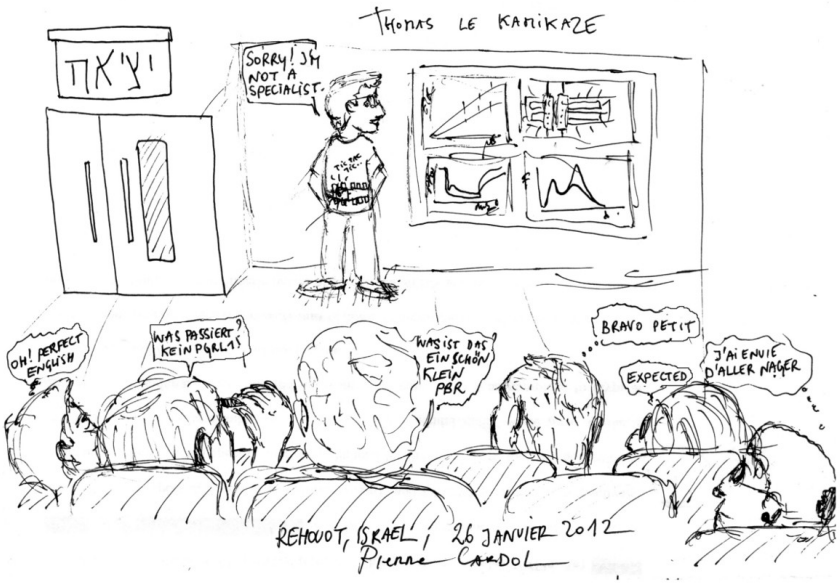

Ce croquis si bien réalisé par Pierre lors d'un séminaire que j'ai donné en Israël mérite bien une petite place! Saurez-vous reconnaître les membres de l'audience?

Abbreviations

AOX	Alternative oxidase
ATP	Adenosine triphosphate
CCM	Carbon concentrating mechanism
CEF	Cyclic electron transport around PSI
Cyt b_6f	Cytochrom b_6f
DCMU-FR	DCMU fluorescence rise
ΔpH	Proton gradient
DIC	Dissolved inorganic carbon
ETR	Electron transport rate
Fd	Ferredoxin
Flv	Flavodiiron proteins
F_M	Maximum fluorescence level of dark-adapted cells
F'_M	Maximum fluorescence level of light-adapted cells
F_O	Fluorescence level of dark-adapted cells
F_t	Steady-state fluorescence level
F_V/F_M	Maximal PSII photochemical efficiency
H_2O_2	Hydrogen peroxide
LEF	Linear electron transport
LHCI and LHCII	Light-harvesting complexes I and II
NADH	Nicotinamide adenine dinucleotide
NADPH	Nicotinamide adenine dinucleotide phosphate
NDA2	Type II NAD(P)H dehydrogenase
NPQ	Non-photochemical quenching
OEC	Oxygen evolving complex
PC	Plastocyanin
ΦPSII	PSII operating photochemical efficiency
PQ/PQH_2	Plastoquinone/Plastoquinol
PSI/PSII	Photosystem I/Photosystem II
PTOX	Plastid terminal oxidase
Q_A	Primary acceptor quinone in the PSII reaction center
Q_B	Secondary acceptor quinone in the PSII reaction center
qE	High-energy state quenching
qI	Photoinhibition
qP	Photochemistry
qT	State transition
RC	Reaction center
ROS	Reactive oxygen species
UQ/UQH_2	Ubiquinone/Ubiquinol

Contents

1 General introduction **17**

1.1 Carbon cycle 17
1.2 What are microalgae? 19
1.3 Importance of studying microalgae photosynthesis 20
1.4 Respiration 20
1.4.1 General description 20
1.4.2 Oxidative phosphorylation 22
1.5 Photosynthesis 24
1.5.1 General description 24
1.5.2 Light phase : light absorption and conversion in chemical energy 26
1.5.3 Dark phase : assimilation of CO_2 by the Calvin cycle 27
1.5.4 The carbon concentrating mechanism 29
1.5.5 Flexibility of photosynthesis against the metabolic and environmental context 30
1.6 *In vivo* monitoring of the photosynthetic apparatus 38
1.6.1 Chlorophyll fluorescence measurements 38
1.6.2 Polarographic measurement of oxygen evolution 44
1.7 Objectives of this thesis 45

2 From photons to photochemistry : fluorescence study on the remodelling of PSII during state transitions **47**

2.1 Introduction 50
2.2 Material and methods 54
2.3 Results and discussion 56
2.3.1 Rate constant dependence on light intensity 59
2.3.2 The optical cross-section, as determined by the half-time of the fluorescence rise, is proportional to the proportion of PSIIα 62
2.3.3 Development of a protocol to determine PSII antenna size heterogeneity during state transition 64

2.3.4 Transition to state 2 from state 1 is reflected in conversion of PSIIα and PSIIβ 66
2.4 Conclusion 69
2.5 Supplemental data 70

3 From photochemistry to CO_2 fixation : photosynthetic adaptations to high and low CO_2 conditions in laboratory grown cultures of *Chlamydomonas reinhardtii* 73
3.1 Introduction 77
3.2 Material and methods 81
3.3 Results and discussion 83
3.3.1 Combined effects of CO_2 supply and light intensity on growth rates 83
3.3.2 Evidence for a light-dependent electron flow to O_2 in low CO_2 conditions 84
3.3.3 A decreased PSII photochemical yield in CO_2-limiting conditions 99
3.3.4 qE is enhanced in CO_2-limiting conditions 100
3.3.5 A decreased PSII antenna size and a state 2 transition in high CO_2 conditions 103
3.4 Conclusion 105
3.5 Annex 106

4 From CO_2 to biomass : photosynthetic adaptations to high and low CO_2 conditions in outdoor microalgae mass cultures of *Scenedesmus obliquus* 111
4.1 Introduction 114
4.2 Material and methods 116
4.3 Results and discussion 119
4.3.1 Productivity and photosynthetic efficiency of *Scenedesmus obliquus* in high and low CO_2 conditions 119
4.3.2 Characterisation of the photosynthetic apparatus in high and low CO_2 conditions 123
4.4 Conclusion 130
4.5 Appendix 131

5 General discussion 133
5.1 What chlorophyll fluorescence can and cannot do for you . . 133
5.2 Perspectives 138
5.2.1 Determination of the cell redox state in high and low CO_2 conditions 138

5.2.2 What is the relative contribution of light-dependent O_2 uptake and CEF? 139
5.2.3 Measuring O_2 evolution in physiological conditions . . 139
5.2.4 Determining the light-dependent O_2 uptake pathway in physiological conditions 140
5.2.5 Why measuring chlorophyll fluorescence on microalgae mass cultures is not an easy task 141

6 Annex **143**

List of Figures **147**

Bibliography **149**

Chapter 1

General introduction

Contents

1.1 Carbon cycle 17
1.2 What are microalgae? 19
1.3 Importance of studying microalgae photosynthesis 20
1.4 Respiration 20
1.4.1 General description 20
1.4.2 Oxidative phosphorylation 22
1.5 Photosynthesis 24
1.5.1 General description 24
1.5.2 Light phase : light absorption and conversion in chemical energy 26
1.5.3 Dark phase : assimilation of CO_2 by the Calvin cycle 27
1.5.4 The carbon concentrating mechanism 29
1.5.5 Flexibility of photosynthesis against the metabolic and environmental context 30
1.6 *In vivo* monitoring of the photosynthetic apparatus 38
1.6.1 Chlorophyll fluorescence measurements 38
1.6.2 Polarographic measurement of oxygen evolution . 44
1.7 Objectives of this thesis 45

1.1 Carbon cycle

All living things are made of carbon-based biomolecules. Carbon is incorporated in your body by the food you eat and is stocked mainly in the form

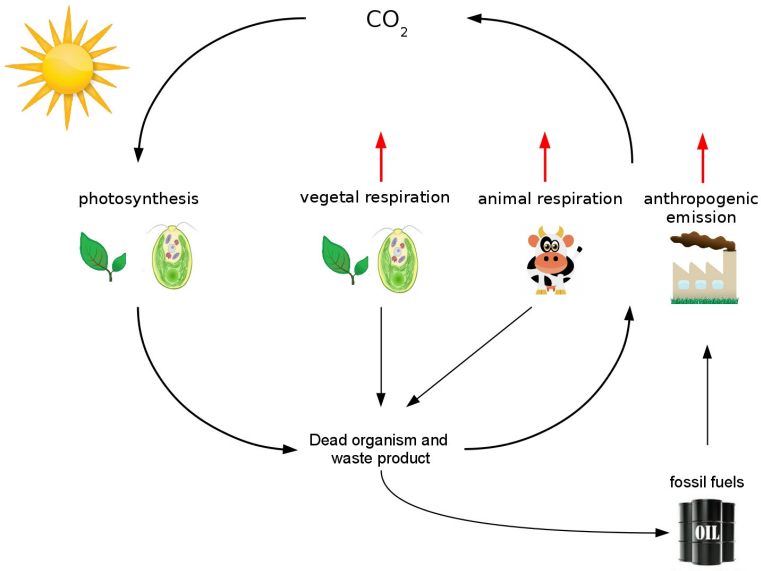

Figure 1.1: Simplified carbon cycle showing CO_2 emission by respiration and anthropogenic factors and its reabsorption into living organism by photosynthesis.

of sugars and lipids, in which carbon is hydrogenated. The energy needed to live results from the oxidation of these energetic molecules into carbon dioxide, which is then released in the atmosphere. Carbon is also the major constituent of fossil fuels like coal, petroleum and natural gas. Like for living things, the energy produced by burning fuels results from the replacement of hydrogen by oxygen in complex molecules which are then decomposed into CO_2.

CO_2 emitted by these processes is released in the atmosphere and constitutes one of the greenhouse gas until it is reincorporated in the carbon cycle by its fixation into biomass by photosynthesis of higher plants and microalgae. The fixation of CO_2 and its reduction to form organic compounds is also termed primary production. This carbon cycle has been unbalanced in the last century by the massive emission of CO_2 by industry. This led to the accumulation of CO_2 in the atmosphere and to a general increase of the earth surface temperature due to the increased greenhouse effect.

Photosynthesis being the base of the food chain and of the life on earth, understanding the impact of variations in CO_2 concentration on this process is thus of primordial importance.

1.2 What are microalgae?

The term microalgae refers to a polyphyletic group (without a common ancestor) of prokaryotic and eukaryotic unicellular photosynthetic microorganisms. Microalgae may live either individually or grouped in small colonies with sizes varying from a few micrometers to hundreds of micrometers. These organisms have adapted to a wide range of environmental conditions that include saline, freshwater and terrestrial environments, hot and cold climates and a great range of mineral compositions. The biodiversity of microalgae has been estimated to about $\approx$ 72000 species (Guiry, 2012).

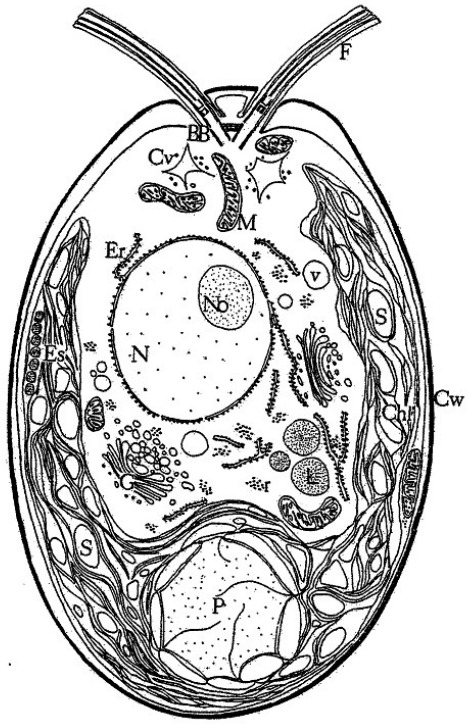

Figure 1.2: Representation of a *Chlamydomonas* cell. Cell length, 10 μm; BB, basal bodies; Chl, chloroplast; Cv, contractile vacuole; Cw, cell wall; Er, endoplasmic reticulum; Es, eyespot; F, flagella; G, Golgi apparatus; L, lipid body; Mi, mitochondria; N, nucleus; No, nucleolus; P, pyrenoid; S, starch grain; V, vacuole. From Harris, 2001.

The eukaryotic species *Chlamydomonas reinhardtii* (fig 1.2) has been used as a model organism since 1960, especially for the study of the flagella apparatus. Nowadays, this green microalgae is still the reference organism for the study of photosynthesis because of the availability of numerous mutants,

its culture facility and the similarity of its metabolism compared to the one of higher plants. Other microalgae species are often studied and cultivated for industrial applications such as *Spirulina platensis*, *Scenedesmus obliquus* and *Chlorella vulgaris* for food and feed production, *Dunaliella salina* for its high β-carotene content and *Haematococcus pluvialis* for astaxanthin production.

1.3 Importance of studying microalgae photosynthesis

In terrestrial ecoregions, primary production is realised mainly by higher plants while in aquatic ecoregions, it is realised mainly by microalgae. Field *et al.* (1998) showed that half of the annual primary production is realised in the oceans by microalgae, which shows the interest of studying microalgae photosynthesis.

Moreover, multiple industrial applications using microalgae have been imagined in the last decade. Due to their carbon dioxide fixing and rapid biomass production capacities, microalgae are thought to be potential candidates for biofuel production and for reduction of the concentration in greenhouse gas in the atmosphere. Microalgal biomass can also be used to produce a great variety of molecules for the industry. This includes food and feed, nutraceutical and cosmetic products.

Microalgae are also extensively studied in the laboratory for multiples reasons. First, their culture is facilitated by the fact that they grow quickly with a generation time which can be as small as three hours. Microalgae can grow on simple medium of inorganic salts using photosynthesis as a source of carbon (phototrophic growth). Most of them can also grow in darkness with organic carbon added in the culture media (heterotrophic growth), which facilitates the study of photosynthetic mutants. Mixotrophic growth is also possible if light and an organic carbon source are provided. Moreover, genetic studies are facilitated due to the availability of several genetic tools.

1.4 Respiration

1.4.1 General description

Respiration is the process which permits the cell to oxidize organic compounds in order to produce ATP and NADH which are necessary for the cell metabolism. In eukaryotic cells, most of this process occurs in mitochondria (fig 1.3). Mitochondria comprise an outer membrane and an inner membrane

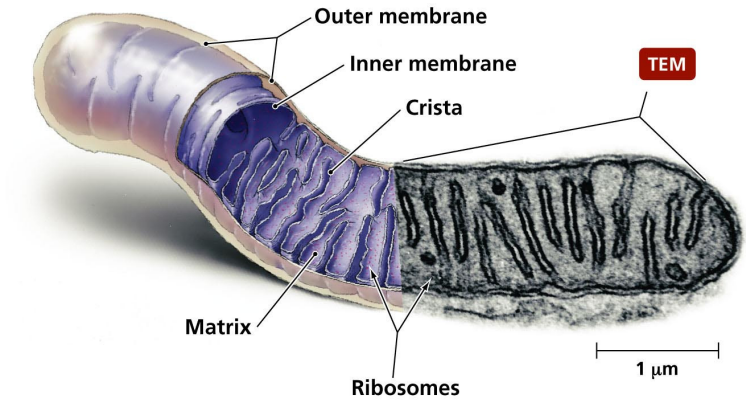

Figure 1.3: Structure of a mitochondrion. Tem, Transmission Electron Microscopy. Copyright 2006 pearson Education, Inc, publishing as Benjamin Cummings.

which delimit the intermembrane space and the matrix. The inner membrane is folded into cristae that increase the surface area for the membrane-bound molecules. The matrix contains enzymes, DNA and ribosomes while the inner membrane contains the complexes of the electron transport chain and the ATP synthase.

Respiration can be described in five steps:

1. The glycolysis oxidizes glucose into pyruvate and generates ATP and NADH.

2. Pyruvate synthesised by the glycolysis is converted into acetyl-CoA, generating ATP and CO_2.

3. Acetyl-CoA enters in the Krebs cycle, leading to the generation of CO_2, GTP and NADH.

4. NADH is oxidized in the mitochondrial electron transport chain. During electron transport to oxygen, protons are translocated from the stroma to the intermembrane space and a transmembrane electrochemical potential is established.

5. ATP is synthesized by an ATP synthase enzyme complex, which couples the dissipation of the transmembrane potential with ADP phosphorylation.

Step 4 and 5 are often referred to as oxidative phosphorylation. The Krebs cycle which is the main source of reductants for the oxidative phosphorylation

is mainly driven by sugar oxidation (glycolysis). However, the Krebs cycle can also be sustained by metabolites generated during by the β-oxidation of lipids or by the oxidation of aminoacids.

1.4.2 Oxidative phosphorylation

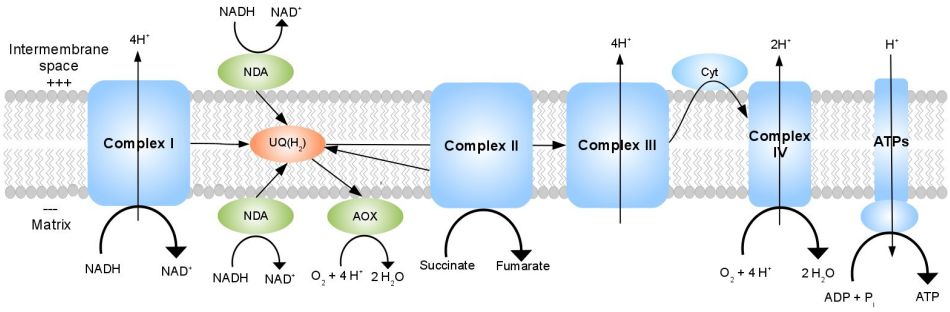

Figure 1.4: Mitochondrial electron transport chain. Complex I, NADH dehydrogenase; Complex II, succinate dehydrogenase; Complex III, cytochrome bc_1; Cyt, cytochrome c; Complex IV, cytochrome c oxidase; ATPs, ATP synthase; AOX, alternative oxidase; $UQ(H_2)$, ubiquinone; NDA, NADH dehydrogenases.

The oxidative phosphorylation is a metabolic pathway which uses the reducing power of NADH to drive an electron transfer coupled to the generation of a transmembrane potential and to ATP synthesis. The mitochondrial electron transport chain consists of several enzymatic complexes and two pathways are generally described, the cytochrome pathway and the alternative oxidase pathway.

Cytochrome pathway

The cytochrome pathway consists of four complexes:

The NADH:ubiquinone oxidoreductase (complex I) NADH is oxidized and two electrons are transferred to the ubiquinone (UQ) while 4 H^+ are pumped from the matrix to the intermembrane space.

The succinate:ubiquinone oxidoreductase (complex II) The succinate from the Krebs cycle can be oxidized in fumarate to reduce the UQ. This process does not drive any H^+ translocation.

The ubiquinol:cytochrome c oxidoreductase (complex III) This complex oxidizes one UQH_2 to reduce two cytochromes c in a series of

oxidation-reduction reactions named Q cycle. During this process, 4 H^+ are translocated into the intermembrane space.

The cytochrome c oxidase (complex IV) The complex IV oxidizes two cytochrome c molecules and transfers the electrons to the last electron acceptor, oxygen, which will be reduced in water while 2 H^+ are pumped from the matrix to the intermembrane space per oxygen atom reduced.

The different proton translocations from the matrix to the intermembrane space result in the formation of an electrochemical gradient that is used by the ATP synthase to phosphorylate ADP into ATP. Plant mitochondria also possess NADH dehydrogenases located on the inner and external faces of the membrane which do not induce proton translocations.

Alternative oxidase pathway

In higher plants, microalgae, fungi and protozoa, there is an alternative oxidase (AOX) which oxidizes UQH_2 and directly reduces O_2. This electron transfer pathway is non-phosphorylating since it does not conduct to any H^+ translocation and ATP synthesis. Molen *et al.* (2006) have shown that the expression of AOX is regulated by two different mechanisms, the first is activated by oxidative stress and leads to a rapid but transient expression of AOX while the second is activated in the presence of NO_3 (Baurain *et al.*, 2003). In *Sauromatum guttatum*, AOX is implicated in heat production in order to disperse the odour molecules and attract pollinators insects (Moore and Siedow, 1991). However the role of this enzyme is not well understood in non-thermogenic tissues. Two major roles have been attributed to it :

1. Its activation could prevent an over-reduction of the electron transport chain in case of stress, over-reduction which could lead to ROS production by complexes I and III.

2. AOX could help to maintain glycolysis and Krebs cycle in case of a low availability in oxidized cofactors (such as NAD^+) by oxidizing UQH_2 in order to permit the regeneration of these cofactors.

These roles have been confirmed in *Chlamydomonas reinhardtii* by a proteomic study conducted by Mathy *et al.* (2010).

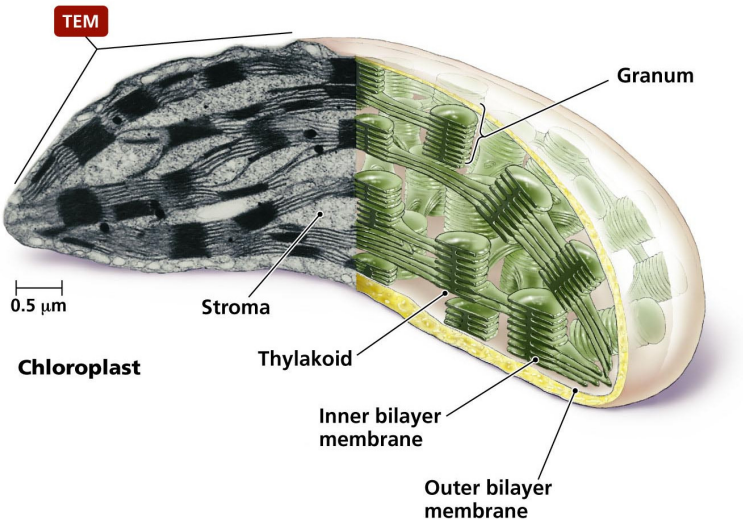

Figure 1.5: Structure of a chloroplast. TEM, Transmission Electron Microscopy. Copyright 2006 Pearson Education, Inc, publishing as Benjamin Cummings.

1.5 Photosynthesis

1.5.1 General description

Photosynthesis is the process by which photosynthetic microorganism use light and convert it into chemical energy which can be used for the absorption and reduction of carbon dioxide and nutrients in order to produce biomass.

This process begins by the absorption of light by the chlorophylls of photosystem I (PSI) and photosystem II (PSII) in the chloroplast. The light energy triggers an electron flux driving the production of NADPH and ATP. This process is named *the light phase*. The reductants are then used by the Calvin cycle during *the dark phase* to assimilate CO_2 and nutrients.

In eukaryotes, photosynthesis takes place in the chloroplast. This organelle is composed of a double membrane, an aqueous matrix (stroma), and an internal membrane forming the thylakoids (fig 1.5). Thylakoids can be free in the stroma or form grana stacks. The reactions of the light phase occur in the thylakoids while these of the dark phase take place in the stroma.

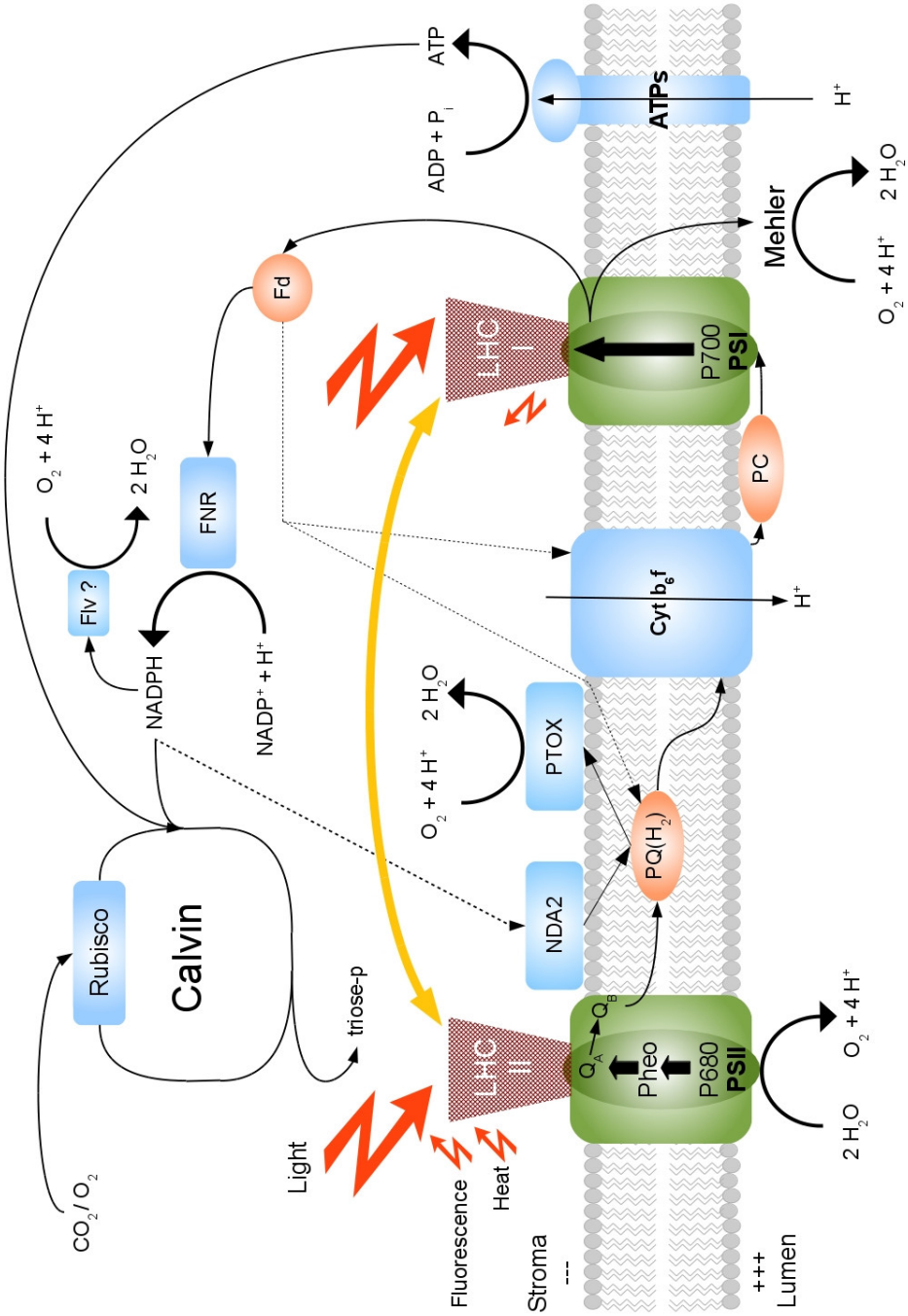

Figure 1.6: This diagram represents the absorption of light and the light-driven electron flux leading to the production of ATP and NADPH in the chloroplastic electron transport chain. ATP and NADPH can then be used to reduce CO_2. Yellow arrow: state transitions; Dashed lines: cyclic electron transport via the NDA2-dependent pathway or the Fd-dependent pathways. See description below.

1.5.2 Light phase : light absorption and conversion in chemical energy

The reactions of the light phase convert light energy in chemical energy in the form of ATP (phosphate bond energy) and NADPH (redox energy). These molecules can then be used by the reactions of the dark phase and by other metabolic processes in order to sustain growth and multiplication of the cell. The electron transport from H_2O to NADPH involves five membrane protein complexes in the thylakoids (fig 1.6) and is called linear electron transport.

Light Harvesting Complexes I and II Though the chlorophyll *a* molecules in a reaction center are able to directly absorb the light, excitation energy is usually transferred from surrounding pigments located in light harvesting complexes chlorophyll-proteins. The antenna light harvesting complexes I and II (LHCI and LHCII) are multi-protein complexes containing chlorophylls and carotenoids that extend the absorbed wavelength range and increase the excitation fluxes in photosystems I and II, respectively. The excited state of a chlorophyll molecule which has absorbed a photon is transferred from chlorophyll to chlorophyll up to the reaction center where photochemistry can take place.

Photosystem II The first step of photosynthesis is the excitation of a special pair of chlorophylls in the photosystem II (PSII) reaction center: P680. The excitation of P680 will cause the transfer of an electron from P680 to pheophytin (primary charge separation). Secondary electron transfer will then result in the reduction of the fixed plastoquinone (PQ) Q_A (a one electron acceptor) which will then reduce exchangeable PQ Q_B. The double reduction of Q_B will conduct to its protonation by two protons from the stroma to form the plastoquinol (PQH_2) which will dissociate from PSII. On the oxidizing side, $P680^+$ will be reduced by an electron from the photolysis of water in the oxygen evolving complex (OEC) via an intermediate tyrozine. After four successive charge separations, an oxygen molecule and 4 H^+ are released into the lumen.

Cytochrome b_6f Binding of a PQH_2 to the site Q_o of the cytochrome b_6f (Cyt b_6f) causes its oxidation by this complex and the release of 2 H^+ in the lumen. One electron passes through the Fe-S site of the RIESKE protein and will reduce one plastocyanin (PC), while the other passes through two cytochromes (b_h and b_l, not shown in figure 1.6) and will partially reduce one PQ at site Q_i. Following a second series of identical reactions, the PQ double reduction conducts to its

protonation and its release. It can then be re-oxidized at Q_o site. During this process, called the Q cycle, 2 electrons are transferred to PC and 4 H^+ are released into the lumen for the net oxidation of one PQH_2.

Photosystem I Excitation of the special pair of chlorophylls (P700) in the photosystem I (PSI) reaction center causes transfer of an electron to a ferredoxin (Fd) via intermediate transporters including Fe-S centers. $NADP^+$ is reduced in NADPH after two charge separations by the ferredoxin-NADP reductase (FNR). After each oxidation, P700 retrieves an electron from a PC.

ATP synthase The different proton translocations from the matrix to the lumen result in the formation of a transmembrane electrochemical gradient which is used by the chloroplastic ATP synthase to phosphorylate ADP to ATP.

1.5.3 Dark phase : assimilation of CO_2 by the Calvin cycle

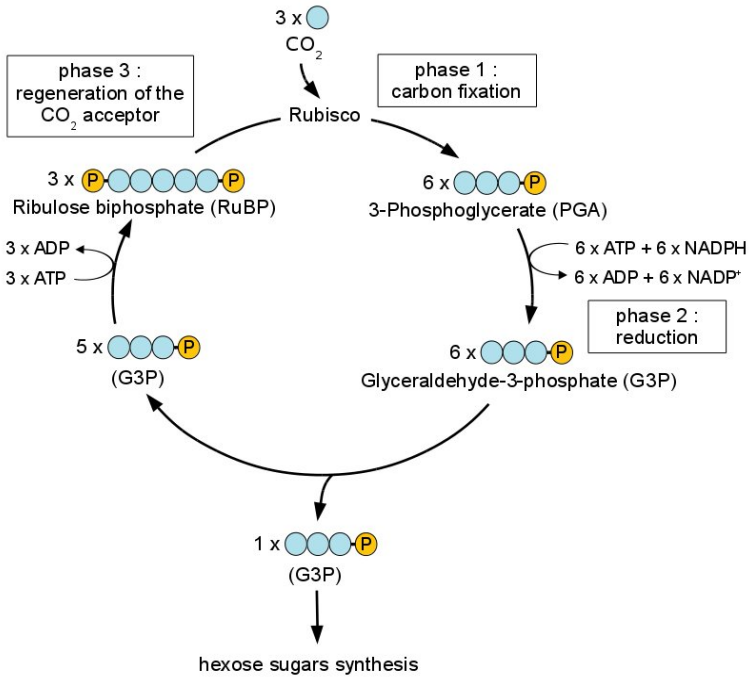

Figure 1.7: Overview of the major steps of the Calvin cycle. See description below.

During the dark phase, the ATP and NADPH produced during the light phase are used by the Calvin cycle to assimilate CO_2 and convert it to glyceraldehyde-3-phosphate (G3P) which will then be exported in the cytosol to be used as a building block for the production of hexose sugars.

The sum of reactions in the Calvin cycle is the following:

$$3CO_2 + 6NADPH + 5H_2O + 9ATP \rightarrow G3P + 2H^+ + 6NADP^+ + 9ADP + 8P_i$$

The Calvin cycle occurs in three major steps (fig 1.7):

Phase 1 : carbon fixation The fixation of CO_2 is catalysed by the ribulose 1,5-biphosphate carboxylase/oxygenase (Rubisco) from ribulose biphosphate (RuBP) and generates 3-phosphoglycerate (PGA). In *Chlamydomonas*, Rubisco is mainly located in the pyrenoid. The catalytic rate of the Rubisco being very slow, this enzyme is present in high concentration in photosynthetic organisms. For this reason, it is probably the most abundant protein on earth (Ellis, 1979).

Phase 2 : reduction For PGA reduction to glyceraldehyde-3-phosphate (G3P) by NADPH, an activation energy barrier must be overpassed. This is achieved by a transient activation of PGA through its phosphorylation to bis-PGA. This is why the reduction phase consumes two ATP molecules per fixed CO_2. The fate of glyceraldehyde-3-phosphate is complex: some is exported in the cytosol to be converted in hexose sugars or is used in the chloroplast to generate starch, but most of it (5/6) is used to regenerate ribulose bisphosphate.

Phase 3 : regeneration of the CO_2 acceptor ribulose bisphosphate Ribulose bisphosphate is regenerated from glyceraldehyde-3-phosphate in a complex pathway involving nine enzymes. At the end of this phase, one ATP molecule is used in the phosphorylation of ribulose 5-phosphate to each ribulose bisphosphate.

Altogether the assimilation of one CO_2 molecule requires three molecules of ATP (two in the reduction phase and one in the regeneration phase) and two molecules of NADPH. It has been calculated that the ratio ATP/NADPH produced by linear electron transport is lower (1.28 ATP produced by NADPH) than the ratio of 1.5 required for the dark phase. In this case, the missing ATP should be produced by auxiliary pathways (see section 1.5.5).

The particular case of photorespiration The main reaction catalysed by Rubisco is the carboxilation of ribulose biphosphate carboxylation. However, when the ratio CO_2/O_2 near the enzyme is low, Rubisco catalyses the

oxygenation of the ribulose biphosphate to yield PGA and phosphoglycolate, a two carbon compound. PGA is the normal product of carboxylation and enters in the Calvin cycle. Phosphoglycolate, however, is toxic and has to be recycled. In higher plants, its recycling involves a series of reactions in the chloroplast, the peroxisome and the mitochondria (Moroney *et al.*, 2013). The sum of photorespiratory reactions is the following:

$$2O_2 + 2\text{RuBP} + \text{ATP} + 2\text{NADH} + 2H^+ \rightarrow 3\text{PGA} + CO_2$$

Photorespiration may be considered as a waste process for the cell since energy and potential biomass are simultaneously consumed. A suggested explanation for Rubisco's inability to discriminate CO_2 and O_2 is that it is an evolutionary relic: the early atmosphere in which primitive plants originated contained very little oxygen, thus the evolution pressure did not select a CO_2 fixing enzyme with a low affinity for O_2. Attempts have been made by genetic engineering to obtain Rubisco with low affinity for O_2 but in each case, the affinity for CO_2 was similarly lowered. Nevertheless, the role of photorespiration is perhaps not only negative. It is assumed that it is involved in the cells photoprotection by oxidizing reductants and ATP in case of stress such as high light or low CO_2 availability, thus preventing ROS production.

1.5.4 The carbon concentrating mechanism

In order to reduce photorespiration and favor CO_2 assimilation, microalgae have developed a mechanism called the Carbon Concentrating Mechanism (CCM), which helps to increase the concentration in Dissolved Inorganic Carbon (DIC) in the Rubisco vicinity. The CCM is induced under low CO_2 concentration and repressed under high CO_2 concentration. In eukaryotic microalgae, the CCM is composed of carbonic anhydrases (CAs), HCO_3^- transporters and the pyrenoid, a microcompartment for the delivery of CO_2 to Rubisco. CA are zinc-metalloenzymes which accelerate the interconversion of CO_2 and HCO_3^- following the reaction : $CO_2 + H_2O \rightleftharpoons HCO_3^- + H^+$. In *Chlamydomonas reinhardtii*, 12 CA genes have been identified, and 6 of them were shown to code for CA localized in the mitochondria, in the chloroplast and in the periplasm (Moroney *et al.*, 2011). CAs can have multiple roles. One is to provide the DIC specie (HCO_3^- or CO_2) needed for a specific metabolic reaction such as the carboxylation of ribulose biphosphate which uses only CO_2. A second role is to deliver DIC to the correct location within the cell (mainly the pyrenoid in the chloroplast). The uptake is thought to be achieved through the action of transport proteins as well as CAs (fig 1.8). A third role would be to prevent CO_2 leakage from the cell. The membranes

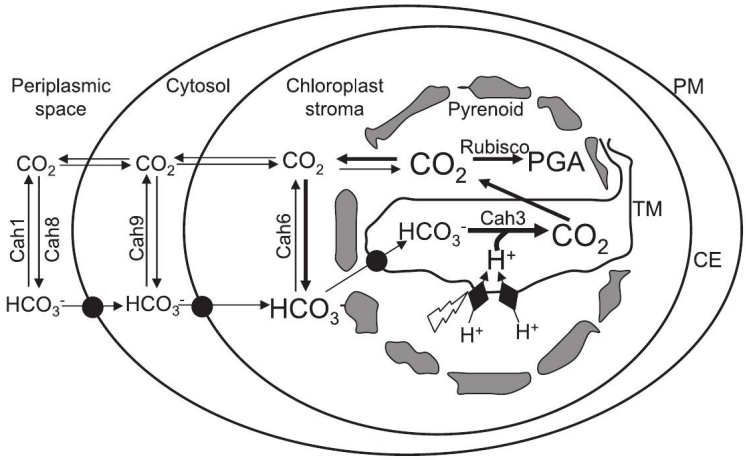

Figure 1.8: The figure depicts an algal cell with a single chloroplast containing a single pyrenoid. CAH1, CAH3, CAH6, CAH8, and CAH9 stand for specific CA isoforms. PM, plasma membrane; CE, chloroplast envelope; TM, thylakoid membrane. The filled circles indicate possible bicarbonate transporters, and the closed diamonds indicate the photosynthetic electron transport chain. From Moroney and Ynalvez, 2007.

are highly permeable to this gas and conversion to HCO_3^-, which is one million times less permeable than CO_2, helps to prevent DIC loss.

1.5.5 Flexibility of photosynthesis against the metabolic and environmental context

In nature, photosynthetic microorganisms have to cope with constantly fluctuating light exposure. The light intensity may exceed the capacity of its use by the photosynthetic apparatus. That capacity is variable and is influenced by various factors such as the CO_2 availability as a sink for the electrons, or the temperature which influences the metabolic reaction rates.

The metabolic context of the cell may also require a precise adjustment of the balance between the ATP and NADPH produced during the light phase of photosynthesis. Indeed, the stoichiometric requirements for the reduction of one CO_2 molecule by the Calvin cycle are 3 ATP and 2 NADPH molecules, i.e. a ratio of 9:6, while the ATP/NADPH ratio produced by linear electron flow is 9:7 (Allen, 2003). The CO_2 availability has also an effect on the ATP/NADPH balance needed during photosynthesis. Under low CO_2 availability, the concentration of one CO_2 molecule from the extracellular space to the pyrenoid by the CCM requires 1.0-1.5 ATP molecule to power the bicarbonate transporters (Spalding and Portis Jr, 1985; Lucker and Kramer,

2013). Under this condition, the optimal ATP/NADPH ratio for carbon fixation increases to 10.0-10.5:6. The adjustment of the ATP/NADPH ratio required to meet the metabolic needs can be realized by alternative pathways to the linear electron transport such as cyclic electron transport around PSI, chlororespiration or the Mehler reaction.

Under high light stress conditions, the photosynthetic electron transport chain is over-reduced and this may lead to ROS production and cell damages. Photosynthetic organisms have developed different mechanisms to reduce the excitation pressure on photosystems. All known mechanisms are associated with PSII and are referred to non-photochemical quenching (NPQ) because they lower the fluorescence yield of PSII chlorophylls. NPQ comprises three different processes: high energy-state quenching (qE), state transitions (qT) and photoinhibition (qI). In addition to these three photoprotective mechanisms, alternative pathways can also participate in the oxidation of the electron transport chain by dissipating reducing power.

High-energy state quenching: increased thermal dissipation

High-energy state quenching (qE) is a mechanism developed to reduce the excitation pressure on the photosynthetic apparatus. It consists in dissipating absorbed light energy as heat directly by antennae pigments (Horton *et al.*, 1996). It is associated with the development of a low pH in the thylakoid lumen (Wraight and Crofts, 1970; Briantais *et al.*, 1979) and, in higher plants and some algae, with the deepoxidation of violaxanthin to zeaxanthin (Demmig-Adams, 1990; Förster *et al.*, 2001). The increase in the ΔpH resulting from the photosynthetic electron transport is thought to induce a conformational change of the thylakoid membrane (Bilger and Bjorkman, 1994) and of the LHCII which opens a channel for energy dissipation by transfer to a bound carotenoid (Ruban *et al.*, 2007). The increase in the ΔpH can also trigger the activation of the violaxanthin-deepoxydase (VDE) which converts violaxanthin in zeaxanthin. A constitutively expressed protein, the zeaxanthin epoxydase, catalyses the opposite reaction to reduce qE in non-stressed conditions. The mechanism of increased thermal dissipation following deepoxydation is not clear. Two theories have emerged:

1. Xanthophylls would favour the conformational aggregation of LHCII, which would increase thermal dissipation (Crofts and Yerkes, 1994; Horton *et al.*, 1996; Johnson *et al.*, 2011).

2. Energy would be transferred directly to zeaxanthin and dissipated (Chow, 1994; Frank *et al.*, 1994).

In *Chlamydomonas reinhardtii*, recent studies have shown the importance of the LHCSR3 protein for high-energy state quenching (Peers *et al.*, 2009).

Binding of LHCSR3 to PSII-LHCII supercomplexes and its protonation in an acidified lumen modifies LHC antennas conformation, creating quenching centres (Bonente *et al.*, 2011b; Tokutsu and Minagawa, 2013a).

Chlamydomonas reinhardtii shows a restricted ability to develop efficient qE. In this alga, strong NPQ comparable to what is commonly observed in higher plants under high light has only been reported after adaptation to low CO_2 conditions (Allorent *et al.*, 2013), or when CO_2 assimilation was impaired by low temperature or by Rubisco deficiency (Finazzi *et al.*, 2006).

While high-energy state quenching is well developed in higher plants and mosses (Morosinotto and Bassi, 2014), *Chlamydomonas reinhardtii* shows a restricted ability do develop efficient qE. It seems that the observed NPQ in this organism may be confused with state transitions (Finazzi *et al.*, 2006).

State transitions

The antenna of PSI is enriched in chlorophyll *a* and absorbs at longer wavelengths than PSII which contains a higher proportion of chlorophyll *b*. Due to this, photosystems can be excited at different rates depending on the excitation light quality and this can lead to an imbalance of the electron transport chain. In order to correct this imbalance, LHCII antenna complexes can migrate between PSI and PSII. This leads to changes in PSI and PSII optical cross-sections, and thereby restores the excitation balance (yellow arrow in fig 1.6). This phenomenon, termed *state transitions* has been discovered independently by Bonaventura and Myers (1969) and Murata (1969).

State transitions have been extensively studied in *Chlamydomonas reinhardtii* because in this organism, up to 80% of the LHCII can migrate between the photosystems, against about 20-25% for higher plants (Delosme *et al.*, 1996). The redox state of the PQ pool is the main determinant of state transitions through binding of plastoquinol to the Q_o site of Cyt b_6f (Vener *et al.*, 1997; Zito *et al.*, 1999). Under conditions of over reduction of the PQ pool (due to over-excitation of PSII or to non-photochemical reduction by the NAD(P)H dehydrogenase NDA2), the kinase STT7 phosphorylates LHCII antennae proteins which then migrate to PSI leading to state 2 (Depege *et al.*, 2003). Under conditions where the PQ pool is oxidized, the STT7 kinase is inactivated and a constitutively active phosphatase dephosphorylates LHCII antennae proteins, which then migrate back to PSII, leading to state 1 (Shapiguzov *et al.*, 2010; Pribil *et al.*, 2010). Rintamäki *et al.* (2000) showed that STT7 activation is not only under control of the PQ pool redox state but is also part of a complex network involving the thioredoxin/ferredoxin system.

It should be mentioned that all the PSII dissociated phospho-LHCII may

not bind to PSI. It has been shown that part of dissociated phospho-LHCII may aggregate and form an energy-dissipative complex (Ruban and Johnson, 2008; Tokutsu *et al.*, 2009). More recently, Unlu *et al.* (2014) suggested that, although LHCs indeed detach from photosystem II in state 2 conditions, only a fraction attaches to photosystem I. However, the existence of a LHCII energy dissipative complex is in contradiction with results of Delosme *et al.* (1996) who showed a complementary change in LHCII association with PSI and PSII upon state transition. The experimental evidences and the arguments in favor or against a complementary change in PSI and PSII optical cross-sections during state transitions are discussed in the annex.

In addition (and in relation) to their function in regulating the distribution of antenna pigment-proteins between PSI and PSII, state transitions have long been thought to control the relative electron fluxes through linear and cyclic electron transports (Finazzi *et al.*, 1999; Wollman, 2001). However, the implication of state transitions in CEF regulation is still a matter of debate (Alric, 2010; Lucker and Kramer, 2013).

Photoinhibition: lowered PSII activity under intense stress

Under intense and maintained high-light stress, when the usual photoprotective responses cannot compensate for the excess light energy, a photoinactivation of PSII is observed. This process, known as photoinhibition (qI), is the consequence of the photodestruction of the D1 polypeptide in the PSII. In contrast to PSII, PSI seems to be more efficiently protected from (or less sensitive to) photoinhibition as it was shown that PSI photoinhibition occurs only under specific conditions in some photosynthetic microorganism (Sonoike, 2011).

PSII photodamage occurs in fact continuously in photosynthetic organism. To prevent the accumulation of photodamaged PSII, photosynthetic organisms have developed a repair process involving (1) a highly regulated reversible phosphorylation of several PSII core subunits, (2) migration of the PSII core from the grana to the stroma lamellae, (3) proteolysis of the damaged proteins, and finally (4) replacement of the damaged proteins followed by (5) the reassembly and the photoactivation of the PSII complexe (Aro *et al.*, 1993; Aro, 2004). Photoinhibition is thus the result of an imbalance between the rate of photodamage of PSII and the rate of its repair.

It was previously thought that excess light energy was responsible for photodamage to PSII by a mechanism implicating an over-reduction of Q_A leading to its dissociation from the PSII followed by an accumulation of $TyrZ^+$, Chl^+ and $P680^+$ and finally to the degradation of D1 (Prasil *et al.*, 1992). However, more recent studies showed that neither impairing CO_2 fixation or inducing environmental stress accelerate PSII photodamages. In

contrast, it inhibited the repair mechanism. This suggests that photoinhibition is the result of suppression of the repair mechanism rather than an increase of photodamage (Nishiyama *et al.*, 2005; Nishiyama *et al.*, 2006; Murata *et al.*, 2007).

Cyclic electron transport

In addition to the linear transport of electrons from water to ferredoxin, there is a cyclic electron transport (CEF) around the PSI and cyt b_6f leading to the synthesis of ATP only. Depending on the pathway of PQ reduction, two routes for CEF can be distinguished: the NAD(P)H-dehydrogenase (NDA2)-dependent pathway and the ferredoxin-dependent pathway (dashed lines in fig 1.6). It is not clear if Fd reduces PQ via the cyt b_6f or via an unknown ferredoxin:PQ oxidoreductase (FQR) (Arnon *et al.*, 1967; Arnon and Chain, 1975; Joliot and Joliot, 2002). This cyclic electron transport permits the synthesis of extra ATP by the generation of a trans-thylakoidal electrochemical gradient in the absence of net production of reducing equivalents, thus allowing an increase of the ATP/NADPH ratio during the light phase of photosynthesis. It has been calculated that the CEF flow rate would have to be in the range of 6 to 16% of the LEF flow rate to supplement the ATP synthesis needed by the Calvin cycle under non-limiting CO_2 (Alric, 2010).

The existence of a functional supercomplex facilitating Fd-dependent CEF has been described in *Arabidopsis thaliana* (DalCorso *et al.*, 2008). This supercomplex would favour CEF by compartmentalizing the electron carriers and the components needed for CEF. It would be composed of the cyt b_6f, the PSI, the FNR and the proteins PGR5 (Proton Gradient Regulation 5) and PGRL1 (Proton Gradient Regulation Like 1). In *Chlamydomonas reinhardtii*, PGRL1 involvement in CEF has been demonstrated (Tolleter *et al.*, 2011) while the presence or absence of PGR5 is still under debate (Johnson *et al.*, 2014; Iwai *et al.*, 2010). The functional mechanism of this supercomplex is still unclear. Recently, PGRL1 has been proposed to be the unknown FQR in *A. thaliana* (Hertle *et al.*, 2013).

Cyclic electron transport has long been thought to be regulated by state transitions and has been shown to be particularly active in state 2 (Finazzi *et al.*, 1999; Finazzi *et al.*, 2002; Cardol *et al.*, 2003; Finazzi and Forti, 2004; Finazzi, 2005). However, this view has been recently challenged (Alric, 2010; Lucker and Kramer, 2013; Strand *et al.*, 2013; Alric, 2014; Johnson *et al.*, 2014). For the latter authors, CEF would be essentially regulated by the redox status of the electrons carriers PQ and $NADP^+$ independently of state transitions. If the pool of PQH_2 and PC is fully oxidized, CEF would be impaired due to the lack of reductants. On the other hand, if the pool of

NADPH is fully reduced, CEF would again be impaired, due to the lack of electron acceptors. It has been proposed that CEF is maximal when the PQ pool is half reduced (Allen, 2003).

CEF was shown to be implicated in high-energy state quenching qE by increasing the ΔpH across the thylakoid membrane (Munekage *et al.*, 2004). In this respect, NPQ was shown to be severely decreased in the *pgrl1* mutant in *Chlamydomonas reinhardtii* (Tolleter *et al.*, 2011).

The Mehler reaction

The Mehler reaction was first described by Mehler (1951) based on the observation that isolated thylakoids were able to reduce O_2. Later, PSI was identified as an efficient photoreducing site of O_2 (Asada *et al.*, 1974). Two molecular pathways have since then been identified for O_2 reduction at the PSI reducing side (fig 1.6):

1. O_2 can be reduced directly at the level of PSI either by ferredoxin (Furbank and Badger, 1983) or by the Fe/S center F_X in the PSI complex (Asada, 1999). This pathway defines the Mehler reaction *stricto sensu* and leads to the generation of superoxide ion $O_2^{\bullet -}$ which is dismutated in H_2O_2 by the superoxide dismutase. H_2O_2 is then reduced into water by the ascorbate peroxidase (Asada, 1999). This series of reactions, when they follow water oxidation by PSII, are classically referred to as the Water-to-Water Cycle (WWC) associated to the Mehler reaction.

2. O_2 could also be reduced by NAD(P)H in a reaction catalyzed by flavodiiron proteins (Flv) in the chloroplasts. In cyanobacteria, flavodiiron proteins have been shown to be involved in O_2 reduction in what is often called a Mehler-like reaction (Helman *et al.*, 2003). Two Flv clusters have been identified: FlvA and FlvB. FlvA proteins would be involved in O_2 photoreduction (Helman *et al.*, 2003) while FlvB proteins would be involved in PSII photoprotection (Zhang *et al.*, 2009). Because of the significant sequence conservation with their cyanobacterial counterparts, it has been proposed that Flv proteins of eukaryote microalgae could catalyse the Mehler-like reaction in these organisms (Peltier *et al.*, 2010). Flv proteins catalyse O_2 reduction to water, therefore the Flv-mediated Mehler-like reaction would operate without ROS production (Vicente *et al.*, 2002; Helman *et al.*, 2003).

The occurrence, relative rate and physiological functions of O_2-dependent electron flow through the Mehler reaction *in vivo* are matters of debate

(Badger *et al.*, 2000). In *Symbiodinium*, it was shown that a significant light-dependent O_2 uptake occurs mainly through a Mehler or Mehler-like reaction (Roberty *et al.*, 2014). In *Chlamydomonas reinhardtii*, a Mehler-type O_2 uptake has been evidenced during the induction of photosynthesis (Franck and Houyoux, 2008). Its relative rate during steady-state photosynthesis is, however, controversial. Indeed, conflicting views have been expressed on the amplitude of Mehler-type O_2 uptake in steady-state regimes (Sueltemeyer *et al.*, 1986; Sültemeyer *et al.*, 1993; Peltier and Thibault, 1985).

The function of this O_2-dependent electron flux is not clear. It could be a way to dissipate excess reducing power in DIC-limited condition in order to prevent photoinhibition and ROS production. It could also be a way to meet the additional ATP metabolic requirement for instance by the CCM to concentrate CO_2 when its availability is restricted. Indeed, this alternative electron flow generates ATP without producing NADPH and can then be used to adjust the ATP/NAD(P)H balance in the chloroplast.

Chlororespiration

Thirty years ago, Bennoun (1982) first suggested that a chloroplast-localized respiratory chain, or chlororespiration, occurs in green microalgae such as *Chlamydomonas reinhardtii* and *Chlorella vulgaris*. This pathway oxidizes NAD(P)H to reduce the PQ pool which is then oxidized at the expense of O_2. In *Chlamydomonas reinhardtii*, the enzyme mainly responsible for the oxidation of NAD(P)H was found to be the type II NADPH-dehydrogenase NDA2 (Jans *et al.*, 2008) while the protein responsible for the oxidation of the PQ pool and the reduction of O_2 to H_2O was found to be a plastid-terminal oxidase (PTOX). Two genes encoding for the oxidase have been found in the *Chlamydomonas* genome: *ptox1* and *ptox2*. PTOX2 is the most predominantly involved in chlororespiration in this algal species (Houille-Vernes *et al.*, 2011a). Observations based on immunoblots on fractionated chloroplasts indicate that PTOX would be located on the stromal side of the thylakoid membrane (Lennon *et al.*, 2003). Because NDA2 is non-electrogenic and that the protons resulting from the oxidation of PQH_2 are directly consumed by PTOX to reduce O_2, chlororespiration is thought to be non-electrogenic.

Two major roles have been ascribed to the PTOX pathway:

1. PTOX is often described as an electron safety valve preventing over-reduction of the PQ pool and protecting the photosynthetic apparatus from photodamage under excess light exposure (Niyogi, 2000). However, this has been questioned because of the low abundance of PTOX in photosynthetic membranes of higher plant plastids (Lennon *et al.*, 2003)

and the limited contribution of the chlororespiratory electron flux to the total electron flow under optimal growth conditions in spinach thylakoids (Feild *et al.*, 1998). Nevertheless, PTOX has been shown to play an important photoprotection role under specific severe stresses such as low temperatures and high salinity conditions (McDonald *et al.*, 2011). Interestingly, in a deep/low-light adapted strain of the green microalgae *Ostreococcus*, the PSI content is greatly reduced compared to a surface/high-light adapted strain and half of the chloroplastic electron flux has been shown to be rerouted to PTOX (Cardol *et al.*, 2008). PTOX has also been shown to play an important photoprotective role in condition of iron limitation when PSI content is low in the cyanobacteria *Synechococcus* (Bailey *et al.*, 2008).

2. In higher plants, PTOX plays a role in carotenoid biosynthesis. Plants lacking PTOX activity, such as the *immutans* mutants of *Arabidopsis thaliana*, accumulate large amounts of phytoene, an intermediate of xantophyll carotenoids. The enzyme which oxidized phytoene requires oxidized PQ and it has been proposed that PTOX would be responsible for oxidizing PQ and making it available for the phytoene desaturase (Wu *et al.*, 1999; Carol *et al.*, 1999).

Chloroplast-mitochondria interactions

Chloroplasts and mitochondria are usually considered to be semi-autonomous organelles but they are tightly linked. It is obvious that mitochondrial respiration depends on carbon substrates but the opposite is also true, mitochondrial metabolism is essential for sustaining photosynthetic carbon assimilation. Indeed, the mitochondria are involved in different processes linked to photosynthesis such as: (1) The recycling of phosphoglycolate produced by photorespiration (Moroney *et al.*, 2013). (2) The oxidation of NAD(P)H in order to produce ATP and balance the ATP/NADPH ratio to meet the Calvin cycle needs. In this respect, state 2 transition, thought to be involved in increased ATP production by promoting CEF, has been shown to be promoted in mutants affected in respiration, thus indicating that mitochondrial respiration is effectively involved in ATP synthesis in the light (Bulté *et al.*, 1990; Cardol *et al.*, 2003; Cardol *et al.*, 2009). (3) The protection against photoinhibition by oxidizing excess reductants under excessive illumination and/or in condition of reduced CO_2 availability (Saradadevi and Raghavendra, 1992).

The cooperation between mitochondria and chloroplast relies on the exchange of metabolites such as ATP, NAD(P)H and carbon compounds. Several transport systems have been identified such as the malate/oxaloacetate

shuttle, the malate/aspartate shuttle or the DHAP/3-PGA shuttle (for an extensive review, see Hoefnagel *et al.*, 1998).

The tight coupling between mitochondria and chloroplast has been widely used to study state transitions. Indeed, inhibition of mitochondrial respiration leads to a depletion of ATP which leads to an increased glycolytic production of reductants, a phenomenon known as the *Pasteur effect* (Bulté *et al.*, 1990). The resulting accumulation of reductants promotes a non-photochemical reduction of the PQ pool by NADPH, which results in a transition to state 2.

1.6 *In vivo* monitoring of the photosynthetic apparatus

Several technical approaches have been developed to measure the performances of a photosynthetic sample such as the chlorophyll fluorescence measurements, the oxygen evolution measurements, the photoacoustic and the absorption spectroscopy. In this study, we performed chlorophyll fluorescence and oxygen evolution measurements. These methods are described below.

1.6.1 Chlorophyll fluorescence measurements

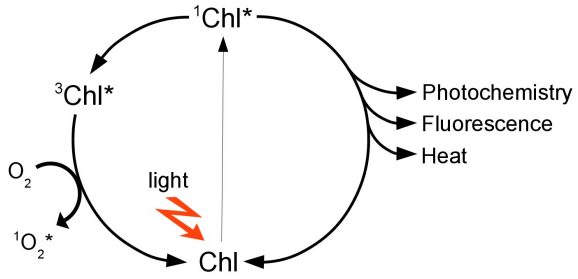

Figure 1.9: The absorption of light results in the excitation of a chlorophyll molecule to the singlet state ^{1}Chl*. ^{1}Chl* can loose its energy and return to the ground singlet state via four pathways: (1) By driving photosynthesis. (2) By dissipating its energy as heat in the PSII antennas. (3) By fluorescence emission. (4) Or by decay via the triplet state ^{3}Chl*, which in turn is able to interact with oxygen to produce $^1O_2$*, a very reactive oxygen species.

The absorption of light results in the excitation of chlorophyll molecules to the singlet excited state ^{1}Chl*. ^{1}Chl* can return to the ground singlet state via four pathways (fig 1.9) :

1. By transferring the 'excited' electron to an acceptor, thereby performing a charge separation to drive photosynthesis.

2. By dissipating as heat the energy difference between the excited and ground state.

3. By emitting a light quantum (fluorescence).

4. It can decay via the triplet state ^{3}Chl*, which in turn can decay to the ground singlet state. ^{3}Chl* is also able to interact with oxygen $^3O_2$ to produce $^1O_2$*, a very reactive oxygen species. However, this pathway seems to occur at low yield *in vivo* and is usually neglected (Vander-Meulen and Govindjee, 1973).

These processes occur in competition, such that any increase in the efficiency of one will result in a decrease in the yield of the others. Hence, by measuring the yield of chlorophyll fluorescence, informations about changes in the efficiency of photochemistry and heat dissipation can be gained.

Changes in the chlorophyll fluorescence yield were first described by Kautsky and Hirsch (1931). They showed that there was a transient increase followed by a slight decrease in fluorescence when transferring photosynthetic material from darkness to light. This was later explained by the Q (quencher) hypothesis (Duysens and Sweers, 1963b), that states that an electron acceptor in PSII, noted Q, acts as a chlorophyll fluorescence quencher when it is in the oxidized state. Q was later identified as the primary, bound plastoquinone electron acceptor Q_A located in the PSII reaction center. The rapid and transient increase of PSII fluorescence yield upon sudden transfer from dark to light is explained as reflecting the transient block in photochemistry that parallels Q_A reduction when the electron transport chain is transiently saturated. During this time, the reaction center of PSII is said to be closed. It is thus possible to obtain informations on the redox state of the electron transport chain by measuring the fluorescence emitted by PSII.

Nowadays, chlorophyll fluorescence has become one of the most common technique used to assess the photochemistry of photosynthetic organisms due to its non-invasiveness, sensitivity and to the wide availability of measuring instruments (Masojídek *et al.*, 2010). Several technical approaches have been developed to measure the PSII chlorophyll fluorescence emission. Among them, the measurerements of the fast chlorophyll *a* fluorescence transient (OJIP) and the PAM fluorimetry are the most frequently used.

Fast chlorophyll *a* fluorescence transient (OJIP)

All oxygenic photosynthetic organisms adapted to darkness and exposed to light show a rapid rise in fluorescence from a F_O level to a F_M level which

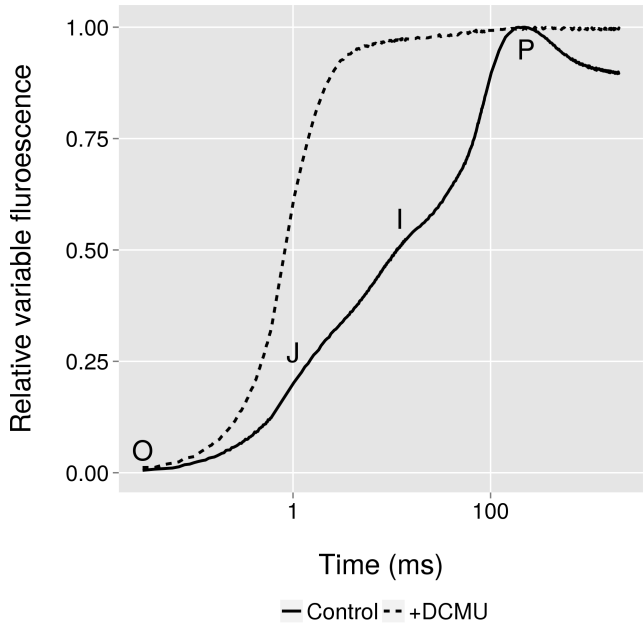

Figure 1.10: Fast chlorophyll *a* fluorescence transient of a *Chlamydomonas reinhardtii* suspension in absence (control) or in presence of DCMU 20µM (+DCMU). These transients are presented on a logarithmic time-axis and were double normalised between F_O and F_M.

corresponds to the reduction of Q_A in the reaction center of PSII (fig 1.10). This rapid increase in fluorescence is not linear but can be divided into several phases. To discern these phases, the measuring device must possess certain characteristics (Lazár, 2006):

1. The intensity of the exciting light must be very high: approximately 3,000 µmol PAR.m^{-2}.s^{-1}.

2. This maximum intensity has to be reached very quickly (short ignition time in the µs range).

3. The time resolution of the fluorescence detector must be very good given the speed of the observed process.

Delosme (1967) studied this phenomenon on a *Chlorella* suspension by using a .22 long rifle pointing on a metal plate between a xenon lamp and a sample. This allowed a sudden and homogeneous illumination of the sample when the bullet hit the metal plate. He showed the existence of two phases:

1. A photochemical phase whose the fluorescence yield at time t is determined by the number of photons absorbed by the system.

2. A thermal phase whose the fluorescence yield depends not only on the number of absorbed photons but is strongly influenced by temperature.

Since then, more detailed studies showed that there were in fact two inflection points during the fluorescence rise (Neubauer and Schreiber, 1987). Strasser *et al.* (1995) used fluorimeters equipped with LED light sources and proposed the OJIP nomenclature (fig 1.10):

1. The OJ phase (1-2 ms) corresponds to the partial reduction of Q_A in the PSII reaction centers and is called the photochemical phase. The initial slope and the relative amplitude of this phase depend on the intensity of the exciting light.

2. The JI and IP phases are thermal phases associated with the re-oxidation of Q_A^- by the PQ pool, which slows down Q_A^- accumulation and therefore the fluorescence rise.

There were several proposals to explain the well-defined biphasicity of the thermal part of the rise (reviewed in Stirbet and Govindjee, 2012). Briefly, these include the influence of electron transport towards PSI on the rise kinetics, a specific correlation between the IP phase and the disappearance of a secondary quencher or the establishment of a trans-thylakoidal electrochemical gradient, or a relationship between the two phases and two distinct PSII populations. The case is not settled at present.

DCMU is often used to isolate the photochemical phase of the fast chlorophyll *a* fluorescence transient (fig 1.10). This inhibitor binds the Q_B pocket of PSII and permits the photochemical reduction of the primary quinone Q_A without influence of its reoxidation by plastoquinones.

Modulated fluorescence (PAM)

The study of the photosynthetic apparatus using fluorimetry boomed in the eighties when Quick and Horton (1984) used a modulated measurement system. In this type of system, the light used for measuring the fluorescence is modulated (switched on and off at high frequency) and the detector is configured to detect only the modulated fluorescence emitted in response to the modulated light. This allows to measure the fluorescence yield in the presence of additional continuous lighting required for the purposes of the experiment. Without this system, the fluorescence intensity would be

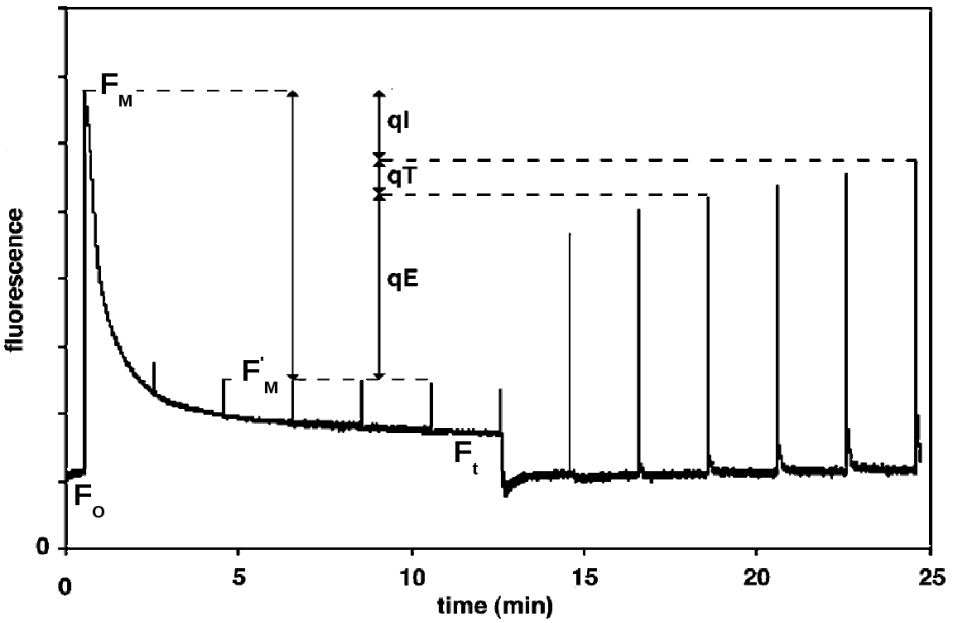

Figure 1.11: Typical chlorophyll fluorescence measurement with a PAM fluorimeter. In the presence of only weak measuring light, the minimal fluorescence (F_O) is seen. When a saturating continuous actinic light is given, the photosynthetic light reactions are saturated and fluorescence reaches a maximum level F_M (in general, when the actinic light in not saturating, a saturating light pulse is given before illumination to obtain F_M). Upon continuous illumination with actinic light, the maximal fluorescence level (F'_M) decreases due to the development of NPQ and the steady-state fluorescence (F_t) increases due to the saturation of the electron transport chain leading to PSII closure. After switching off the light, the different relaxation kinetics of F_M reflects the relaxation of the three components of NPQ: qE, qT and qI. Diagram modified from Muller *et al.*, 2001.

directly affected by the different excitation lights and it would be impossible to determine the variations of the fluorescence yield.

In order to obtain informations on photosynthetic performances of a sample, it is necessary to distinguish the extinction of fluorescence due to the photochemistry (called 'photochemical quenching' qP) from other process that also affect the fluorescence yield, namely 'non-photochemical quenching' (NPQ). For this, it is possible to remove the photochemical quenching qP using the technique of the saturating pulse. In this approach, a short high intensity flash (1s) is given, which leads to the temporarily closure of all PSII reaction centers and to the transient suppression of qP. This gives the

maximum level of fluorescence in the absence of photochemistry: F'_M.

Figure 1.11 shows the data obtained for a typical PAM fluorimetry experiment. Several parameters have been developed to calculate the photosynthetic performances of a sample.

Maximal photochemical efficiency of PSII (F_V/F_M) is a parameter that characterizes the proportion of absorbed light quanta which can be used by PSII to drive charge separations:

$$\frac{F_V}{F_M} = \Phi PSII_{dark} = \frac{F_M - F_O}{F_M} \tag{1.1}$$

where F_M is the maximal fluorescence level obtained by applying a saturating pulse and F_O is the minimal fluorescence level in darkness. This parameter is determined after dark-adaptation and its optimal value is about 0.7-0.8, meaning that in optimal conditions, about 70 to 80% of the absorbed light quanta are used for photochemistry while the rest is wasted as heat or fluorescence.

Another useful parameter is the PSII operating photochemical efficiency (ΦPSII) which is determined in the same way as F_V/F_M except that it is measured under actinic light, usually at steady-state:

$$\Phi PSII = \frac{F'_M - F_t}{F'_M} \tag{1.2}$$

where F'_M is the maximal fluorescence level obtained by applying a saturating pulse under a particular actinic light intensity and F_t is the steady-state fluorescence level. While F_V/F_M is a measure of the maximal photochemical capacity of PSII, ΦPSII is a measure of the actual photochemical capacity of PSII when photosynthesis is active. This means that any stress affecting a component of the photosynthetic apparatus will be reflected by a decreased ΦPSII.

Finally, non-photochemical quenching (NPQ) is a third parameter which is often calculated to determine if photoprotective mechanisms are activated to deal with excessive absorbed light energy. NPQ is reflected as a general decrease of the fluorescence level and it is calculated as:

$$NPQ = \frac{F_M - F'_M}{F'_M} \tag{1.3}$$

NPQ is composed of three components: high-energy state quenching quenching qE, which reflects an increased heat dissipation in the antennas, state transition qT which reflects a dissociation of light-harvesting complexes from PSII and photoinhibition qI, which reflects photodamage to PSII. These different components have different relaxation times ranging from a

few seconds (qE) to several minutes (qT and qI) and thus, the kinetics of relaxation of these different processes can be used to distinguish them. It is noteworthy that the expression 1.3 generally used for NPQ quantitation reflects the idea that NPQ would follow a Stern-Volmer principle, for which NPQ would be proportional to the concentration of a hypothetic quencher. Although this may apply to qE, it is certainly not appropriate for qT or qI.

1.6.2 Polarographic measurement of oxygen evolution

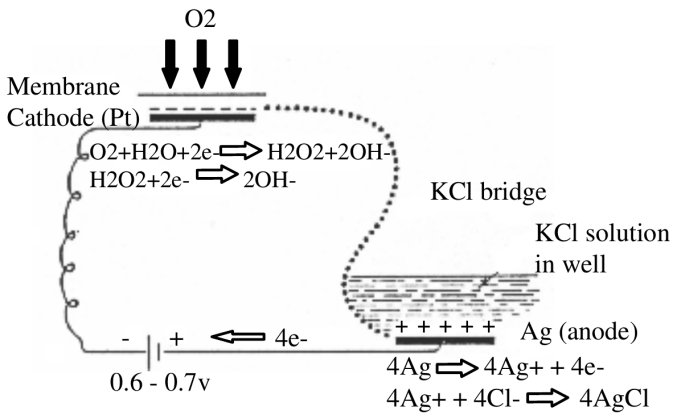

Figure 1.12: Representation of oxygen electrode reactions: when a potentiating voltage is applied across the two electrodes, the platinum (Pt) becomes negative (i.e. becomes the cathode), and the silver (Ag) becomes positive (the anode). Oxygen diffuses through the membrane and is reduced at the cathode surface so that a current flows through the circuit (which is completed by a thin layer of KCl solution as electrolyte). The silver is oxidized and silver chloride deposited on the anode. The current which is generated bears a direct, stoichiometric, relationship to the oxygen reduced. From Walker and Walker, 1987.

Most of the methods used to measure photosynthetic oxygen emission in living algae are based on amperometric detection, using most generally a platinum electrode negatively polarized with respect to a reference electrode (Joliot *et al.*, 2004). In the Clark electrode (Clark Jr, 1956), a thin layer of Teflon permeable to oxygen protects the platinum electrode from any contaminant present in the suspension (fig 1.12). The reduction of oxygen at the cathode produces a current which is used to determine the O_2 concentration in the cuvette. A photosynthetic sample can then be submitted to an illumination protocol in order to determine the O_2 evolution under illumination and the O_2 consumption under darkness. Two parameters are

usually used to characterise the photosynthetic O_2 evolution: (1) the net oxygen evolution (P_{net}) which is the result between O_2 evolution at PSII and O_2 consumption processes, and (2) the gross oxygen evolution (P_{gross}) which represents the total O_2 evolution at PSII. Usually, when measuring O_2 evolution with a Clark electrode, P_{gross} is calculated as $P_{gross} = P_{net} - R_{dark}$, where R_{dark} is the respiration measured in the dark. This means that some O_2 consuming processes occurring in the light (photorespiration, Mehler and PTOX-dependent O_2 uptake) are still included in P_{gross}.

1.7 Objectives of this thesis

Recently, there has been an increased interest in microalgae. Firstly, they are responsible for about 50% of primary production (Field *et al.*, 1998) and for this reason, they are carefully studied by ecologists. Secondly, microalgae can also produce a great variety of molecules for the industry. This includes food and feed, nutraceutical and cosmetic products. The main advantages of microalgae on higher plants are: (1) A higher production yield per hectare. (2) A possible culture in inhospitable places such as deserts with a low requirement in water resources. Indeed, microalgae culture can be carried out in saline or seawater on non-arable lands. (3) A great metabolic flexibility, which offers the possibility to modify their biochemical pathways and cellular compositions by varying the culture conditions.

However, currently, microalgae mass culture production yields remain lower than the yields estimated from the maximum photosynthetic efficiency. Several explanations can be advanced in order to explain poor algal productivity yields with respect to the potential maximum. First, the local light intensities in the different layers of the culture suspensions are rarely optimal (Grobbelaar, 2010). Furthermore, different stresses affecting photosynthesis can occur. In order to optimize production yields, it is essential to analyze the functioning of the photosynthetic apparatus under different culture conditions. On the ecophysiological level, a good understanding of the photosynthesis of microalgae from different habitats is also desired. The main objectives of this thesis were:

1. To develop methods which allow effective use of fluorescence and oxygen experimental signals for a more complete analysis of the functioning of the photosynthetic apparatus of green microalgae under different conditions.

2. To apply these methods to analyze the adaptations of the photosynthetic apparatus under selected conditions, especially regarding CO_2 supply.

The results of this thesis are divided into three chapters:

Chapter 2: From photons to photochemistry The initial goal of this study was to apply a fluorescence based method for determining the PSII antenna size by analyzing the kinetics of the fast chlorophyll *a* fluorescence transient in presence of DCMU (or DCMU-Fluorescence Rise). A more detailed analysis of the different phases of this rise associated with different types of PSII (PSII heterogeneity) in *Chlamydomonas reinhardtii* allowed us to show that state transitions can be explained by an inter-conversion of two types of PSII formerly described as PSIIα and PSIIβ.

Chapter 3: From photochemistry to CO_2 fixation In this work, we studied the photosynthetic adaptations of laboratory grown *Chlamydomonas reinhardtii* under high and low CO_2 conditions. We developed a method to quantify the alternative electron transport to O_2, based on simultaneous measurements of oxygen evolution and fluorescence. We showed that this alternative, Mehler-type electron transport represented a substantial part of total linear electron transport in cells exposed to CO_2 limitations but not in CO_2 replete cells. PAM fluorimetry indicated that the PSII photochemical yield was reduced in the low CO_2 condition and that more absorbed energy was dissipated as heat in this condition than in high CO_2 condition. Surprisingly, low temperature fluorescence spectra and DCMU-FR measurements showed that the PSII antenna size was reduced in high CO_2 cells when compared to low CO_2 cells.

Chapter 4: From CO_2 to biomass In the last chapter, two outdoor open thin-layer cascade systems operated as batch cultures with the alga *Scenedesmus obliquus* were used to compare the productivity in control and CO_2 supplemented cultures in relation with the outdoor light irradiance. We found that the culture productivity was strongly limited by CO_2 availability. The methods developed in previous chapters were then applied to study the photosynthetic adaptations in both cultures. We found that ETR and oxygen evolution light saturation curves, as well as light-dependent O_2 uptake were similar in algal samples from both cultures when the CO_2 limitation was removed. We also found a decreased PSII photochemical efficiency and increased capacity for light-induced heat-dissipation in the control culture compared to the CO_2 supplemented culture.

Chapter 2

From photons to photochemistry : fluorescence study on the remodelling of PSII during state transitions

Contents

2.1 Introduction 50
2.2 Material and methods 54
2.3 Results and discussion 56
2.3.1 Rate constant dependence on light intensity . . . 59
2.3.2 The optical cross-section, as determined by the half-time of the fluorescence rise, is proportional to the proportion of PSIIα 62
2.3.3 Development of a protocol to determine PSII antenna size heterogeneity during state transition . 64
2.3.4 Transition to state 2 from state 1 is reflected in conversion of PSIIα and PSIIβ 66
2.4 Conclusion 69
2.5 Supplemental data 70

Analysis of PSII antenna size heterogeneity of *Chlamydomonas reinhardtii* during state transitions

Thomas de Marchin[a], Bart Ghysels[a], Samuel Nicolay[b] and Fabrice Franck[a]

[a]Laboratory of Bioenergetics, B22, University of Liège, B-4000 Liège/Sart-Tilman, Belgium
[b]Department of Mathematics, B37, University of Liège, B-4000 Liège/Sart-Tilman, Belgium

Accepted for publication in *Biochimica et Biophysica Acta (BBA) - Bioenergetics*, July 18, 2013. The original publication is available at http://www.sciencedirect.com/science/article/pii/S0005272813001266

PSII antenna size heterogeneity has been intensively studied in the past. Based on DCMU fluorescence rise kinetics, multiple types of photosystems with different properties were described. However, due to the complexity of fluorescence signal analysis, multiple questions remain unanswered. The number of different types of PSII is still debated as well as their degree of connectivity. In *Chlamydomonas reinhardtii* we found that PSIIα possesses a high degree of connectivity and an antenna 2-3 times larger than PSIIβ, as described previously. We also found some connectivity for PSIIβ in contrast with the majority of previous studies. This is in agreement with biochemical studies which describe PSII mega-, super- and core- complexes in *Chlamydomonas*. In these studies, the smallest unit of PSII *in vivo* would be a dimer of two core complexes hence allowing connectivity. We discuss the possible relationships between PSIIα and PSIIβ and the PSII mega-, super- and core- complexes. We also showed that strain and medium dependent variations in the half-time of the fluorescence rise can be explained by variations in the proportions of PSIIα and PSIIβ. When analyzing the state transition process in vivo, we found that this process induces an interconversion of PSIIα and PSIIβ. During a transition from state 2 to state 1, DCMU fluorescence rise kinetics are satisfactorily fitted by considering two PSII populations with constant kinetic parameters. We discuss our findings about PSII heterogeneity during state transitions in relation with recent results on the remodelling of the pigment-protein PSII architecture during this process.

2.1 Introduction

Photosynthesis is the process by which light energy is converted into chemical energy (ATP and NAD(P)H) usable for the synthesis of organic compounds. The first step of this process is the absorption of light by antenna pigments of PSI and PSII. Excitation energy is then transferred to reaction centers of the photosystems where photochemistry drives a flow of electrons and protons across the thylakoïd membrane, which permits the synthesis of ATP and NAD(P)H. The antenna of PSI is enriched in chlorophyll *a* and absorbs to longer wavelength than PSII which is enriched in chlorophyll *b*. Due to this, photosystems can be excited differently depending of the excitation light quality and this can lead to an imbalance of the electron transport chain. In order to correct this imbalance, LHCII antenna complexes can migrate between PSI and PSII and make their cross-section to vary, thus restoring the excitation balance. This phenomenon, termed 'state transitions' has been discovered independently by Bonaventura and Myers (1969) and by Murata (1969).

State transitions have been extensively studied in *Chlamydomonas reinhardtii* because in this organism, up to 80% of the LHCII can migrate between the photosystems (Delosme *et al.*, 1996), against about 20-25% for higher plants. In *Chlamydomonas*, like in other studied organisms, the redox state of the plastoquinone (PQ) pool is the main determinant of state transitions through binding of plastoquinol to the Q_o site of Cyt b_6f (Vener *et al.*, 1997; Zito *et al.*, 1999). Under conditions of over reduction of the PQ pool (due to over-excitation of PSII or to non-photochemical reduction by the NAD(P)H dehydrogenase NDA2), the kinase STT7 phosphorylates LHCII which then migrates to PSI (state 2) (Depege *et al.*, 2003). Under conditions where the PQ pool is oxidized, STT7 kinase is inactivated and a constitutively active phosphatase dephosphorylates LHCII antenna which then migrates to PSII (state 1) (Shapiguzov *et al.*, 2010; Pribil *et al.*, 2010). Rintamäki *et al.* (2000) showed that STT7 activation is not only under control of the PQ pool redox state but is also part of a complex network involving the thioredoxin/ferredoxin system.

In addition (and in relation) to their function in regulating the distribution of antenna pigment-proteins between PSI and PSII, state transitions can also control the relative electron fluxes through linear and cyclic electron transports (Finazzi *et al.*, 1999; Wollman, 2001). For cyclic electron transport to occur, it is admitted that ferredoxin reduced by PSI can reduce the PQ pool via the cyt b_6f, via an unknown ferredoxin:PQ oxidoreductase or via NAD(P)H thanks to NDA2 (Arnon *et al.*, 1967; Arnon and Chain, 1975; Joliot and Joliot, 2002). Cyclic electron transport is favoured over linear electron transport in state 2, which permits the synthesis of extra

ATP by the generation of a trans-thylakoidal electrochemical gradient in the absence of net production of reducing equivalents. Thus, regulation of cyclic electron transport by state transitions allows the cell to regulate the ratio of ATP to NADPH produced during the light-phase of photosynthesis.

It is well known that PSI and PSII are not homogeneously dispersed in the thylakoïd membrane. PSII is located mainly in the grana (appressed membrane region) but a small part is present in the stroma exposed (non-appressed) membrane region while PSI is strictly present in the latter (Anderson and Melis, 1983; Vallon *et al.*, 1986). In addition to these heterogeneities, structural and functional heterogeneity has also been shown for different PSII sub-populations. PSII heterogeneity was first described by Melis and Homann (1975) based on previous observations that the fluorescence rise of dark-adapted chloroplast did not follow a first order reaction kinetics (Joliot and Joliot, 1964; Doschek and Kok, 1972). Melis and Homann (1975) concluded to the existence of two PSII populations, namely the PSIIα and the PSIIβ (Melis and Homann, 1975; Melis and Homann, 1976). This was inferred from the analysis of the semilogarithmic plot of the kinetics of the complementary area (CA) above the fluorescence rise curve in presence of the inhibitor DCMU. This inhibitor binds the pocket Q_B of PSII and permits the photochemical reduction of the primary quinone Q_A without influence of its reoxidation by plastoquinones. Previous works showed (Murata *et al.*, 1966; Bennoun and Li, 1973; Malkin and Kok, 1966) that the complementary area over the fluorescence rise curve (area between the fluorescence curve and a horizontal line at the maximal fluorescence level F_M) in presence of DCMU is proportional to the number of photosystems able to realize reduction of Q_A. Melis and Homann (1975) found two phases in the time-dependent increase of the CA and ascribed them to the two populations of PSII. Since then, many studies have been conducted on this subject and a third phase has been discovered: phase γ (Hsu and Lee, 1991; Hsu *et al.*, 1989).

Phase α is ascribed to a sub-population of dimeric PSII localized in the appressed membrane region of the thylakoid (Melis and Anderson, 1983). They are characterized by an antenna of 210-250 chlorophylls (Melis and Anderson, 1983) and connectivity (p). This term was proposed by Joliot and Joliot (1964) and is related to the transfer of absorbed energy from a closed reaction center (in which Q_A is already reduced) to an open neighboring unit. Connectivity is reflected by a sigmoidal fluorescence rise. Phase β is ascribed to a population of monomeric PSII localized in the non-appressed membrane region of the thylakoid. They are characterized by an antenna 2 to 3 times smaller than PSIIα ($\backsim$130 Chl) and do not possess connectivity, which is reflected as an exponential fluorescence rise. The last γ phase is characterized by a rate 10 to 40 times slower than phase α but it seems

that, in contrast to the two previous phases, it is not directly related to photoreduction of Q_A. Indeed, the rate constant of this γ phase behaves in a non-linear way towards light intensity (Lazár *et al.*, 2001). The existence of four phases has been suggested (Sinclair and Spence, 1990) but most studies report only three phases (see Lavergne and Briantais, 2004 for a review).

It is most often considered that the increase in fluorescence intensity during the DCMU-FR is essentially due to Q_A reduction, following the original theory of Duysens and Sweers (1963a), but other theories with different explanations for the slow phases of the DCMU-FR have emerged (reviewed in in Stirbet *et al.*, 2012) such as fluorescence yield variations due to conformational changes (Moise and Moya, 2004a; Moise and Moya, 2004b; Schansker *et al.*, 2011). Even if the different phases in the DCMU-FR are interpreted as reflecting different Q_A reduction kinetics, antenna size heterogeneity is not the only possible interpretation for these phases (other interpretations are reviewed in Lavergne and Briantais, 2004). Differences in trapping efficiency could also result in the appearance of several phases. For example, a lower photochemical quantum yield for PSIIβ versus PSIIα would lead to an overestimation of the proportion of PSIIβ with the analysis of the semilogarithmic plot of the kinetics of the CA above the fluorescence rise curve. The comparison of the PSIIβ and PSIIα quantum yields has been conducted in the past. Although lower quantum yield for PSII associated to the slow phase of the induction kinetics (usually ascribed to phase β) has been reported (Melis and Duysens, 1979; Doschek and Kok, 1972; Lavergne and Rappaport, 1998; Joliot and Joliot, 1977), other studies showed similar quantum yields for both types of PSII (Thielen and Gorkom, 1981; Roelofs *et al.*, 1992). It is clear that the case is not settled. In any case, even if a proportion of PSII had a lower quantum efficiency, the amplitude of this difference is too low to account entirely for the proportion of PSIIβ (Lavergne and Briantais, 2004). It was also suggested that the β phase was related to PSII being less sensitive to DCMU addition (Schreiber and Pfister, 1982), but this could be circumvented by using a sufficiently high DCMU concentration (20 µM) (Black *et al.*, 1986a). In any case, Melis and Duysens (1979) showed a very good correlation between the different phases in the absorbance changes at 320nm (reflecting Q_A reduction) and the different phases in DCMU-FR. Moreover, biochemical studies demonstrated the existence of multiple PSII complexes with different antenna sizes (see below) and it must necessarily be reflected in a multi-phasic character of the DCMU-FR.

It should also be mentioned that other type of PSII heterogeneities (not related to the sole photoreduction of Q_A in presence of DCMU) have been described such as PSII reducing side heterogeneity, which refers to the ability of a reaction center to transfer electron to the secondary acceptor Q_B

(Lavergne and Briantais, 2004). These will not be addressed here.

The proportions of PSIIα and PSIIβ are not fixed and vary with culture conditions as well as with sample preparation. It has been reported that protein phosphorylation of chloroplast membrane, that simulates state transition, leads to an increase in the amplitude of phase β whether by conversion of PSIIα into PSIIβ (Kyle *et al.*, 1982) or by preferential quenching of PSIIα (Horton and Black, 1981; Horton and Black, 1983). However, these studies, like most studies on PSII heterogeneity (with exception of the work of Lazár *et al.* (2001) and Nedbal *et al.* (1999)) were conducted on chloroplast preparations or isolated thylakoids. The method of isolation of these organelles and their resuspension in various media are likely to influence the properties of the photosynthetic apparatus and the relevance of the results to the *in vivo* situation can be questioned. Other factors influencing the proportion of PSIIα and PSIIβ have been described such as temperature (Mathur *et al.*, 2011; Bukhov and Carpentier, 2000), concentration in Mg^{2+} (Horton and Black, 1983) , pH (Melis and Homann, 1976) and greening time in the case of higher plants (Melis and Akoyunoglou, 1977; Barthélemy *et al.*, 1997).

In addition to this description of heterogeneity by functional analysis of the fluorescence rise of PSII *in vivo*, biochemical studies have been conducted more recently. Methods used were mainly based on isolation of PSII complexes and subsequent analysis. Most studies report the existence of PSII megacomplexes composed of a dimer of supercomplex C_2S_2 where C refer to the PSII core complex and S to the *strongly* bound LHCII trimer (one LHC trimer and two LHC monomer). Other complexes have been reported in spinach chloroplast such as the $C_2S_2M_2$ supercomplex where two *moderately* bound LCHII trimers and one monomer bind the C_2S_2 supercomplex (Boekema *et al.*, 2000). A third type of L (for *loosely* bound) LHC trimer may bind the supercomplex but the resulting complex would be rare (Kouřil *et al.*, 2012). In *Chlamydomonas reinhardtii*, the largest supercomplex detected is C_2S_2, probably due to the lack of CP24 (Nield *et al.*, 2004), which is needed to bind M trimers.

A stepwise mechanistic model has been proposed for LHCII dissociation from PSII and reassociation with PSI after phosphorylation by the STT7 kinase during state transitions in *Chlamydomonas* (Iwai *et al.*, 2008; Minagawa, 2011b). Initially, cells are in state 1 and unphosphorylated LHCII stabilize the PSII–LHCII megacomplex. First, the phosphorylation of LHCII type I in the major LHCII trimers triggers the dissociation of the megacomplex, resulting in individual C_2S_2 supercomplexes. Secondly, the increase in the phosphorylation of CP26 and CP29, as well as the PSII core subunits D2 and CP43 (although the role of the latter remains unclear), induces the displacement of remaining LHCII from the PSII core complex, resulting in discrete C_2 core complex. Finally, a part of dissociated phospho-LHCII migrates

from the PSII-rich appressed region membrane to the PSI-rich non-appressed region membrane and associates with PSI (Kyle *et al.*, 1983; Black *et al.*, 1986b; Larsson *et al.*, 1983; Takahashi *et al.*, 2006), leading to state 2 while the other part may aggregate to form an energy-dissipative complex (Ruban and Johnson, 2008; Tokutsu *et al.*, 2009). Nevertheless, the existence of a LHCII energy dissipative complex is in contradiction with results of Delosme *et al.* (1996) who showed a complementary change in LHCII association with PSI and PSII upon state transition. Recent results in *Arabidopsis thaliana* suggest that in addition to the control of LHC phosphorylation by STN7 kinase, the association/dissociation of supercomplexes is under the control of a new parallel but independent regulatory pathway involving Psb27 and PsbW proteins (García-Cerdán *et al.*, 2011; Dietzel *et al.*, 2011).

The structural PSII heterogeneity, and the complexity of the rearrangement of pigment-protein complexes during state transitions, outlined above, are likely to have their counterpart in terms of changes in functional antenna size during state transitions. However, an in situ analysis of functional PSII heterogeneity from the fluorescence rise curve in presence of DCMU has not been performed. Here, we analyze PSII heterogeneity related to DCMU-FR in *Chlamydomonas reinhardtii* cells, we show how this heterogeneity is affected during state transitions and discuss the results in terms of changes in antenna size heterogeneity.

2.2 Material and methods

Strains and Growth Conditions The *Chlamydomonas reinhardtii* wild-type strain *1690* used in this work was obtained from the *Chlamydomonas Resource Center*. The mutant *stt7* unable to realize state transitions was obtained from J.-D. Rochaix (Fleischmann *et al.*, 1999). Cells were grown at 25° C in Tris-acetate-phosphate medium (Gorman and Levine, 1965) under 80 µmol PAR $m^{-2}.s^{-1}$ continuous white light and regularly diluted to ensure that cells were in exponential phase. In section 2.3.2, other wild-type strain were used, such as strain *25* (derived from the CC-400 cw15 (Davies and Plaskitt, 1971)) and strain *2'* (derived from the *wt* strain 137c (Harris, 1989)). In that section, cells were grown in Tris-acetate-phosphate medium and in Tris-buffered mineral media.

Chlorophyll concentration determination Pigments were extracted from whole cells in ethanol and debris were removed by centrifugation at 10,000g for 5 min. The Chl (a + b) concentration was determined according to Lichtenthaler (1987) with a lambda 20 UV/Vis spectrophotometer (Perkin Elmer, Norwalk, CT).

Chlorophyll fluorescence measurement Chlorophyll fluorescence emission measurements were made using a PAM (pulse amplitude modulated) chlorophyll fluorimeter (type FMS 1, Hansatech instruments, UK). Prior to each measurement, cultures were dark-adapted for 30 minutes. The analytical light was provided by light-emitting diodes with an emission maximum at 594 nm. The frequency of measuring flashes was 1500 per second and their integral light intensity was less than 0.1 µmol PAR $m^{-2}.s^{-1}$. F_M level was obtained by applying a pulse of saturating light (6000 µmol PAR $m^{-2}.s^{-1}$) provided by a halogen light source. Measurements of chlorophyll fluorescence rise curve in presence of 20µM DCMU were made in cell suspensions (2 ml) using a AquaPen AP-C 100 fluorimeter (PSI, Czech Republic). The maximal intensity (100%) was 1670 µmol PAR $m^{-2}.s^{-1}$ at 455 nm. Chlorophyll concentration was adjusted to 10 $\mu g.ml^{-1}$ for PAM measurements and to 1 $\mu g.ml^{-1}$ for chlorophyll fluorescence rise curve measurements.

Low temperature fluorescence spectra Fluorescence emission spectra at 77K were recorded using a LS 50B spectrofluorimeter (Perkin Elmer). The excitation wavelength was 440 nm. Excitation and emission spectral width slits were 10 and 5 nm, respectively. A broad blue filter (CS-4-96, Corning, Corning, NY) was placed between the excitation window and the sample to minimize stray light. Cells were frozen in liquid nitrogen. Chlorophyll concentration was lower than 2 $\mu g.ml^{-1}$, and it was verified that no changes in the intensity ratio of the 685 and 715 nm emission bands arose from reabsorption artefacts. Spectra were normalized to a fluorescence intensity of 1 at 685 nm.

Curve fitting Fitting of the fluorescence rise in presence of DCMU was realized with the R package *nls* and the *port* algorithm. R is an open-source statistical software freely available under GNU license (Team, 2011). *Nls* package allows the simultaneous direct fitting of several curves of the DCMU-FR, which permits an increase in the reliability and accuracy in the determination of the model parameters (Lazár *et al.*, 2001). It also gives the possibility to control which parameter is allowed to vary between curves and which cannot, depending of the experimental design (see Pinheiro *et al.* (2011) for a good manual on *nls*). The principle of non-linear regression is to minimize the square of the distance between experimental data and a theoretical curve (χ^2) by testing multiple combinations of parameters. The parameters giving the minimal χ^2 are then choosen for subsequent analysis. Comparison of the quality of fit by different models was realized using the R function *AIC*. When specified, the error range was determined using the R function *confint.nls*. This function calculates the χ^2 subsequent to a stepwise

change of each parameter and determines if the new χ^2 is significantly worse than the χ^2 determined by the best fitting. This gives a confidence interval. The confidence level was set to 90%. For more information on error range determination, see Johnson and Faunt (1992) and Roelofs *et al.* (1992).

2.3 Results and discussion

Different approaches have been proposed for the determination of PSII antenna heterogeneity from the fluorescence rise in presence of DCMU (DCMU-FR). The original procedure of Melis and Homann (1975) is based on deconvoluting the time-course of the complementary area (CA) over the fluorescence rise curve. This approach suffers from two main problems. First, it requires a very accurate determination of the maximum level of fluorescence F_M. This can be difficult since small distortions of the signal not attributable to photochemistry occur, such as caused by non-photochemical quenching (NPQ) and technical limitations of experimental apparatus. Bell and Hipkins (1985) showed that an error of 2% in F_M determination leads to an error of 150% in the amplitudes and rates of different photosystems. Secondly, the determination of the contributions of the different phases starts by calculating the rate and amplitude of the slowest phase and subtracting it from the kinetics of the whole complementary area. This operation is repeated from the slowest phase to the last fastest phase. This implies that any small error in the determination of the first slow phase (the most inaccurate) affects the calculation of the next phases. Moreover, as discussed before, the slowest phase (γ) is not related to the photoreduction of Q_A and for this reason, determination of its kinetics and extent by the time course of the CA is not relevant.

In 1995, Lavergne and Trissl (1995) and Trissl and Lavergne (1995) introduced a new method of determination of PSII heterogeneity based on direct fitting of the time course of the fluorescence rise. This method is more accurate than the Melis and Homann (1976)'s original approach because mistakes due to an erroneous determination of F_M are avoided. Lazár *et al.* (2001) used this approach to determine PSII antenna heterogeneity of PSII on wheat leaves and *Chlamydomonas reinhardtii* cells. The novelty of their study was in the simultaneous direct fitting of several curves of the DCMU-FR at different light intensities. This increases the reliability and accuracy of the determination of the model parameters.

In the presence of DCMU, the fluorescence rise (DCMU-FR) can be fitted with the equation :

$$rF_V(t) = \sum_{i=1}^{3} F\mathrm{PSII}_i \frac{(1-p_i)\mathrm{PSII}_i^{closed}(t)}{1-p_i\mathrm{PSII}_i^{closed}(t)} \tag{2.1}$$

where $rF_V(t)$ is the normalized rise of fluorescence intensity, $F\mathrm{PSII}_i$ is the proportion of variable fluorescence associated to PSII of type i, p_i is the connectivity parameter described by Joliot and Joliot (1964), t is the time and $\mathrm{PSII}_{\mathrm{i}}^{\mathrm{closed}}(t)$ is the proportion of closed PSII of type i at time t. This last term is described by the equation

$$\mathrm{PSII}_i^{closed}(t) = \mathrm{PSII}_{i,0}^{open}(1-e^{(-k_i t)}) \tag{2.2}$$

where $\mathrm{PSII}_{i,0}^{open}$ is the proportion of open PSII of type i at time 0 (which is 1 in case of dark adapted material) and k_i is the rate constant of reduction of the PSII. These equations, derived from Lazár *et al.* (2001), allows a good fit of the DCMU-FR.

In theory, k_i is not a constant but varies with time due to excitation energy transfer between closed and open PSII. As the time increases, the increase in the proportion of closed PSII leads to an increase in the effective antenna size of open PSII. Thus, k_i(t) vary according to :

$$\mathrm{k}_i(t) = \frac{\mathrm{k}_i^0}{1-p_i\mathrm{PSII}_i^{closed}(t)} \tag{2.3}$$

where k_i^0 is the initial rate constant when all PSII are open. However, there is no explicit solution to these 3 equations (see supplemental data), thus preventing the use of non-linear regression algorithm. To circumvent this problem, we could use an iterative process to fit our data (as used in Lazár *et al.*, 2001). The problem with such process is that it is difficult to know if the algorithm has converged to a suitable solution. In order to be able to use a regression algorithm, we considered k_i as a constant, characterizing the kinetics of a whole phase (thus, in our case, such a value k_i cannot be interpreted as a quantification of the initial rate constant k_i^0).

It is important to note that the proportion of fluorescence $F\mathrm{PSII}_i$ associated to each photosystem type represents the proportion of chlorophylls associated with each type of photosystem and is not a quantification of the proportion of each type of photosystem, due to their differences in antenna size. The proportion of photosystems $\omega\mathrm{PSII}_i$ can only be calculated from their contributions to the complementary area over the fluorescence rise curve (CA) (Murata *et al.*, 1966; Malkin and Kok, 1966). The proportion CA_i of the CA that corresponds to PSII_i has been calculated from the fluorescence rise associated to each PSII type. This is mathematically calculated after the regression procedure giving the p_i, k_i and $F\mathrm{PSII}_i$ parameters.

Most earlier fluorescence studies report the existence of three PSII types: PSIIα, PSIIβ and PSIIγ in which only PSIIα are able to share excitation energy (connectivity) between individuals units (Lavergne and Briantais, 2004). Is is tempting to ascribe the PSII mega-,super- and core- complexes described in most recent biochemical studies to the PSIIα, PSIIβ and PSIIγ. However, in earlier functional studies, the ability to share excitation energy between individuals units was restricted only to PSIIα while new biochemical evidences suggest a dimeric organization, and therefore the possibility for energy transfer between neighbouring units for all PSII complexes. There is, therefore, a need of comparing the suitability of models, which consider a connectivity term (p) either for PSIIα only, for PSIIα and PSIIβ or for all PSII types.

In order to decide which model is best adapted, we fitted DCMU-FR curves measured at different light intensities (same data as section 2.3.1) with the three models. In model 1, connectivity was allowed only for PSIIα. In model 2, it was allowed for PSIIα and PSIIβ whereas in model 3, it was allowed for all type of PSII. Usually, the quality of a fit is determined on the value of the χ^2. The lower it is, the higher is the efficiency of the fit to describe the experimental data. However, comparing quality of models with different number of variables (in our case, more parameters due to connectivity for PSIIβ and PSIIγ) with the χ^2 is not appropriate because adding variables increases the complexity of the model and the number of solutions possible for the fit. It will always be possible to add artificial, non-biologically meaning parameters and increase the quality of the fit. Thus, to avoid overfitting, it is necessary to take into account the complexity of the model in the assessment of the quality of the fit. The *Akaike's information criterion* (AIC) permits the comparison of different models with different number of variables by judging the quality of the fit and introducing a penalty for the number of parameters used (Akaike, 1974). AIC was determined according to equation 2.4 where k is the number of parameters and L is the maximized value of the likelihood function for the estimated model. For more information on AIC, see Burnham and Anderson (2002).

$$\mathrm{AIC} = 2k - 2\ln(L) \tag{2.4}$$

AIC for the three models is shown in table 2.1. The AIC of model 2 is lower than that of model 1 and model 3, which is an indication that model 2 describes the experimental data better than other models. Moreover, the difference between the two best models AIC_{model3} - AIC_{model2} is 18. Considering the rule of thumb given in Burnham and Anderson (2002), which requires a difference in AIC of more than 10 to definitely choose one model over another model, we decided to make the subsequent fitting of DCMU-FR

curve with model 2. Residuals of the fit for the three models are shown in figure 2.5. In contrast to what was described in most previous studies, we had to conclude that PSIIβ are characterized by a non 0 connectivity (only the two former studies of Lavergne and Trissl (1995) and Lazár *et al.* (2001) came to the same conclusion).

model	AIC	Δ_i
1: connectivity allowed only for PSIIα	-14599	2416
2: connectivity allowed for PSIIα and PSIIβ	-17025	0
3: connectivity allowed for PSIIα, PSIIβ and PSIIγ	-17007	18

Table 2.1: Determination of the best model to analyse PSII antenna size heterogeneity by calculating the AIC on the entire data set of section 2.3.1. In model 1, connectivity was allowed only for PSIIα. In model 2, it was allowed for PSIIα and PSIIβ whereas in model 3, it was allowed for all type of PSII. Δ_i represents the AIC differences : Δ_i = AIC$_i$ - AIC$_{min}$. Model 2 has been selected because it had the lower AIC value.

2.3.1 Rate constant dependence on light intensity

We began our analysis by comparing fluorescence rise curves in presence of DCMU at different light intensities. The purpose of such a procedure is to verify the photochemical character of the different phases. This also helped us to validate our method by comparing our results with those of Lazár *et al.* (2001). Due to the complexity and to the high number of parameters in equation 2.1, multiple possibilities exist for fitting the experimental data although they do not always have a biological sense. We thus forced the fitting program to find common values for some parameters. In this case, connectivity and proportion of each type of photosystems had to remain unaltered between individuals sample. This makes sense since the only difference between samples is the intensity of illumination. Thus, the only parameter which may change are the rate constants of Q_A reduction k_i.

Figure 2.1A shows the DCMU-FR measured at different light intensities and the corresponding fits. The curves are plotted from time 0 to the time when rF_V reaches 1. Figure 2.1B shows the effect of light intensity on the rate constant values k for each type of photosystem. We see that for PSIIα and PSIIβ, the value is linearly correlated to the intensity of illumination, which confirms the photochemical character of the fluorescence rise for these two PSII types. This is not the case for PSIIγ (or γ phase) for which a different pattern is observed (Fig. 2.1B, inset). Therefore, the γ phase seems influenced by other factors than the absorption of light. This phase did

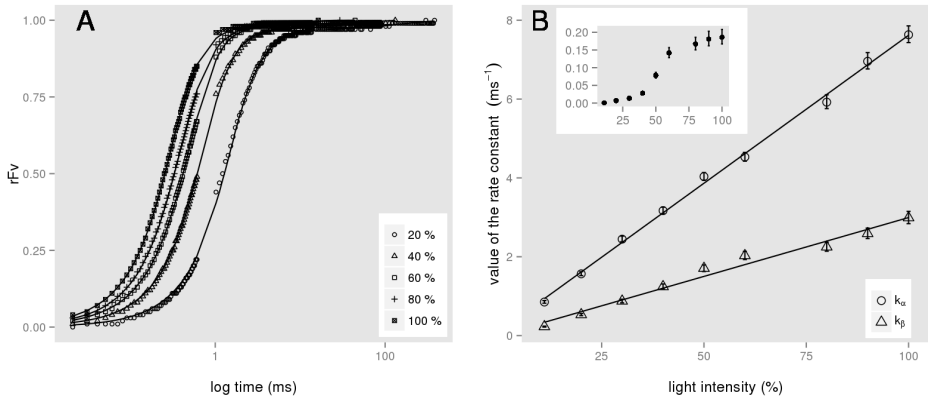

Figure 2.1: A: Time course of the DCMU-FR measured at different light intensities on the *wt* strain *1690* grown on Tris-buffered mineral media. Only 5 intensities are shown for clarity. 100 % = 1670 µmol PAR $m^{-2}.s^{-1}$. Experimental curves and fits are shown as dots and full lines, respectively. B: value of the rate constant of photochemistry of PSIIα and PSIIβ plotted against the intensity of illumination. Inset shows the rate constant of photochemistry of PSIIγ. The errors bars were calculated according to section 2.2. Data are representative of one experiment out of at least three independent determinations.

not represente more than 4% of the variable fluorescence intensity (results not shown) while it represented a fraction of the CA that varied with light intensity. For this reason, determination of the kinetics and extent of this phase by the time course of the CA is considered not relevant. Thus in the subsequent analysis, phase γ was mathematically removed from the results to avoid any error in the determination of the proportion and kinetics of PSIIα and PSIIβ by the method of the CA.

Proportions, rate constants of photoreduction and connectivity of the three types of photosystem are detailed in table 2.2.

If one admits that the rate constant of a phase of the DCMU-FR curve reflects the size of the light-harvesting antenna associated with the corresponding type of PSII, it is possible to calculate the ratio $\frac{\mathrm{Chl}_{\mathrm{PSII}\alpha}}{\mathrm{Chl}_{\mathrm{PSII}\beta}}$ which is determined from the ratio of $\frac{\mathrm{k}_\alpha}{\mathrm{k}_\beta}$ in most studies. However, the rate constant as determined in this study represents the kinetics of a whole phase and not the initial rate constant k_i^0 (see above). It is thus influenced not only by the antenna size but also by the connectivity. A better approach to calculate the ratio $\frac{\mathrm{Chl}_{\mathrm{PSII}\alpha}}{\mathrm{Chl}_{\mathrm{PSII}\beta}}$ is based on the proportion of each type of photosystems ($\omega\mathrm{PSII}_i$) and the proportion of chlorophyll fluorescence associated to them

type	%	k (s^{-1})	p
PSIIα	52	46.6 ± 1.4	0.75
PSIIβ	48	17.4 ± 2.4	0.58

Table 2.2: Proportion (%), rate constant of Q_A photoreduction (k) and connectivity (p) of each type of photosystem determined by fitting model 2 on FR-DCMU curves of the *wt* strain *1690* measured at different light intensities. Rate constant was determined by averaging individual rate constants for particular light intensities recalculated for an intensity of illumination of 10 µmol PAR $m^{-2}.s^{-1}$ in order to allow an easy comparison with previous studies (see Table 2 from Lazár *et al.* (2001)).

($F\mathrm{PSII}_i$) following equation 2.5 :

$$\frac{\mathrm{Chl}_{\mathrm{PSII}\alpha}}{\mathrm{Chl}_{\mathrm{PSII}\beta}} = \frac{\mathrm{FPSII}_\alpha/\omega\mathrm{PSII}_\alpha}{\mathrm{FPSII}_\beta/\omega\mathrm{PSII}_\beta} \tag{2.5}$$

The average ratio $\frac{\mathrm{Chl}_{\mathrm{PSII}\alpha}}{\mathrm{Chl}_{\mathrm{PSII}\beta}}$ determined here by this approach was 2.14 ± 0.39. This would mean that the PSIIα antenna is about 2-3 times larger than PSIIβ antenna if the pigments of both PSII types were equally excited. The excitation wavelength in this study (430 nm) however preferentially excites Chl *a*, which would tend to an overestimation of PSIIβ antenna size and proportion if the Chl a/b ratio is higher for PSIIβ. In earlier studies ratios between 1,65 and 8 were obtained (see Table 2 from Lazár *et al.*, 2001). Such variations are probably caused by the different species and preparations studied.

The question arises whether the PSII heterogeneity evidenced here can be explained in terms of structural differences between the PSII populations that were previously separated using gel filtration (Iwai *et al.*, 2008; Minagawa, 2011b). Only two functional populations of PSII are predicted by DCMU-FR analysis (PSIIα and PSIIβ) while gel filtration analysis predicts three different PSII populations (mega-, super- and core- complexes). Iwai *et al.* (2008) performed functional optical cross-section analysis on PSII fractions obtained by gel filtration separation. Fractions composed mainly of PSII mega- and super- complexes had a similar optical cross section in contrast to the fraction composed mainly of PSII core complexes for which it was approximately two times lower. This indicates that PSII mega- and super-complexes are hardly distinguishable by functional analysis of the DCMU-FR since PSII antenna size heterogeneity determination cannot discriminate two PSII populations with the same antenna size. It could be argued that although the antenna size of PSII mega- and super- complexes is the same, the connectivity may change. However, the accuracy for the decomposition

of induction kinetics is not sufficient to reliably resolve them on this basis. Taking into account that the reduction rate constant found in this study for PSIIα is 2-3 times higher than for PSIIβ, it is tempting to conclude that PSIIα phase refers to PSII mega- and super- complexes and that PSIIβ phase refers to PSII core complexes.

2.3.2 The optical cross-section, as determined by the half-time of the fluorescence rise, is proportional to the proportion of PSIIα

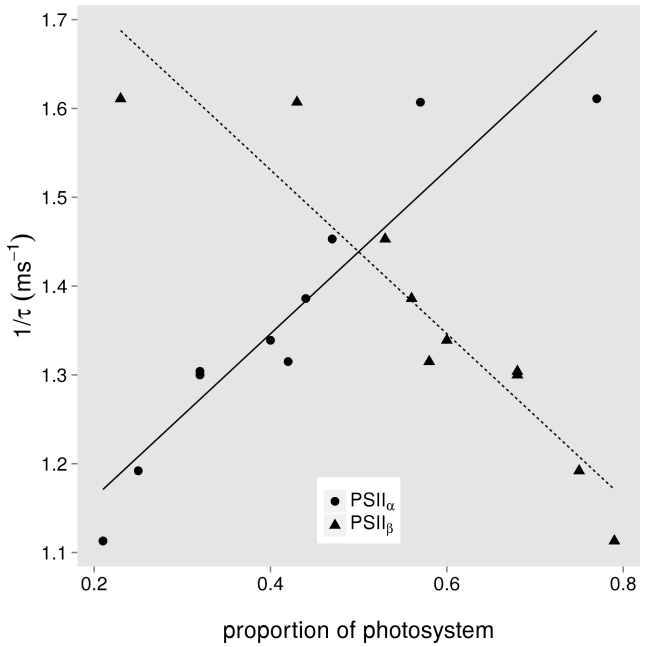

Figure 2.2: Correlation between $\frac{1}{\tau}$ and the proportions of PSIIα and PSIIβ. τ is the time when the normalized variable fluorescence level reaches 0.5. R^2 for linear regression was 0.8 for both types of photosystem. The different *wt* strains (2', 1690, 25) were grown in different media (Tris-buffered acetate or mineral media).

To have an idea of the variations in the proportions of different PSII types in *Chlamydomonas reinhardtii*, we applied our analysis to several DCMU-FR of suspensions of different *wt* strains (2', 1690, 25) grown in different media (TAP, TMP, Bold) after dark-adaptation. We noticed large variations between samples. In other words, the proportions of PSIIα and PSIIβ vary extensively for dark-adapted cells.

We took advantage of these variations in order to investigate the relationship between the proportions of different PSII types and the half-time of the whole fluorescence rise, a parameter that is frequently used to characterize the PSII average optical cross-section (Lavaud *et al.*, 2002; Havaux and Tardy, 1999; Cadoret *et al.*, 2004; Dall'Osto *et al.*, 2006). It is indeed possible to characterize the rate of the fluorescence rise by determining the half-time τ of the fluorescence increase as the time when the normalised variable fluorescence level reaches 0.5.

Figure 2.2 shows a positive and negative correlations between $\frac{1}{\tau}$ and the variable proportions of PSIIα and PSIIβ, respectively. In other words, the cell seems to adapt its ability to harvest light at PSII by converting fast PSIIα into slow PSIIβ and inversely. From these results, it appears that dark adaptation (usually used as standard condition) does not necessarily conduct to cells which are in the same state. It is known that growth condition can influence the amount of PSII-free and PSII-bound LHCII (Anderson, 1986), thus modifying the ratio between different PSII types. This result could also explain the large variation in the determination of PSII heterogeneity observed in previous studies (see table 2 from Lazár *et al.*, 2001) where amounts of PSIIα and PSIIβ ranged from 13.5% to 76% and from 9% to 40%, respectively.

type	k (s^{-1})	p
PSIIα	72.4 ± 9.9	0.89 ± 0.07
PSIIβ	14.1 ± 3.8	0.11 ± 0.21

Table 2.3: Summary of connectivity and rate constant of PSIIα and PSIIβ. Values are averages of the samples used in figure 2.2. Values of rate constant are recalculated for an intensity of illumination of 10 µmol PAR $m^{-2}.s^{-1}$ to allow an easy comparison with previous studies. Error ranges represent standard deviations.

Average values for rate constants of photoreduction (k) and connectivities (p) of PSIIα and PSIIβ are given in table 2.3. Values of k are in accordance with section 2.3.1 and previous studies (see Table 2 from Lazár *et al.*, 2001). A non-zero connectivity term for PSIIβ is found again, although its value is here quite variable and lower compared to its value in section 2.3.1. The p value for PSIIα is higher than in section 2.3.1 and may be overestimated. Indeed, according to Lavergne and Trissl (1995), it is possible to calculate the antenna size enhancement for open PSII surrounded by closed ones as J+1, where $J = p/(1-p)$, which makes J very sensitive to small errors in p determination. For a p value of 0.89, this antenna size enhancement

would be around 9, which would indicate a connectivity between several super/mega complexes. Commonly found p values around 0.7 give an antenna size enhancement of 3.3. Here, p values of 0.75 (section 2.3.1) and 0.62 (see below, section 2.3.4) lead to antenna size enhancements of 4.0 and 2.63, respectively, which do not require connectivity between super/mega complexes. More data and higher reliability on p would be necessary to conclude on this issue.

The variations in PSII heterogeneity and in half-time of the fluorescence rise from one sample to another were most probably due to uncontrolled variations in the PQ pool redox state. Such variations are easily produced as consequences of changes in the medium composition of cultured cells (acetate concentration), or depending on the extent of aeration of the culture and dark-adaptation time before measurements. Therefore, changes in PSII optical cross-section from one sample to another were most probably due to changes in metabolic status of the cells and thus to changes in excitation energy distribution between PSII and PSI (state transitions). In the next sections, we investigated changes in PSII heterogeneity during experimentally controlled state transitions.

2.3.3 Development of a protocol to determine PSII antenna size heterogeneity during state transition

We then tried to determine the changes in PSII antenna size heterogeneity during state transitions. To trigger a transition from state 1 to state 2, we used the method described by Bulté *et al.* (1990), which consists of inhibiting mitochondrial respiration either by using inhibitors/uncouplers of respiration, or by anoxia. Impairment of mitochondrial respiration leads to a depletion of ATP and a non-photochemical reduction of the PQ pool by the NAD(P)H dehydrogenase NDA2, thus inducing a transition to state 2. State 1 (or a state close to it) is usually achieved first by dark-adapting well-aerated cells in order to oxidize the PQ pool (this is only valid for cells grown on mineral media).

To determine PSII heterogeneity, we performed measurements of the DCMU-FR on cells dark-adapted for 30 min (state 1) or cells in presence of mitochondrial inhibitors KCN (potassium cyanide) and SHAM (salicylhydroxamic acid) for 20 min (state 2). The fluorescence rise was first found faster in state 2 than in state 1 which is in contradiction with the common sense if PSII antenna size is smaller in state 2. The results were similar if mitochondrial respiration was impaired by the addition of the uncoupler FCCP or by an anoxia caused by the addition of glucose oxydase and glucose (results not shown). In state 2 condition, there was an increase and a decrease in F_O and F_M levels, respectively. The decrease of F_M is explained by the

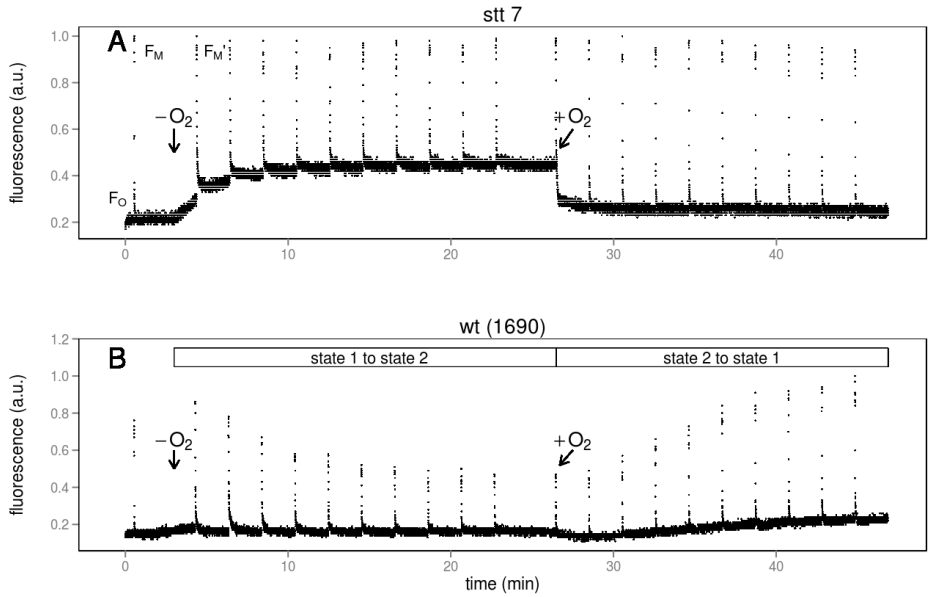

Figure 2.3: Determination of changes in the redox status of PQ pool and state transitions by PAM fluorimetry as described in section 2.2. A: state transition deficient mutant *stt7*. B: wild type strain *1690*. Strains were grown on Tris-buffered acetate media. O_2 is removed or added when indicated. Removal is realized by bubbling N_2 and closing the electrode chamber and addition is realized by opening the closed chamber and bubbling air. Data are representative of one experiment out of at least three independent determinations.

reduced PSII antenna size in state 2. The increase of F_O can be explained by the fact that binding of DCMU in the dark can induce a back transfer of electron from PSII-bound semiquinone Q_B^- to Q_A (Velthuys and Amesz, 1974; Bulté and Wollman, 1990). In the case when the PQ pool is highly reduced like in state 2 inducing conditions (due to a constant non-photochemical reduction) many PSII centers may have a Q_B^- bound and the addition of DCMU leads to Q_A reduction before the illumination. Therefore, in this situation, the fluorescence rise under illumination only represents a small pool of initially oxidized PSII.

In order to probe all the PSII pool in state 2, PQ pool had to be rapidly oxidized before the addition of DCMU. We thus used a different approach to reoxidize the PQ pool after reaching state 2. For this, instead of using respiration inhibitors to induce PQ reduction and state 2, we bubbled N_2 in

a closed electrode chamber of algal suspension and let the cells consume the remaining O_2 through respiration in order to cause anoxia and a transition to state 2. When state 2 was reached, opening of the electrode chamber and adding air led to the arrest of non-photochemical reduction and to re-oxidation of the PQ pool. This was confirmed by PAM fluorimetry measurements during the whole procedure (Fig. 2.3). The fluorescence level of PSII measured under low analytic modulated light is dependent on the redox state of Q_A in the reaction center of PSII and, indirectly, by the subsequent intermediates in the photosynthetic electron transport chain together with state transitions. In order to monitor the redox state of Q_A without the influence of state transitions, we first performed experiments with the mutant strain *stt7* which lacks the ability to realize state transition. Figure 2.3A shows the PAM fluorescence trace of the *stt7* strain. Removal of oxygen induces a rapid increase of F_O which reflects the non-photochemical reduction of PQ pool. Then, addition of oxygen (air) induces a fast decrease of F_O which reflects the re-oxidation of PQ pool, thus confirming that PQ pool can be oxidized almost instantly by O_2 most probably via the plastid terminal oxydaze (PTOX).

In contrast to the *stt7* strain, the increase of F_O after removal of oxygen in the *wt* strain *1690* (Fig 2.3B) is not so apparent because it is counterbalanced by a general fluorescence decrease due to detachment of LHCII from PSII (transition to state 2) as indicated by the decrease of maximum level F'_M. Addition of oxygen after transition to state 2 leads to a slight decrease of F_O which reflects PQ pool re-oxidation. This is followed by a transition back to state 1 as indicated by the increase of F'_M caused by the re-association of LHCII to PSII.

In both cases (*stt7* and *wt* strains), the re-oxidation of PQ pool by O_2 is realized in less than 2 minutes after its addition (as indicated by the duration of the decrease of F_O). Moreover, in the *wt* strain, F_M did not increase within this time, indicating that back transition to state 1 did not start yet (this is confirmed by the non-significant variation in the low temperature fluorescence ratio between 0 and 2 min after O_2 addition, see fig 2.4A). Therefore, PSII antenna heterogeneity analysis could be realized on samples taken from 2 min after the addition of O_2 (state 2) to the end of the transition to state 1.

2.3.4 Transition to state 2 from state 1 is reflected in conversion of PSIIα and PSIIβ

PSII antenna heterogeneity variations were determined on samples taken from 2 to 20 minutes after addition of O_2. First, it was verified that state transition was occurring in theses samples by measuring low temperature

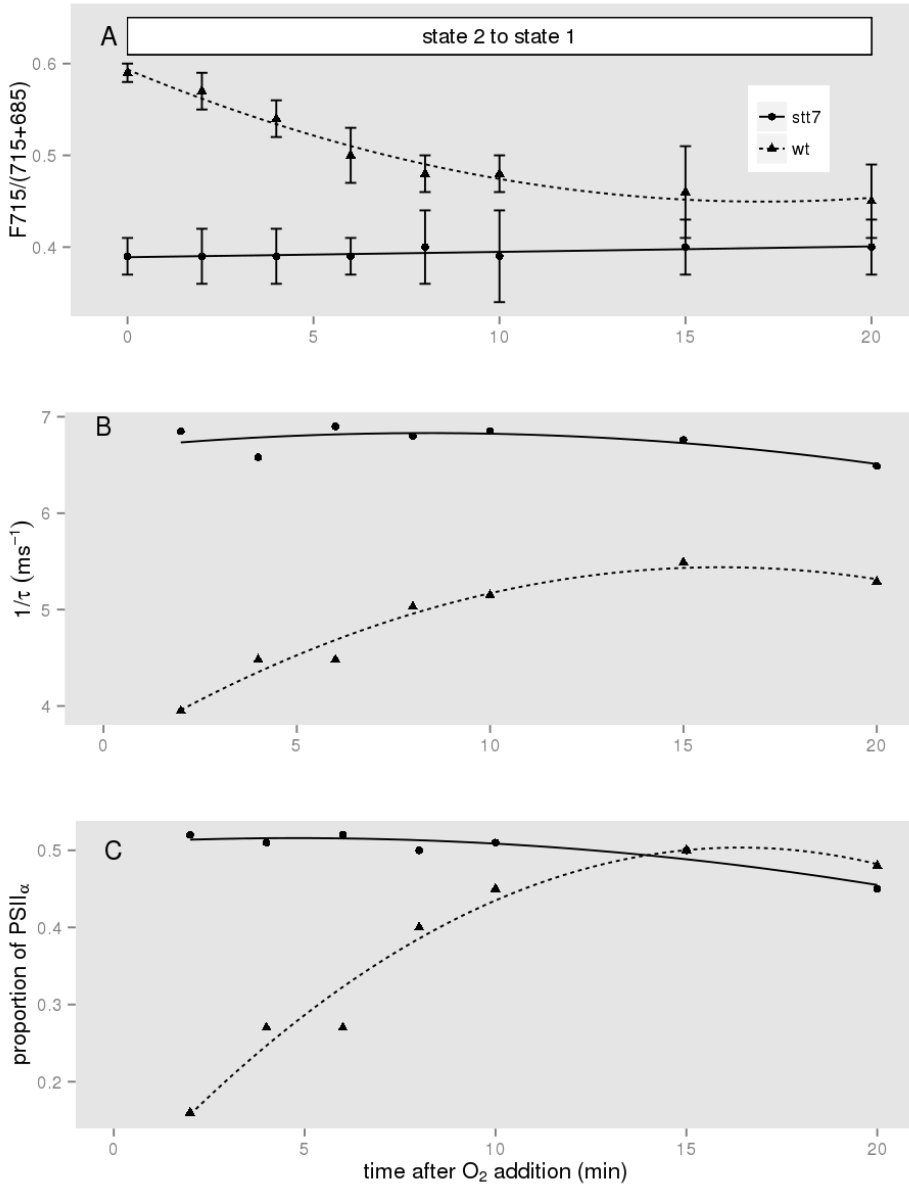

Figure 2.4: A: variation in the ratio of fluorescence emitted at 715 and 685 nm at 77K indicating a state transition from state 2 to state 1 in the *wt* strain but not in the *stt7* strain. Each value is the mean of 3 independent experiments. Error bars represent standard deviations. B: variation of $1/\tau$ indicating a decrease of the optical cross-section of PSII during transition from state 2 to state 1. C: Variations in proportions of PSIIα during transition from state 2 to state 1. DCMU-FR were measured at 100% of maximal light intensity. Strains were grown on Tris-buffered acetate media. For B and C, data are representative of one experiment out of at least three independent determinations.

(77K) fluorescence spectra. At this temperature, fluorescence emission by PSI and PSII can be distinguished. The 685 nm fluorescence is emitted by PSII while the 715 nm fluorescence is emitted by PSI. Variation of this ratio indicates variation in distribution of excitation energy between PSI and PSII. Figure 2.4A shows a decrease of the ratio F715/(715+685) from 2 minutes to 20 minutes after O_2 addition in the case of *wt* strain, indicating a transition from state 2 to state 1 (high and low values of F715/(715+685), respectively). In contrast, in the *stt7* strain, there is no significant variation of this ratio, as expected.

We then determined changes in proportions and properties of PSIIα and PSIIβ from DCMU-FR curves during the transition from state 2 to state 1. Since biochemical studies on PSII complexes indicate that state transitions are caused by changes in relative abundances in different PSII subpopulations (Iwai *et al.*, 2008; Minagawa, 2011b), we forced the fitting program to find common values for rate constants of photoreduction (k) and connectivity (p) for each PSII type during state transition. Fits and corresponding residuals for the *wt* strain 1690 in state 1 and in state 2 (corresponding to 2 and 20 min after O_2 addition, respectively) are shown in figure 2.6. Rate constants of photoreduction (k) and connectivities (p) of PSIIα and PSIIβ for the *wt* and *stt7* strains are detailed in table 2.4. Values of k and p are in accordance with previous section and previous studies (see Table 2 from Lazár *et al.*, 2001).

	p_α	p_β	k_α (s^{-1})	k_β (s^{-1})	$\frac{k_\alpha}{k_\beta}$
wt	0.62	0.15	48.6	15.4	3.1
stt7	0.64	0.16	64	19	3.3

Table 2.4: Summary of connectivity and rate constant of PSIIα and PSIIβ. Values are averages of the 7 samples used in figure 2.4. Values of rate constant are recalculated for an intensity of illumination of 10 µmol PAR $m^{-2}.s^{-1}$ to allow an easy comparison with previous studies. Data are representative of one experiment out of at least three independent determinations.

Changes in proportions of PSIIα in the course of state transition are shown in figure 2.4C. In the *wt* strain, during transition from state 2 to state 1, about 32% of slow PSIIβ is converted into fast PSIIα with the same kinetics than the variation of the ratio F715/(715+685) and the half-time of the whole fluorescence rise. In contrast, no significant variation is observed in the state transition deficient strain *stt7*. These results show for the first time *in vivo* that state transition induces an inter-conversion of two types of photosystems.

This is in agreement with recent models based on biochemical and structural analysis of PSII after gel filtration separation which indicate a conversion of PSII mega- and super- complexes (that we suggest to be related to PSIIα) in PSII core complexes (that we suggest to be related to PSIIβ) during state transitions (Iwai *et al.*, 2008; Minagawa, 2011b). In contrast to the frequent implicit view that state 1 and state 2 are characterized by specific PSII states, it appears that the two PSII populations are present in both states but in different proportions.

2.4 Conclusion

In this study, we showed that variations in the optical cross-section of PSII (as indicated by half-time estimations of the DCMU-FR) can be described as changes in PSIIα/PSIIβ heterogeneity. Our results on PSII heterogeneity during a transition from state 2 to state 1 showed for the first time *in vivo* that this transition correlates with a conversion of PSIIβ to PSIIα. Considering our results and recent biochemical and structural researches on PSII, we suggest that in *Chlamydomonas reinhardtii* PSIIα refers to two PSII populations with the same antenna size and a high degree of connectivity, namely the PSII mega- and super- complexes whereas PSIIβ refers to a PSII population with a 2-3 times smaller antenna size and a reduced connectivity, namely the PSII core complexes. We think that the procedure of PSII antenna size heterogeneity determination described in this study could be useful to study PSII antenna size heterogeneity in other photosynthetic organisms as well as in antenna size mutants.

Acknowledgments

This study was supported by FP7-funded Sunbiopath project (GA 245070). Thomas de Marchin thanks the F.R.I.A. for the award of a fellowship. Fabrice Franck is senior research associate of the Fonds de la Recherche Scientifique F.R.S-FNRS. Many thanks are given to Dr F.A. Wollman, Dr P. Tocquin and Dr P. Cardol and the anonymous reviewers for their helpful suggestions during this work.

2.5 Supplemental data

There is no explicit solution to the equations (2.1), (2.2) and (2.3)

By re-writing equation (2.1), one can explicitly express PSII_i^{closed} as a function of $rF_{V,i}$ and p_i :

$$\mathrm{PSII}_i^{closed}(t) = \frac{rF_{V,i}(t)}{p_i rF_{V,i}(t) + 1 - p_i}. \tag{2.6}$$

Combined with equation (2.2), this equation leads to

$$e^{-k_i(t)t} = \frac{(1 - rF_{V,i}(t))(1 - p_i)}{1 - p_i(1 - rF_{V,i}(t))}. \tag{2.7}$$

One thus have,

$$\begin{aligned} k_i(t) = \frac{1}{t}\Big(& \ln\Big(1 - p_i(1 - rF_{V,i}(t))\Big) \\ & - \ln\big(1 - rF_{V,i}(t)\big) - \ln(1 - p_i)\Big). \end{aligned} \tag{2.8}$$

Finally, equation (2.3) implies

$$\begin{aligned} \mathrm{k}_i^0 \;=\; & \frac{1 - p_i}{t(p_i rF_{V,i}(t) + 1 - p_i)} \\ & \Big(\ln\big(1 - p_i(1 - rF_{V,i}(t))\big) \\ & - \ln\big(1 - rF_{V,i}(t)\big) - \ln(1 - p_i)\Big). \end{aligned} \tag{2.9}$$

This relation shows that k_i^0 depends on p_i and $rF_{V,i}$, both being unknown. Therefore k_i^0 cannot be determined using a non-linear regression algorithm simultaneously with other parameters of equations (2.1) and (2.2).

Residuals of the fit for model 1, 2 and 3

Figure 2.5 indicates that model 1 is worse than model 2 and model 3 in describing the experimental data. The residuals of model 2 and model 3 are identical because a 0 connectivity is found for γ phase in model 3. Thus, the fit is exactly the same for model 2 and model 3. The choice of model 2 by the AIC criterion is based on the reduced number of parameters in this model.

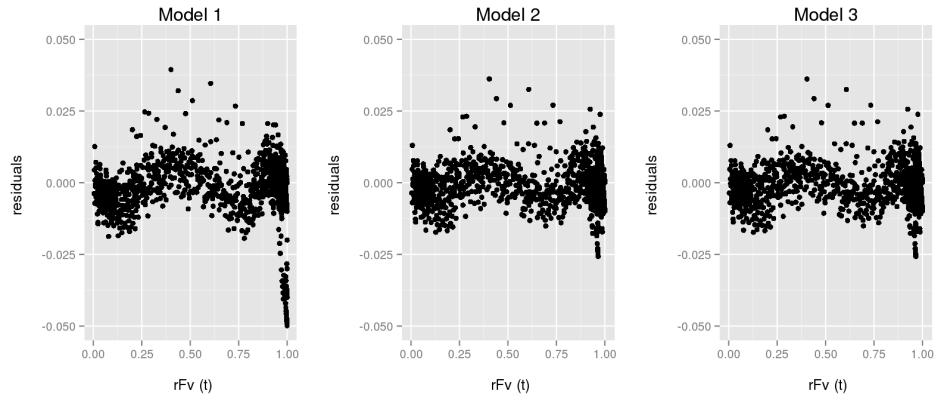

Figure 2.5: Residuals of the fits on data of section 2.3.1 for model 1 (connectivity allowed only for PSIIα) , model 2 (connectivity allowed for PSIIα and PSIIβ) and model 3 (connectivity allowed for PSIIα, PSIIβ and PSIIγ).

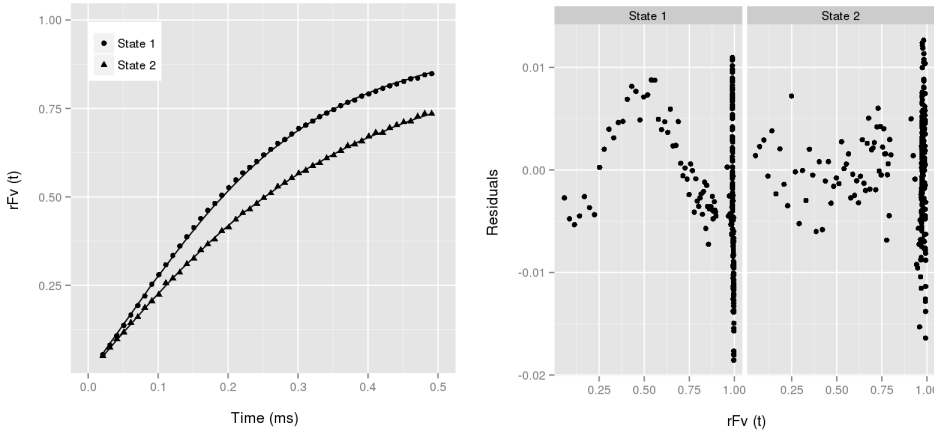

Figure 2.6: Upper panel, DCMU-FR of *wt* strain 1690 in state 1 and in state 2. Symbols : experimental data, line : fit. Lower panel, Residuals for the fits in state 1 and in state 2.

Fits and corresponding residuals for state 1 and for state 2

Upper panel of figure 2.6 shows a decrease in the rate of fluorescence increase under illumination in state 2 compared to state 1, as expected. Lower panel shows that the residuals for the fit in state 1 and in state 2 are small. This indicates that the fit prediction is very close to the experimental data.

Chapter 3

From photochemistry to CO_2 fixation : photosynthetic adaptations to high and low CO_2 conditions in laboratory grown cultures of *Chlamydomonas reinhardtii*

Contents

3.1 Introduction 77
3.2 Material and methods 81
3.3 Results and discussion 83
3.3.1 Combined effects of CO_2 supply and light intensity on growth rates 83
3.3.2 Evidence for a light-dependent electron flow to O_2 in low CO_2 conditions 84
3.3.3 A decreased PSII photochemical yield in CO_2-limiting conditions 99
3.3.4 qE is enhanced in CO_2-limiting conditions 100
3.3.5 A decreased PSII antenna size and a state 2 transition in high CO_2 conditions 103
3.4 Conclusion 105
3.5 Annex 106

Study of the acclimation of the photosynthetic apparatus of *Chlamydomonas reinhardtii* to CO_2 limitation, with emphasis on alternative electron transport

Thomas de Marchin[a], Bart Ghysels[a], Anthony Fratamico[a], Stéphane Roberty[b] and Fabrice Franck[a]

[a]Laboratory of Bioenergetics, B22, University of Liège, B-4000 Liège/Sart-Tilman, Belgium
[b]Laboratory of Ecophysiology and animal physiology, B22, University of Liège, B-4000 Liège/Sart-Tilman, Belgium

In this study, we used combined fluorescence-based electron transport and oxygen measurements to evaluate the responses to low and high CO_2 in *Chlamydomonas reinhardtii* grown in photobioreactors at different light intensities. We developed a method to rationalize the relationship between the apparent quantum yields of oxygen evolution and of electron transport at PSII while taking into account the variations in the proportion of energy absorbed by PSII. We used this relationship as a tool to evidence a significant O_2-dependent alternative electron transport in low CO_2 acclimated cells. We showed that this alternative electron transport represented up to 60% of the total electron transport in low CO_2 cells even when the CO_2 limitation was removed during the measurement by bicarbonate addition. In contrast, no significant alternative electron transport was detected in high CO_2 acclimated cells. We suggest that the high alternative electron transport to O_2 observed in low CO_2 cells represents an adaptation that could help to meet the higher ATP demand for the concentration of CO_2 by the CCM. In contrast, in high CO_2 conditions, the absence of the CCM would reduce the need for ATP and thus the need for electron transport to O_2. Using mutants and inhibitors, we studied the involvement of mitochondrial respiration (the cytochrome pathway and the alternative oxidase pathway) and chlororespiration in this light-dependent O_2 uptake and we found no evidence for the involvement of any of these processes. The alternative electron transport was even higher in the *dum22* mitochondrial mutant devoid of complexes I and III and

we suggest that this alternative electron transport could compensate for the absence of mitochondrial ATP synthesis in the mutant. We observed the expression of FlvA, a protein which is supposed to be involved in a Mehler-like reaction in green microalgae, in low but also, surprisingly, in high CO_2 conditions. H_2O_2 production measurements suggested that if a Mehler reaction is involved in the alternative electron transport to O_2, then the H_2O_2 produced is efficiently scavenged. From fluorescence measurements performed directly in the cultures, we found a lowest PSII photosynthetic efficiency and a higher qE NPQ under low CO_2. This higher qE NPQ was accompanied by a higher xanthophyll de-epoxydation index as well as an increased expression of the LHCSR3 protein. Our results indicate that *Chlamydomonas reinhardtii* is capable of inducing significant thermal dissipation of excitation energy and the extent of this process is influenced essentially by the CO_2 availability. In contrast with results obtained in previous studies, low temperature fluorescence spectra showed that in high light, high CO_2 cells were characterised by a higher proportion of light energy absorbed by PSI compared to low CO_2 cells. This was accompanied by a decreased PSII antenna size as shown by DCMU-FR measurements. These findings which suggested that high CO_2 cells were more in state 2 than low CO_2 cells were discussed in relation with the conflicting theories concerning the regulation of the cyclic electron transport around PSI. Our results support the idea that CEF is regulated by the redox state of the chloroplast rather than by state transitions.

3.1 Introduction

In photoautotophic atmospheric conditions, microalgae often have to deal with limited CO_2 availability. The unicellular green algae *Chlamydomonas reinhardtii* can adapt to low CO_2 concentrations due to a highly efficient inorganic carbon concentration mechanism (CCM), which has been extensively studied in the past (Moroney *et al.*, 2011). However, other functional adaptations of the photosynthetic apparatus to CO_2 limitation have been much less studied.

Several mechanisms are thought to allow photosynthetic organisms to cope with acceptor side limitation at the photosynthetic electron transport chain. This limitation can be caused by excess light and/or CO_2 limitation, and would otherwise lead to damage at PSII, which appears as the main target of photoinhibition. Protecting processes reduce excitation pressure at PSII either by down-regulating the effective excitation flux or by engaging alternative pathways or sinks for electrons in order to decrease reducing pressure. Part of excess excitation energy at PSII can be dissipated thermally at light-harvesting complexes (LHCII) through high-energy state, non-photochemical quenching qE. Part of the LHCII can also dissociate from PSII in a process known as state transitions or qT (Baker, 2008). Finally, cyclic electron transport at PSI and/or electron transfer pathways to O_2 can become more active under limitation in CO_2 availability.

High-energy state quenching (qE) is evidenced through a light-induced decrease of PSII fluorescence yield, which is rapidly reversed in darkness and is part of the so called non-photochemical quenching of fluorescence (NPQ). This process is associated with an increased thermal dissipation in the antennas (Horton *et al.*, 1996), with the development of a low pH in the thylakoid lumen (Wraight and Crofts, 1970; Briantais *et al.*, 1979) and in some cases with the de-epoxidation of violaxanthin to zeaxanthin (Demmig-Adams, 1990; Förster *et al.*, 2001). In *C. reinhardtii*, recent studies showed the importance of the LHCSR3 protein for high-energy state quenching (Peers *et al.*, 2009; Bonente *et al.*, 2011b; Tokutsu and Minagawa, 2013b).

State transitions modulate the binding properties of mobile LHCII to photosystems, and are another component of NPQ. They have been extensively studied in *Chlamydomonas reinhardtii* because up to 80% of the LHCII can migrate between the photosystems in this organism (Delosme *et al.*, 1996), against about 20-25% for higher plants. The redox state of the plastoquinone (PQ) pool is the main determinant of state transitions through binding of plastoquinol to the Q_0 site of Cyt b_6f (Vener *et al.*, 1997; Zito *et al.*, 1999). Under conditions of over reduction of the PQ pool, the kinase STT7 phosphorylates LHCII which then migrates to PSI leading to state 2 (Depege *et al.*, 2003). In addition to its role in photoprotection, the

state 2 transition has been proposed to favour ATP synthesis by enhancing cyclic electron flow around PSI (Vallon *et al.*, 1991; Finazzi *et al.*, 2002; Finazzi and Forti, 2004; Cardol *et al.*, 2009). However, the implication of state transitions in CEF modulation is still a matter of debate (Alric, 2010; Lucker and Kramer, 2013).

The metabolic context of the cell also requires precise adjustments of the photosynthetic apparatus. In particular, the ratio of the phosphorylating and reducing power (ATP/NADPH) produced by photosynthesis has to be precisely adjusted according to the metabolic needs. Indeed, the stoichiometric requirement for the reduction of one CO_2 molecule by the Calvin cycle is 3 ATP for 2 NADPH molecules, i.e. a ratio of 9:6, while the ATP/NADPH ratio produced by linear electron flow (LEF) is 9:7 (Allen, 2003). The concentration of CO_2 by the CCM mechanism emphasizes the need for a higher ATP/NADPH ratio because 1 molecule of ATP is needed for the transport of one molecule of HCO_3^- from the extracellular space to the pyrenoid (Spalding and Portis Jr, 1985). Clearly, alternative pathways are needed to produce the extra ATP costs which are not meet by the LEF. Cyclic electron transport around PSI (CEF) has long been thought to be the mechanism responsible for the adjustment of the ATP/NADPH ratio (Spalding *et al.*, 1984; Miyachi *et al.*, 2003; Lucker and Kramer, 2013). However, this was recently challenged by a study of a *Chlamydomonas* mutant deficient in CEF (Dang *et al.*, 2014). The authors showed that the growth rate of a CEF mutant was similar to the *wild-type* under a wide range of illumination and CO_2 concentrations and that a combination of mitochondrial cooperation and oxygen photoreduction downstream of PSI (Mehler reactions) may provide the ATP needed to supply the CCM.

The photosynthetic electron transport chain of microalgae is endowed with great flexibility due to the existence of auxiliary electron transfer pathways (Peltier *et al.*, 2010), such as electron transfer to O_2. Electron transfer to O_2, also known as water-water cycle, has been found earlier to be very effective in the green microalga *Chlamydomonas reinhardtii* (Sueltemeyer *et al.*, 1986; Bassi *et al.*, 2012). Three physiological roles have been proposed for the water-water cycle: (1) It could act as a photoprotective mechanism to dissipate reducing power in DIC-limited condition in order to prevent reactive oxygen species (ROS) production. (2) Because it allows linear electron flow even when the electron acceptor CO_2 is not available, a proton gradient across the thylakoïd membrane is generated, which permits the development of energy-dependent NPQ. (3) It allows the regulation of the ratio ATP/NADPH produced by photosynthesis by conducting to the synthesis of ATP without the generation of NADPH. This would permit to maintain a chloroplastic electron flow in order to allow the synthesis of the ATP needed by the CCM to concentrate CO_2 when its availability is

restricted (Sültemeyer *et al.*, 1993; Roberty *et al.*, 2014).

Photoreduction of O_2 can occur through different pathways:

1. O_2 can be reduced at PSI in a reaction known as the Mehler reaction (Mehler, 1951). Two molecular pathways have been identified as the possible catalysts for the PSI-mediated O_2 photoreduction: (1) O_2 can be reduced directly at PSI, either by ferredoxin (Furbank and Badger, 1983) or by the Fe/S center F_X in the PSI complex (Asada, 1999). These processes form the Mehler reaction *stricto sensu* and lead to the generation of reactive oxygen species (ROS) which are rapidly detoxified by enzymes of the water-water cycle (Asada, 1999). (2) O_2 can also be reduced by flavodiiron proteins in the chloroplast. In cyanobacteria, flavodiiron (Flv) proteins have been shown to be involved in O_2 reduction in a Mehler-like reaction (Helman *et al.*, 2003). Two Flv clusters have been identified: FlvA and FlvB. FlvA proteins would be involved in O_2 photoreduction (Helman *et al.*, 2003) while FlvB proteins would be involved in PSII photoprotection (Zhang *et al.*, 2009). Because of the significant sequence conservation with their cyanobacterial counterparts, it has been proposed that Flv proteins of eukaryote microalgae could catalyse the Mehler-like reaction in these organisms (Peltier *et al.*, 2010). In contrast to the Mehler reaction, the Flv-mediated Mehler-like reaction operates without significant ROS production (Vicente *et al.*, 2002; Helman *et al.*, 2003).

2. Photoreduction of O_2 can also occur with plastoquinol as electron donor via the plastid terminal oxidase (PTOX) located in the thylakoïd membrane. PTOX-mediated O_2 reduction is also part of chlororespiration (Bennoun, 1982; McDonald *et al.*, 2011).

3. O_2 can be consumed in the mitochondria with the transport of reductants via the malate valve (Scheibe, 1987; Xue *et al.*, 1996; Hoefnagel *et al.*, 1998; Yoshida and Noguchi, 2011).

4. Additionnally, O_2 can be taken up by the oxygenase activity of Rubisco, and this will lead to consumption of reducing equivalents through the associated process of photorespiration (Moroney *et al.*, 2013).

Different technical approaches have been employed to show directly or indirectly the occurrence of light-dependent O_2 uptake activities in microalgae. First of all, in order to study the light-dependent O_2 uptake pathways without the influence of the O_2 uptake associated with photorespiration, manipulation of O_2 and CO_2 levels is a common strategy employed. This approach assumes that Rubisco oxygenase activity is suppressed at high CO_2/O_2 level

while other O_2 uptake pathways are not, due to their high affinity for O_2 compared to photorespiration (Badger *et al.*, 2000). Another method relies on the use of Calvin cycle inhibitors to suppress photorespiration.

A first approach to study alternative electron flow to O_2 is based upon mass spectrophotometric isotopic discrimination of O_2 uptake and O_2 evolution. A second one is based upon the comparison of the electron flux determined by fluorimetry measurements (PAM or FRR) with the rate of O_2 evolution or the rate of CO_2 fixation.

Mass spectrometry approaches provided evidence for non-photorespiratory, light-dependent O_2 uptake in the green microalga *Scenedesmus* during photosynthetic induction (Radmer and Kok, 1976), as well as during steady-state photosynthesis in a manner that was dependent on CO_2 supply during pre-cultivation (Radmer and Ollinger, 1980). In *Chlamydomonas reinhardtii*, non-photorespiratory O_2 uptake was found also at steady-state, especially in cells raised under low-CO_2 conditions. However, it was not clear if the O_2-uptake was due to chlororespiration or Mehler reaction (Sueltemeyer *et al.*, 1986; Sültemeyer *et al.*, 1993) or rather to a light-dependent enhanced mitochondrial respiration (Peltier and Thibault, 1985).

Concomitant measurements of fluorescence-based electron transport rate and of polarographically-measured O_2 exchanges have also suggested in some studies that alternative electron transport to O_2 made a significant part of total electron transport during the photosynthetic induction of *C. reinhardtii* (Franck and Houyoux, 2008) as well as at steady-state for a variety of microalgae species (Flameling and Kromkamp, 1998), although it was not always observed (Heinze *et al.*, 1996). In the green microalga *Dunaliella* sp., it was clearly shown that this alternative electron transport was not linked to photorespiration (Rees *et al.*, 1992). A recent study of our group on the dinoflagellate *Symbiodinium* sp. showed that alternative electron transport at saturating light intensities occurred mainly through a Mehler or Mehler-like reaction (Roberty *et al.*, 2014), but the effect of CO_2 supply during algal growth was not investigated.

For the sake of a better understanding of the adaptations of the photosynthetic electron transport chain to CO_2 limitation in *Chlamydomonas reinhardtii*, we combined electron transport and oxygen measurements and rationalized the relationship between the apparent quantum yields of oxygen evolution and of electron transport at PSII. We used this relationship as a tool to appreciate quantitatively the importance of the O_2-dependent alternative electron transport in different conditions of light intensity and CO_2 concentrations. Furthermore, we analyzed the development of high energy state quenching and energy distribution between the two photosystems in response to CO_2 availability.

3.2 Material and methods

Strains and Growth Conditions The *Chlamydomonas reinhardtii wild-type* strain *1690* used in this work was obtained from the *Chlamydomonas Resource Center* (US). The *dum22* mutant was kindly provided by Dr. C. Remacle from the laboratory of genetics of microorganisms at ULg (Belgium). The *ptox2* mutant and its corresponding *wild-type jex4* were kindly provided by the Institut de Biologie Physico-Chimique at Paris (France). Cells were grown at 25°C in Tris-buffered Bold 3N media in a Multi-Cultivator MC 1000 from PSI (Czech Republic) under 200-900 µmol PAR.m^{-2}.s^{-1} continuous illumination. Because the *wild-type Jex4* and the *ptox2* mutant are deficient in the nitrate-reductase enzyme, they were cultivated in Pipes-buffered bold 3N media in which nitrate was replaced by ammonium. Cells were grown either with air (low CO_2 condition) or with CO_2 5% as sparging gas (high CO_2 condition). Because the growth was different in the two conditions, the cultures were not at the same concentration at the same time and local irradiance differed due to light attenuation. To avoid the influence of this parameter, cultures were diluted at the same concentration of 10 µg chlorophyll.ml^{-1} three hours before starting the experiments.

Pigment analysis Pigments were extracted from whole cells in ethanol and debris were removed by centrifugation at 10,000g for 5 min. The Chl (*a* and *b*) concentration was determined according to Lichtenthaler (1987) with a lambda 20 UV/Vis spectrophotometer (Perkin Elmer, Norwalk, CT). 100µl of pigment extract was subjected to reverse-phase HPLC analysis using a set-up comprising a 616 pump, a 717 plus autosampler, and a 996 online photodiode array detector (Waters, Milford, MA). A Nova Pak C18, 60A column (150-mm length, 4-µm pore size) was used for separation. Acquisition and data treatment were performed using the Millenium software (Waters). Pigments were eluted during 2 min with a gradient from 100% (v/v) solvent A (80% [v/v] methanol and 20% [v/v] 0.5 M ammonium acetate [pH 7]) to 100% (v/v) solvent B (90% [v/v] acetonitrile in water), then during 20 min with a gradient from 100% (v/v) solvent B to 31% (v/v) solvent B and 69% (v/v) solvent C (ethyl acetate) and during 3 min with a gradient from the latter solvent mixture to 100% (v/v) solvent A. The solvent flow rate was 1 ml.min^{-1}. Concentrations of individual pigments were determined using commercial pigments standards (Sigma-Aldrich).

Chlorophyll fluorescence and O_2 evolution measurements Chlorophyll fluorescence emission measurements were made using either a PAM (pulse amplitude modulated) chlorophyll fluorimeter FMS1 from Hansatech instruments (UK) or using an Aquapen AP-C 100 fluorimeter from PSI

(Czech Republic). Measurements of chlorophyll fluorescence rise curve in presence of 20µM DCMU (DCMU-FR) were made in cell suspensions (2 ml) of 1 µg chlorophyll.ml^{-1} using the AquaPen fluorimeter at an intensity of 1670 µmol PAR.m^{-2}.s^{-1} at 455 nm. All other fluorescence measurements were made with the PAM fluorimeter. For dark-adapted measurements, cultures were dark-adapted for 30 minutes prior to each measurement and the chlorophyll concentration was adjusted to 8 µg.ml^{-1}. The analytical light was provided by light-emitting diodes with an emission maximum at 594 nm. The frequency of measuring flashes was 1500 per second and their integral light intensity was less than 0.1 µmol PAR.m^{-2}.s^{-1}. F_M and F'_M levels were obtained by applying a pulse of saturating light (6000 µmol PAR.m^{-2}.s^{-1}) provided by a halogen light source. Oxygen evolution was simultaneously recorded using a Clark electrode system from Hansatech (UK). The protocol for dark-adapted measurements consisted of 6 light periods of 150 sec with light intensities of 50, 160, 300, 550, 750 and 1000 µmol PAR.m^{-2}.s^{-1} during which we recorded net oxygen evolution. Because mitochondrial respiration is known to increase with light intensity, successive light periods were separated by dark periods of 120 sec during which we recorded the respiration rate (R_{dark}). Gross oxygen evolution was calculated as $P_{gross} = P_{net} - R_{dark}$. Light saturating pulses were given every 60 sec. The PSII operating photochemical efficiency ΦPSII was determined as $(F'_M - F_t)/F'_M$ where F'_M is the maximal fluorescence level determined by applying a saturating pulse and F_t is the steady-state fluorescence level. Non-photochemical quenching NPQ was calculated as $(F_M/F'_M) - 1$ where F_M is the maximal fluorescence level when photoprotective mechanisms are not active. $\Phi O_2(r)$ was calculated according to equation (3.11). The value of $(VO_2/PFD)^{max}$ was measured at 50 µmol PAR.m^{-2}.s^{-1} in healthy high CO_2 cultures grown under 200 µmol PAR.m^{-2}.s^{-1} and was found to be 2.89E-007 µmol O_2.µg chl^{-1}.µmol PAR^{-1}.m^2 ± 7E-009 (n=3). For the light-adapted fluorescence measurements in the cultures, the fluorescence probe was immersed in the photobioreactor and fluorescence was recorded without prior dark-adaptation.

Low temperature fluorescence spectra Fluorescence emission spectra at 77K were recorded using a LS 50B spectrofluorimeter (Perkin Elmer). The excitation wavelength was 440 nm. Excitation and emission spectral width slits were 10 and 5 nm, respectively. A broad blue filter (CS-4-96, Corning, Corning, NY) was placed between the excitation window and the sample to minimize stray light. Cells were frozen in liquid nitrogen. Chlorophyll concentration was lower than 2 µg.ml^{-1}, and it was verified that no changes in the intensity ratio of the 685 and 715 nm emission bands arose from

reabsorption artefacts. Spectra were corrected for wavelength-dependent changes in photomultiplier response.

Immunoblot analysis Whole-cell extracts were rapidly harvested and frozen from photobioreactor cultures. Extracts were then incubated 5 min in a buffer (SDS 2% , glycerol 10% , DTT 0.1M and 0.06M Tris pH 6.8) at 95°C. Proteins were separated by SDS-gel electrophoresis on PAGEr gels 4-12% T-G (Lonza) and subsequently electro-blotted onto nitrocellulose membranes (Amersham). FlvA was detected using a purified rabbit antibody prepared against the peptide antigen CGVFGSFGWSGEAVDE. This antibody was produced by Genscript (USA) and was used at a concentration of 1 $\mu g.ml^{-1}$. LHCSR3 antibody is a gift of Prof R. Bassi and Dr C. Formighieri and was used at a dilution 1:8000. Detection was performed using a Chemiluminescence BM Western blotting kit (Roche, Switzerland) with anti-rabbit peroxidase conjugated antibodies.

H_2O_2 measurements The production of H_2O_2 was evaluated using Amplex Red reagent (Molecular Probes, Life technologies, USA) according to the manufacturer's instructions. Aliquots of cultures (10 µg chlorophyll) were combined with Amplex Red (100 µM) and horseradish peroxidase (0.2 U ml^{-1}) under 0 and 450 µmol $PAR.m^{-2}.s^{-1}$ and at 25°C for 90 min. After treatments, samples were centrifuged briefly to pellet the cells and the fluorescence emitted by the supernatant was measured at 590 nm (excitation 540 nm) using a Synergy Mx multimode microplate reader (Biotek Instruments, USA). Concentrations of H_2O_2 were calculated by comparing absorbance of unknown samples to a series of H_2O_2 standards (0–10 µM) treated with the Amplex Red mixture. As the Amplex red reagent is light sensitive, a Rose Pink screening filter (002, LEE Filters, Andover,UK) was placed over the light tubes to minimize excitation of the reagent by blue-green light (≈450–550 nm).

3.3 Results and discussion

3.3.1 Combined effects of CO_2 supply and light intensity on growth rates

Chlamydomonas reinhardtii was cultivated in reactors bubbled with air (the low CO_2 condition) or with air + CO_2 5% (the high CO_2 condition) under different light intensities in phototrophic growth conditions. Table 3.1 shows that growth is faster in high CO_2 conditions, as expected. The generation time decreased with light intensity except in the low CO_2 condition at 900

µmol PAR.m^{-2}.s^{-1} for which it was higher than when measured at 400 µmol PAR.m^{-2}.s^{-1}, which probably indicates a severe stress at this high light intensity.

Light intensity	Low CO_2	High CO_2
200	68.8±9.2	10.5±1.4
400	33.4±4.1	9.8±0.3
900	55±3.8	6.8±0.2

Table 3.1: Generation time (h) of *Chlamydomonas reinhardtii* cultures under different light intensities in high and low CO_2 conditions. Light intensity is expressed in µmol PAR.m^{-2}.s^{-1}.

3.3.2 Evidence for a light-dependent electron flow to O_2 in low CO_2 conditions

It is known that cells grown in low CO_2 condition require a higher ATP/NADPH ratio due to the supplemental ATP required by the CCM to concentrate the carbon dioxide. Extra-ATP synthesis can be achieved by alternative electron transport pathways such as electron transport to O_2. Electron transport to O_2 can be evidenced by simultaneously measuring electron transport rate at PSII (ETR) and oxygen evolution. Indeed, the electron transport rate measured at PSII reflects the total linear electron flux while oxygen evolution is the balance of the oxygen evolved by PSII and the oxygen consumed by other pathways. The relationship between ETR and O_2 evolution rate is therefore affected by light-dependent O_2 uptake processes.

We measured simultaneously the light-response curves of ETR and O_2 evolution on cells grown in high and low CO_2 conditions under 900 µmol PAR.m^{-2}.s^{-1} (fig 3.1). ETR was calculated from PAM fluorescence measurements while gross O_2 evolution was determined with a Clark electrode. Cultures were dark-adapted for 30 min to permit the relaxation of dissipative and photoprotective processes and the measurements were done in presence of $NaHCO_3$ 10 mM to avoid DIC limitation during the measurement , thereby also avoiding photorespiration (Rees *et al.*, 1992). The protocol consisted of six light periods of 150 sec with light intensities of 50, 160, 300, 550, 750 and 1000 µmol PAR.m^{-2}.s^{-1} separated by dark periods of 120 sec (fig 3.1, a and b). Electron transport rate is usually defined as ETR = ΦPSII $*$ PFD $*$ σ_{PSII}, where PFD is the incident light intensity and σ_{PSII} is the optical cross-section of PSII. Unfortunately, in practice, σ_{PSII} measurements is difficult. At this stage, we thus determined the relative electron transport rate (calculated as rETR = ΦPSII $*$ PFD $*$ 0.5, where the factor 0.5 assumes that half of the light is absorbed by PSII). Figure 3.1c shows that the light-response curves

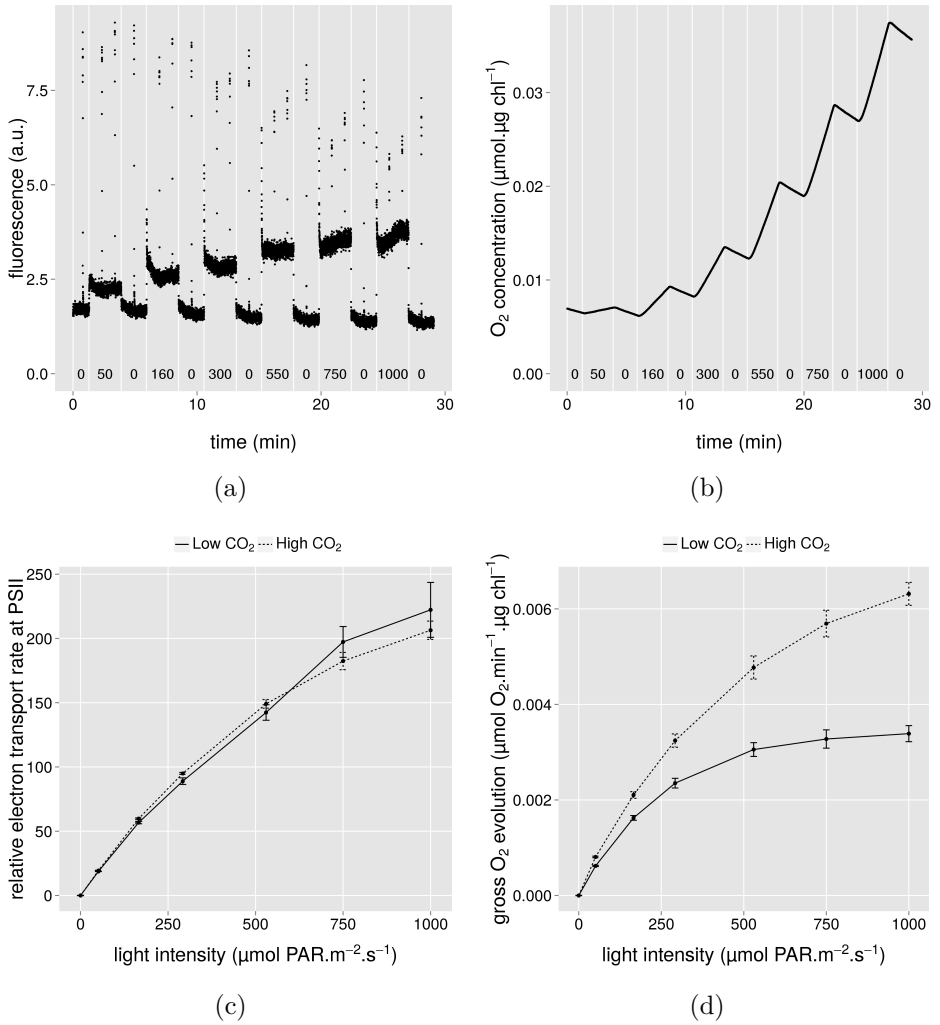

Figure 3.1: (a): Fluorescence trace during a typical experiment. (b): Variation in oxygen concentration during a typical experiment. (c) Light-response curves of the relative electron transport rate at PSII (rETR) calculated from the fluorescence trace. (d) Light-response curves of the gross oxygen evolution calculated from the variations in O_2 concentration. Cells were grown in high and low CO_2 conditions under 900 µmol PAR.m^{-2}.s^{-1} and the measurements were realised in presence of 10mM $NaHCO_3$ after 30 min of dark-adaptation. Shown are means ± SD (n=3). Light intensities (µmol PAR.m^{-2}.s^{-1}) at which measurements were realised are indicated in the figure.

of the rETR are similar in both conditions. This is not the case for the light-response curves of gross O_2 evolution (fig 3.1d) for which low CO_2 cells are characterized by a lower O_2 production than high CO_2 cells.

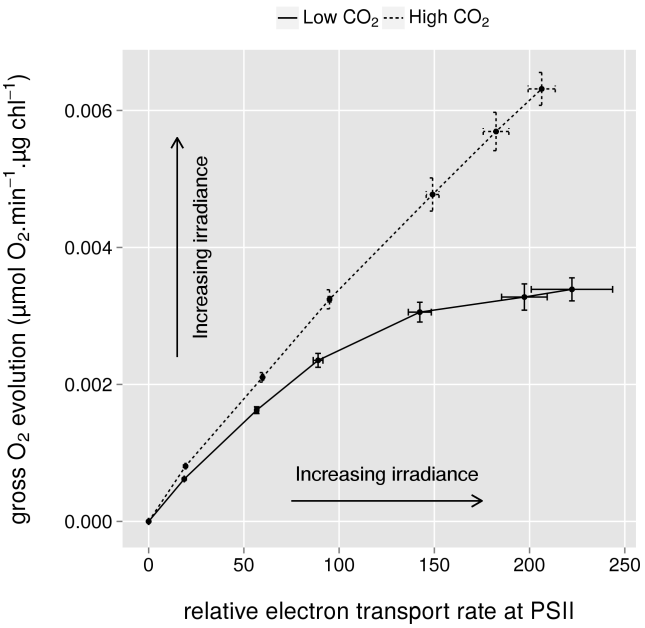

Figure 3.2: Relationship between relative electron transport rate and gross oxygen evolution measured at different light intensities. Cells were grown in high and low CO_2 conditions under 900 µmol PAR.m^{-2}.s^{-1} and the measurements were realised in presence of 10mM $NaHCO_3$ after 30 min of dark-adaptation. Shown are means ± SD (n=3).

We then established the rETR/VO_2 relationships with these data. Figure 3.2 shows that in low CO_2 cells, this relationship is characterized by a curvature which indicates that the flux of electrons is gradually redirected to O_2 with increasing irradiance. Absence of CO_2 limitation during the measurement indicates that this O_2-dependent electron flux becomes structurally more active in low CO_2 cells. By contrast, rETR/VO_2 relationship for high CO_2 cells is characterized by a straight line, which indicates no or less redirection of electrons to O_2. These results show that electron transport to O_2, which cannot be ascribed to photorespiration, occurs in cells grown in low CO_2 conditions.

However, the expression of combined O_2-evolution and fluorescence results in terms of rETR and VO_2 does not allow to derive a quantitative parameter which would express the importance of electron transport to O_2.

As will be shown below, this can be done by comparing the yield of PSII photochemical activity ΦPSII and the yield of oxygen evolution ΦO_2 (see also Heinze *et al.*, 1996; Flameling and Kromkamp, 1998). ΦPSII is easily determined by fluorescence measurements using PAM fluorimetry. This is not the case for ΦO_2 which has to be calculated. We thus developed a theoretical approach to determine a useful parameter to quantify the yield of alternative electron flow to O_2. On the other hand, optical cross-sections of photosystems could vary between measurements. It is thus necessary to identify at which points the interpretation of the results would be dependent on these variations and to introduce the necessary correction factors.

Theoretical considerations on ΦO_2 determination

Absolute value of ΦO_2 is given by :

$$\Phi O_2 = \frac{\text{mol } O_2 \text{ evolved}}{\text{mol photons absorbed}} \tag{3.1}$$

where ´mol O_2 evolved´ is the quantity of oxygen molecules evolved by the photosynthetic apparatus and ´mol photons absorbed´ is the quantity of photons absorbed by the photosynthetic apparatus.

When measuring O_2 evolution with a Clark electrode, two parameters are measured: (1) VO_2, which is expressed as µmol $O_2.ml^{-1}.s^{-1}$. Here, VO_2 is the gross O_2 evolution (P_{gross}) which is calculated as $P_{gross} = P_{net} - R_{dark}$ where P_{net} is the measured O_2 evolution and R_{dark} is the respiration in the dark (see methods). (2) The incident photons flux (PFD), which is expressed as µmol $PAR.m^{-2}.s^{-1}$.

Note that VO_2 is a flux per volume unit while PFD is a flux per surface unit. For a correct expression of ΦO_2 in terms of VO_2 and PFD, we will consider that:

$$VO_2 = \mu\text{mol } O_2.ml^{-1}.s^{-1}.\frac{m^{-2}}{m^{-2}} \tag{3.2}$$

and

$$\frac{ml^{-1}}{m^{-2}} = \frac{m^2}{ml} = \frac{1}{d} \tag{3.3}$$

where ´d´ is the thickness of the sample. Thus,

$$VO_2 = \mu\text{mol } O_2.m^{-2}.s^{-1}.\frac{1}{d} \tag{3.4}$$

To link the incident photon flux PFD to the absorbed photons flux, we can write:

$$\text{Light absorbed} = \alpha.\text{PFD} \tag{3.5}$$

where α is the proportion of incident light absorbed by the photosynthetic pigments of the sample.

By combining equations (3.1), (3.4) and (3.5), one thus have:

$$\Phi O_2 = \frac{VO_2}{PFD}.\frac{d}{\alpha} \tag{3.6}$$

or

$$\Phi O_2 = K.\frac{VO_2}{PFD} \tag{3.7}$$

where

$$K = \frac{d}{\alpha} \tag{3.8}$$

In practice, K is unknown and cannot be easily determined by experimentation. It is thus difficult to calculate an absolute value for ΦO_2. However, it is possible to calculate a relative value $\Phi O_2(r)$ on a normalized scale to its maximal value:

$$\Phi O_2(r) = \frac{\Phi O_2}{\Phi O_2(max)} \tag{3.9}$$

with

$$\Phi O_2(max) = K.\left(\frac{VO_2}{PFD}\right)^{max} \tag{3.10}$$

with $(VO_2/PFD)^{max}$ being the maximal value of the ratio VO_2/PFD found experimentally. In practice, this value is obtained for low PFD ($\approx$ 20-50 µmol PAR.m^{-2}.s^{-1}) where the relation between VO_2 and the PFD is linear for a healthy microalgae sample cultivated in optimal conditions. This value is also equal to the parameter α (initial slope of the light saturation curve) for equations used to fit the VO_2 light saturation curve (Jassby and Platt, 1976).

By combining equations (3.7), (3.9) and (3.10), one thus have:

$$\Phi O_2(r) = \frac{VO_2}{PFD} \Big/ \left(\frac{VO_2}{PFD}\right)^{max} \tag{3.11}$$

as long as K is unchanged. This implies that α has not changed between the measurements of VO_2/PFD and of $(VO_2/PFD)^{max}$. For this, the chlorophyll concentration has to be kept constant, which is the case in our study.

Calculating a quantum yield for alternative electron transport to oxygen

For the purpose of calculation, we can consider that ΦPSII consists of two terms, corresponding to the quantum yields of electron transport leading or not to oxygen evolution $\Phi_{PSII}^{O_2}$ and Φ_{PSII}^{ALT}, respectively. This is formulated as:

$$\Phi\text{PSII} = \Phi_{PSII}^{O_2} + \Phi_{PSII}^{ALT} \tag{3.12}$$

These yield are expressed as mol of electrons per mol of absorbed photons by PSII and are written as:

$$\Phi\text{PSII} = \frac{\text{mol e}^-.\text{m}^{-2}.\text{s}^{-1}}{\text{PFD}.\alpha_{PSII}} \tag{3.13}$$

$$\Phi_{PSII}^{O_2} = \frac{4\text{mol O}_2.\text{m}^{-2}.\text{s}^{-1}}{\text{PFD}.\alpha_{PSII}} \tag{3.14}$$

$$\Phi_{PSII}^{ALT} = \frac{\text{mol e}^-_{ALT}.\text{m}^{-2}.\text{s}^{-1}}{\text{PFD}.\alpha_{PSII}} \tag{3.15}$$

where α_{PSII} is the proportion of incident light absorbed by the PSII.
On the other hand, the quantum yield of O_2 evolution can be written as:

$$\Phi O_2 = \frac{\text{mol O}_2.\text{m}^{-2}.\text{s}^{-1}}{\text{PFD}.\alpha} \tag{3.16}$$

Combining equations (3.14) and (3.16), we obtain:

$$\Phi_{PSII}^{O_2} = 4\Phi O_2 \frac{\alpha}{\alpha_{PSII}} \tag{3.17}$$

Taking into account that the normalized yield $\Phi O_2(r)$ is equal to the absolute yield ΦO_2 multiplied by the minimum quantum requirement for O_2 evolution, which has been estimated to be equal to 10 (Govindjee *et al.*, 1968; Ley and Mauzerall, 1982):

$$\Phi O_2 = \frac{\Phi O_2(r)}{10} \tag{3.18}$$

One thus obtain:

$$\Phi_{PSII}^{O_2} = \Phi O_2(r) \frac{\alpha}{2.5\alpha_{PSII}} \tag{3.19}$$

Combining the equations (3.12) and (3.19):

$$\Phi_{PSII}^{ALT} = \Phi_{PSII} - \Phi O_2(r) \frac{\alpha}{2.5\alpha_{PSII}} \tag{3.20}$$

The alternative electron transport rate can be written as:

$$\mathrm{ETR^{ALT}} = \Phi\mathrm{PSII}.\alpha_{\mathrm{PSII}}.\mathrm{PFD} - \Phi\mathrm{O_2(r)}.\mathrm{PFD}.\frac{\alpha}{2.5} \tag{3.21}$$

Because

$$\mathrm{ETR^{ALT}} = \Phi^{\mathrm{ALT}}_{\mathrm{PSII}}.\alpha_{\mathrm{PSII}}.\mathrm{PFD} \tag{3.22}$$

On the other hand, the total electron transport rate can be written as:

$$\mathrm{ETR} = \Phi\mathrm{PSII}.\alpha_{\mathrm{PSII}}.\mathrm{PFD} \tag{3.23}$$

It results that the ratio of the alternative electron transport rate to the total electron can be calculated with:

$$\frac{\mathrm{ETR^{ALT}}}{\mathrm{ETR}} = 1 - \frac{\Phi\mathrm{O_2(r)}}{\Phi\mathrm{PSII}}\frac{\alpha}{2.5\alpha_{\mathrm{PSII}}} = \frac{\Phi^{\mathrm{ALT}}_{\mathrm{PSII}}}{\Phi\mathrm{PSII}} \tag{3.24}$$

If one knows the $\alpha/\alpha_{\mathrm{PSII}}$ ratio value for each point (each light intensity), it is possible to calculate $\Phi^{\mathrm{ALT}}_{\mathrm{PSII}}$ and $\mathrm{ETR^{ALT}}/\mathrm{ETR}$. In practice, the $\alpha/\alpha_{\mathrm{PSII}}$ ratio is unknown. However, we can consider that in any light condition α_{PSII} is proportional to the $\mathrm{F^{'}_M}$ value measured after the rapid relaxation of qE, and that the maximal $\mathrm{F_M}$ value ($\mathrm{F^{state1}_M}$) corresponds to the situation known as state 1. We thus write :

$$\alpha_{\mathrm{PSII}} = \mathrm{cF^{'}_M} \tag{3.25}$$

where c is a constant. At state 1, α_{PSII} takes its maximal value:

$$\alpha^{\mathrm{state1}}_{\mathrm{PSII}} = \mathrm{cF^{state1}_M} \tag{3.26}$$

where $\alpha^{\mathrm{state1}}_{\mathrm{PSII}}$ is the the proportion of light absorbed by PSII at state 1.

On the other hand, one can show that at state 1 the $\alpha/\alpha_{\mathrm{PSII}}$ ratio is equal to 2. This is obtained from equation (3.20) by admitting that $\Phi\mathrm{O_2(r)} = 1$ (maximal oxygen quantum yield) and that $\Phi^{\mathrm{ALT}}_{\mathrm{PSII}} = 0$ (no alternative electron transport at PSII), conditions which in theory can be met in very low light and with maximal PSII light absorption capacity (state 1). Together with a ΦPSII value of 0.8 corresponding to the maximal value in low light obtained experimentally. It results that:

$$\alpha^{\mathrm{state1}}_{\mathrm{PSII}} = \frac{\alpha}{2} \tag{3.27}$$

Combining equations (3.26) and (3.27) gives:

$$\mathrm{F^{state1}_M} = \frac{\alpha}{2\mathrm{c}} \tag{3.28}$$

The combination of (3.25) and (3.28) gives:

$$\frac{\alpha}{\alpha_{\mathrm{PSII}}} = \frac{2\mathrm{F}_{\mathrm{M}}^{\mathrm{state1}}}{\mathrm{F}_{\mathrm{M}}^{'}} \tag{3.29}$$

In practice, $\mathrm{F}_{\mathrm{M}}^{\mathrm{state1}}$ is obtained under low irradiance in presence of DCMU. $\mathrm{F}_{\mathrm{M}}^{'}$ values were obtained by applying a saturating pulse after 60 seconds of darkness following illumination. In this manner, qE was relaxed while qT was not. This value of $\alpha/\alpha_{\mathrm{PSII}}$ was used in equation (3.20) to calculate $\Phi_{\mathrm{PSII}}^{\mathrm{ALT}}$.

The yield of alternative electron transport to O_2 is enhanced in low CO_2 cells

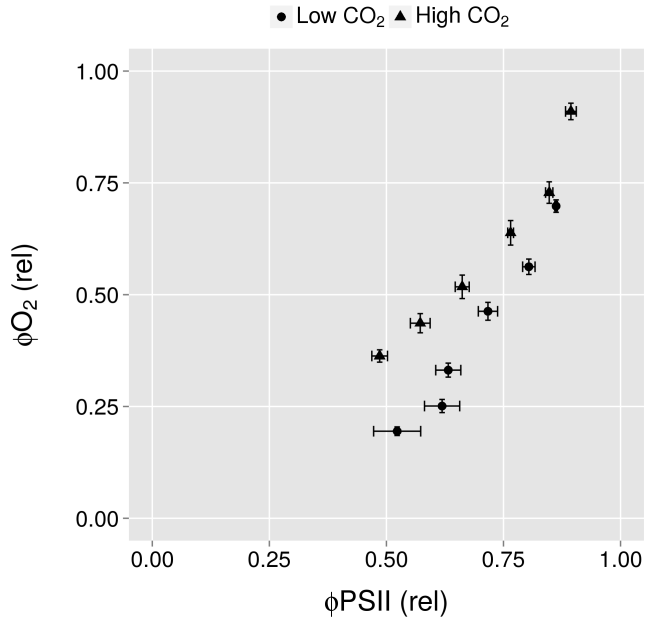

Figure 3.3: Comparison of the $\Phi O_2(r)/\Phi PSII$ relationship in cells cultivated under high and low CO_2 conditions under 900 µmol PAR.m^{-2}.s^{-1}. Cultures were dark-adapted for 30 min and the measurements were realized in presence of 10mM $NaHCO_3$. ΦPSII was normalized relative to its highest value of 0.85 measured after dark-adaptation. Shown are means ± SD (n=3).

We first compared the importance of the alternative electron flux to O_2 in cells cultivated under high and low CO_2 at 900 µmol PAR.m^{-2}.s^{-1} (the highest light intensity in this study). For this, we began by determining

the $\Phi O_2(r)/\Phi PSII$ relationship in the two conditions. Figure 3.3 shows that low CO_2 cells were characterized by a more pronounced deviation from the 1:1 relationship compared to high CO_2 cells. This suggests that the light-dependent O_2 uptake is more efficient in low CO_2 conditions.

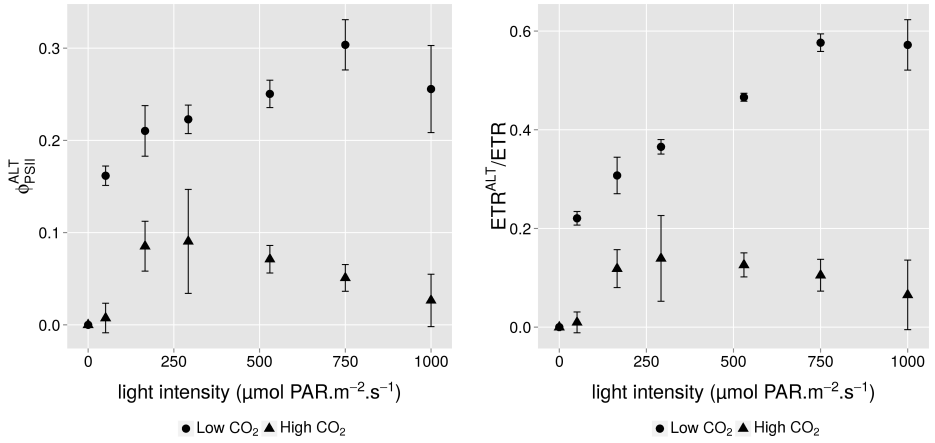

(a) (b)

Figure 3.4: (a): Φ_{PSII}^{ALT} light-response curve. (b): ETR^{ALT}/ETR light-response curve. Cells were grown in high and low CO_2 conditions under 900 µmol PAR.m^{-2}.s^{-1} and the measurements were realized in presence of 10mM $NaHCO_3$ after 30 min of dark-adaptation. Shown are means ± SD (n=3).

This was further investigated by calculating the Φ_{PSII}^{ALT} and ETR^{ALT}/ETR light-response curves according to equations (3.20) and (3.24). Figure 3.4 shows that the yield of alternative electron transport to O_2 was closed to 0 in high CO_2 cells but increased with light intensity in low CO_2 cells. The higher ratio ETR^{ALT}/ETR observed in low CO_2 cells indicates that up to 60% of the electron transport flux is directed to O_2 under an intensity of illumination of 1000 µmol PAR.m^{-2}.s^{-1}. In contrast, high CO_2 cells are characterized by an absence of significant alternative electron transport to O_2. Similar conclusions were obtained for cultures grown at 200 and 400 µmol PAR.m^{-2}.s^{-1} (fig 3.5) although it should be mentioned that negative Φ_{PSII}^{ALT} values were obtained for high CO_2 cells grown at 200 µmol PAR.m^{-2}.s^{-1}. This probably reflects some inaccuracies in the fluorescence and/or O_2 evolution measurements in this set of experiments. However, the difference between high and low CO_2 cells is still evident.

The absence of significant alternative electron transport to O_2 observed in high CO_2 cells is in agreement with a previous study by Heinze *et al.* (1996),

who did not find any deviation between ΦO_2 and ΦPSII measurements under a wide range of light intensities in cultures bubbled with air enriched with CO_2 3% (high CO_2 condition).

Determination of the pathway involved in the light-dependent O_2 uptake

In order to investigate which pathway is involved in the increased alternative electron transport to O_2 in low CO_2 conditions, we determined the Φ_{PSII}^{ALT} and ETR^{ALT}/ETR light-response curves in different mutants or in presence of inhibitors.

Alternative electron transport to O_2 is enhanced in the *dum22* mitochondrial mutant devoid of complexes I and III Oxygen can be consumed in the mitochondria with the transport of chloroplastic reductants via the malate valve. In order to calculate $\Phi O_2(r)$, we took care to deduce the mitochondrial respiration from the O_2 evolution measured in the light for all the results shown in this study. Because it is not possible to measure the mitochondrial respiration during a light period with a Clark electrode, the mitochondrial respiration was determined by measuring the respiration in the dark immediately after the light period. This was shown earlier to provide a good measure of the O_2 consumption rate in the light (Xue *et al.*, 1996). This implies in principle that the alternative electron transport to O_2 evidenced here shouldn't be ascribed to mitochondrial respiration.

In order to confirm that this assumption was correct, we determined the Φ_{PSII}^{ALT} and ETR^{ALT}/ETR light-response curves in the *dum22* mutant, which lacks both complex I and III activities and is thus impaired in the cytochrome pathway (Cardol and Remacle, 2008). If the cytochrome pathway was involved in a light-dependent O_2 uptake, the *dum22* would be characterized by a lower Φ_{PSII}^{ALT} and ETR^{ALT}/ETR than the *wild-type*. Figure 3.6 shows that it is not the case. Surprisingly, the alternative electron transport to O_2 was even much higher for the *dum22* mutant than for the *wild-type*. This result suggests that the alternative light-dependent electron transport to O_2 in the chloroplast has a higher efficiency in the mutant than in the *wild-type*. It also makes it unlikely that the cytochrome pathway is involved in the light-dependent electron transport to O_2 in the *wild-type* and highlights the high capacity of electron transport to O_2 at the level of photosynthetic chain. This could be helpful to compensate for the absence of mitochondrial ATP synthesis in the mutant.

Neither AOX nor PTOX are involved in the alternative electron transport to O_2 We then wanted to investigate if the alternative oxidase

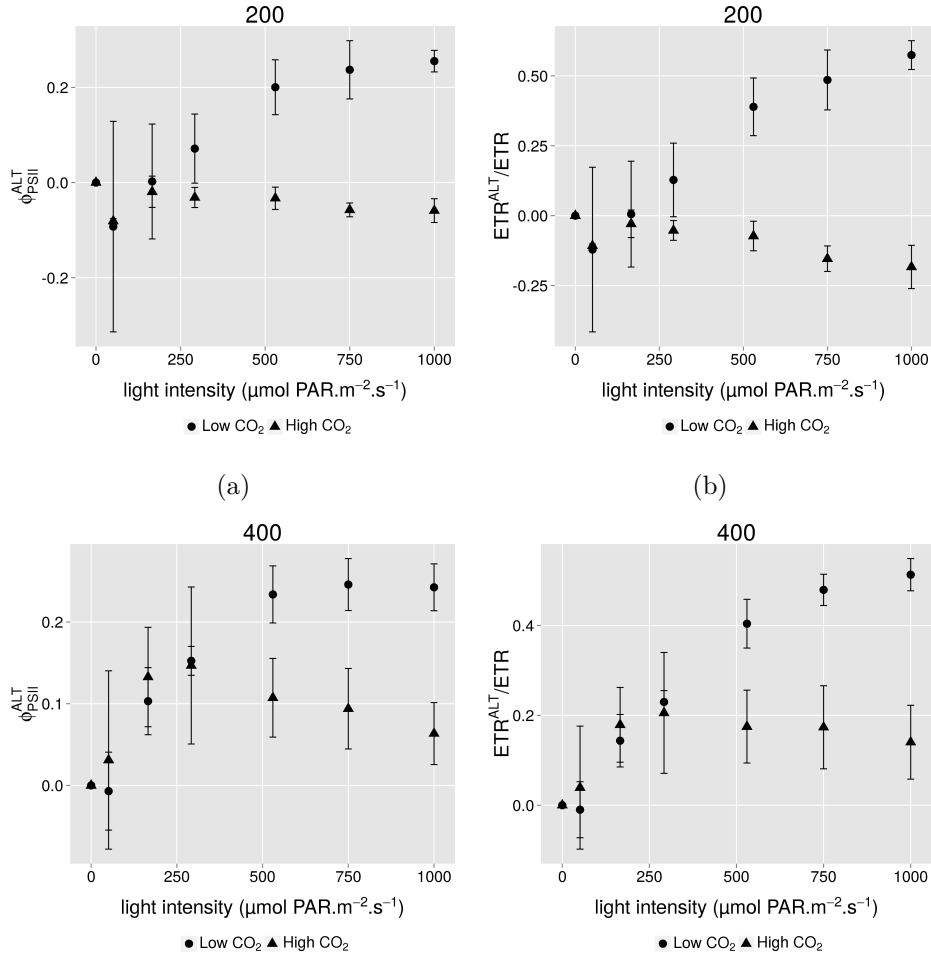

Figure 3.5: (a,c): $\Phi_{\mathrm{PSII}}^{\mathrm{ALT}}$ light-response curve. (b,d): $\mathrm{ETR}^{\mathrm{ALT}}$/ETR light-response curve. Cells were grown in high and low CO_2 conditions at 200 (a,b) and 400 (c,d) µmol PAR.m^{-2}.s^{-1} and the measurements were realized in presence of 10mM $NaHCO_3$ after 30 min of dark-adaptation. Shown are means ± SD (n=3).

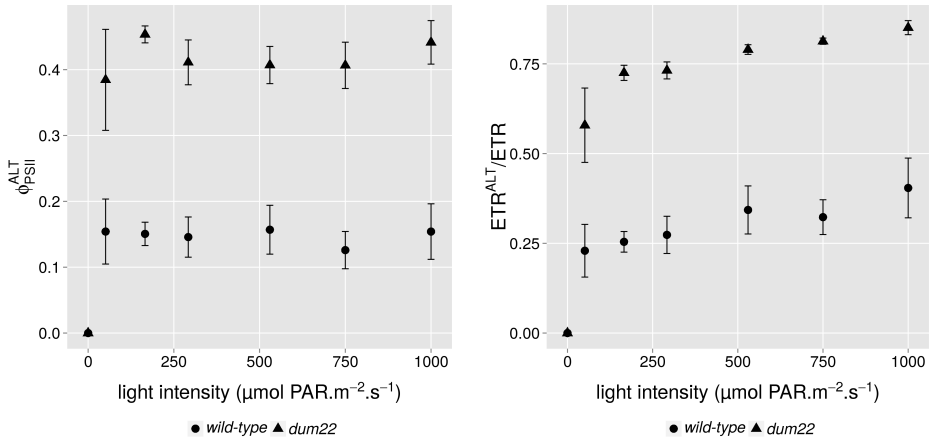

(a) (b)

Figure 3.6: Φ_{PSII}^{ALT} (a) and ETR^{ALT}/ETR (b) light-response curve for the *wild-type* and the *dum22* mutant grown under low CO_2. Cells were cultivated at 400 µmol PAR.m^{-2}.s^{-1} and the measurements were realized in presence of 10mM $NaHCO_3$. Cultures were dark-adapted for 30 min prior to the measurement. Shown are means ± SD (n=3).

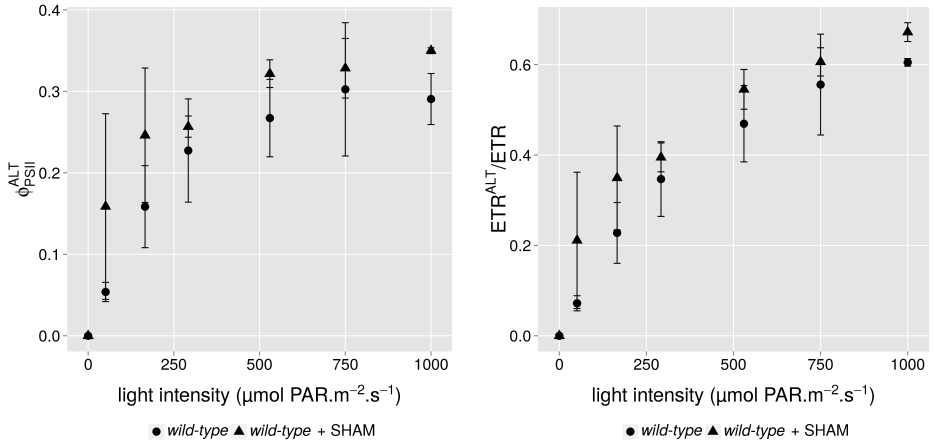

(a) (b)

Figure 3.7: Φ_{PSII}^{ALT} (a) and ETR^{ALT}/ETR (b) light-response curves for the *wild-type* and the *wild-type* in presence of SHAM 2mM. Cultures were cultivated in low CO_2 conditions at 400 µmol PAR.m^{-2}.s^{-1} and the measurements were realized in presence of 10mM $NaHCO_3$. Cultures were dark-adapted for 30 min prior the measurement. Shown are means ± SD (n=3).

(AOX) is involved in alternative electron transport to O_2. For this, we inhibited AOX using salicylhydroxamic acid (SHAM). It should be pointed out that SHAM also inhibits the oxidase involved in chlororespiration PTOX. Figure 3.7 shows that the addition of SHAM does not conduct to significant variations in Φ_{PSII}^{ALT} and ETR^{ALT}/ETR light-response curves. This indicates that neither AOX nor PTOX are involved in the alternative electron transport to O_2 evidenced in this study.

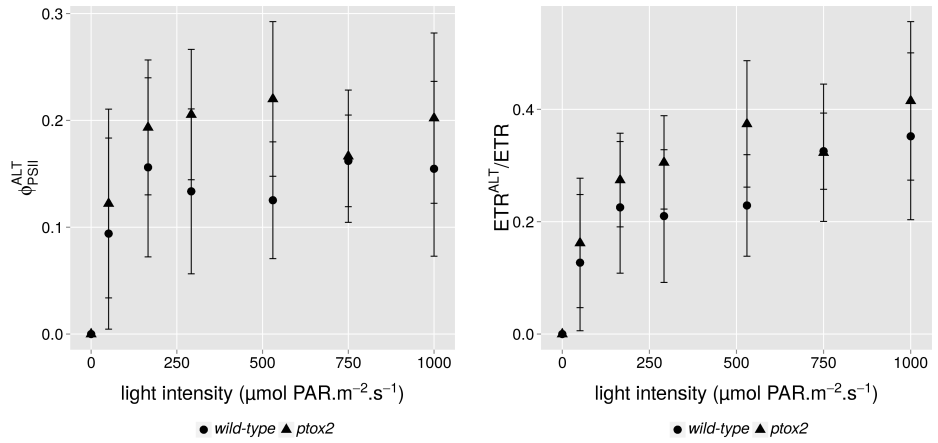

(a) (b)

Figure 3.8: Φ_{PSII}^{ALT} (a) and ETR^{ALT}/ETR (b) light-response curves for the *wild-type Jex4* and the *ptox2* mutant. Cultures were cultivated in low CO_2 conditions at 400 µmol PAR.m^{-2}.s^{-1} and the measurements were realized in presence of 10mM $NaHCO_3$. Cultures were dark-adapted for 30 min prior the measurement. Shown are means ± SD (n=6).

We confirmed that PTOX was not involved in the alternative electron transport to O_2 by measuring Φ_{PSII}^{ALT} and ETR^{ALT}/ETR light-response curves in the chlororespiratory deficient mutant *ptox2* and its corresponding *wild-type jex4* (Houille-Vernes *et al.*, 2011b). Figure 3.8 shows that there is no significant differences in Φ_{PSII}^{ALT} and ETR^{ALT}/ETR light-response curves between the mutant and the *wild-type*. The latter finding is in agreement with the running idea that the contribution of the PTOX-mediated chlororespiratory electron flow to the total chloroplastic electron flow is generally low in standard growth conditions (Feild *et al.*, 1998; Lennon *et al.*, 2003)

Is the light-dependent O_2 uptake mediated by the Mehler reaction or by the Mehler-like reaction? After ruling out several other possibilities such as PTOX, enhanced mitochondrial respiration and photorespiration

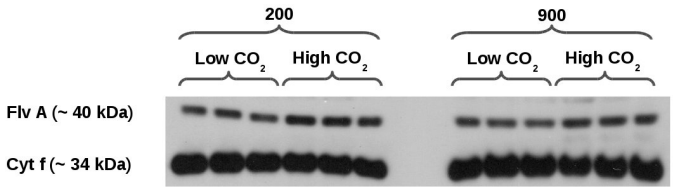

Figure 3.9: Western blot analysis of FlvA abundance in the *wild-type* grown under under 200 or 900 µmol PAR.m^{-2}.s^{-1} in low and high CO_2 conditions. Cyt f was used as a loading control.

(because measurements were realized in presence of saturating bicarbonate concentration), we assumed that the low CO_2 induced alternative electron transport to O_2 must occur either through the Mehler reaction or through a Mehler-like reaction (with Flv proteins as a catalysts). Discrimination between these two pathways is difficult because no inhibitor or mutant is yet available in green microalgae.

We tried to determine if the Mehler-like reaction is involved by measuring the expression of FlvA, a protein which homologues drive the Mehler-like reaction in cyanobacteria. We used western blotting to compare FlvA expression in high and low CO_2 conditions on cells grown under 200 or 900 µmol PAR.m^{-2}.s^{-1} (fig 3.9). Surprisingly, FlvA was expressed in all conditions. The amount of FlvA seems even higher in high CO_2 condition although the light-dependent O_2 uptake was shown to be lower in this condition. FlvA expression in high CO_2 condition has already been observed recently by Dang *et al.* (see fig 6C in Dang *et al.*, 2014) though they did not discuss this result. It must be said that Flv proteins involvement in Mehler-like reaction has been demonstrated in cyanobacteria but the evidence in green microalgae remains to be established. From this result, two assumptions can be made: (1) Either FlvA is involved in the Mehler-like reaction and is expressed regardless of the CO_2 concentration. It would then be activated in low CO_2 condition perhaps by a cofactor or a post-translational modification. (2) Or FlvA is not involved in the light-dependent O_2 uptake and is linked to another function in green microalgae. Clearly, the case is not settled and more studies would be needed to answer to this issue.

In contrast to the Mehler-like reaction, the reduction of O_2 by the Mehler reaction leads to the generation of superoxide ion $O_2^{\bullet -}$ which is dismutated in H_2O_2 by the superoxide dismutase. H_2O_2 is then reduced into water by the ascorbate peroxidase (Asada, 1999). Hence, measurements of H_2O_2 production in high and low CO_2 conditions could indicate if the Mehler reaction is active in these conditions. Measurements of extracellular H_2O_2

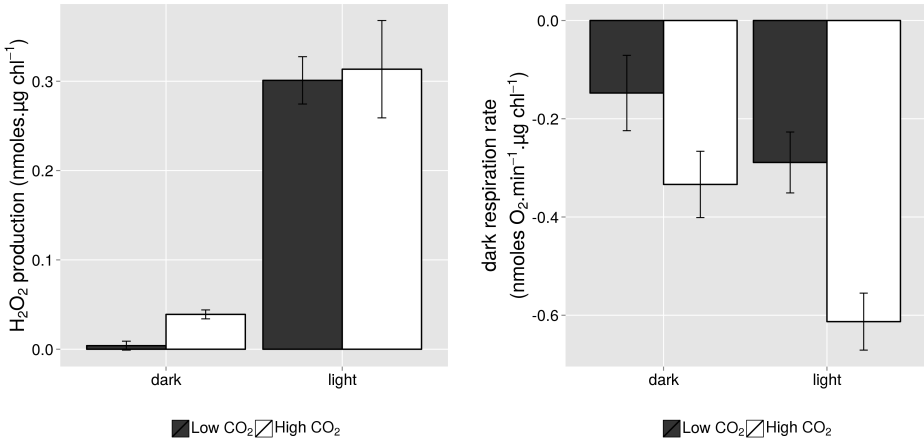

(a) (b)

Figure 3.10: (a): H_2O_2 production determined using AmplexRed probe after 90 min of incubation in high and low CO_2 conditions and in the dark or under 450 µmol PAR.m^{-2}.s^{-1} (light). (b): dark respiration rates in high and low CO_2 conditions measured after dark-adaptation for 30 min (dark) or after illumination at 450 µmol PAR.m^{-2}.s^{-1} (light). Shown are means ± SD (n=3).

generation has already been used as a basis to provide evidences for a Mehler reaction in *Chlamydomonas* (Dang *et al.*, 2014). We thus determined H_2O_2 production using AmplexRed probe after 90 min of incubation in high and low CO_2 conditions and in the dark or under 450 µmol PAR.m^{-2}.s^{-1} (fig 3.10a). In the dark, the H_2O_2 concentration was higher in high CO_2 condition though the Mehler reaction cannot be active in absence of illumination. This surprising result could be explained by the higher dark respiration rate observed in high CO_2 conditions (fig 3.10b) for it is known that mitochondrial respiration leads to ROS production (Purvis, 1997). In addition, Sültemeyer *et al.* (1993) showed a decreased activity of the enzymes that degrade superoxide radicals in high CO_2 conditions compared to low CO_2 conditions.

Under high light illumination, the H_2O_2 concentration was similar in both conditions. One would expect a higher concentration in the low CO_2 condition if a Mehler reaction was engaged in O_2 reduction. Nevertheless: (1) A part of the H_2O_2 is produced by the mitochondrial respiration which is increased in the high CO_2 condition. (2) A significant part of the H_2O_2 is detoxified by the enzymes of the WTW cycle in low CO_2 conditions. This could suggest that more H_2O_2 is effectively produced by a Mehler reaction in low CO_2 conditions. However, we recognize that it is difficult to draw

conclusions on the involvement of the Mehler reaction in the light-dependent O_2 uptake from this single result and that more studies are needed for a definitive conclusion on this point.

3.3.3 A decreased PSII photochemical yield in CO_2-limiting conditions

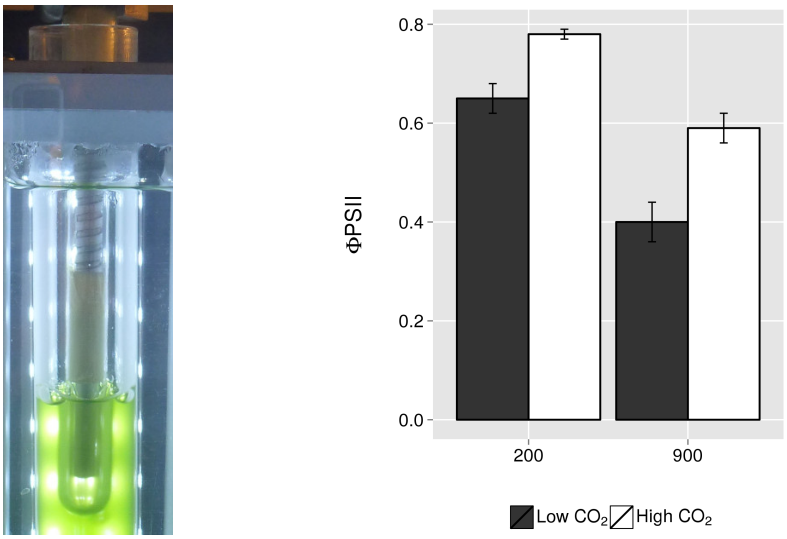

(a) (b)

Figure 3.11: (a): Set-up for the fluorescence measurement directly in the culture. (b): PSII operating photochemical efficiency (ΦPSII) in cultures grown in high and low CO_2 conditions under 200 and 900 µmol PAR.m^{-2}.s^{-1}. Shown are means ± SD (n=3).

After having established the enhancement of the light-induced electron transport to O_2 after growth under low CO_2 conditions (low CO_2 cells), we wanted to determine if variations in the CO_2 availability were conducting to other photosynthetic adaptations. We first measured the PSII operating photochemical efficiency ΦPSII (or the proportion of absorbed light quanta used to drive photochemistry) in cultures grown in high and low CO_2 conditions under 200 and 900 µmol PAR.m^{-2}.s^{-1} by submersing the probe of our fluorimeter directly in the culture (fig 3.11a). In the high CO_2 condition under 200 µmol PAR.m^{-2}.s^{-1}, ΦPSII was close to its maximal value (±0.85) while it was a bit lower in the low CO_2 condition. Under 900 µmol PAR.m^{-2}.s^{-1}, a general decrease was observed, as expected, and the difference between high and low CO_2 conditions was even higher (fig 3.11b). These results indicate that less absorbed light energy was used for

photochemistry in conditions of CO_2 limitation. This is already observed under the non-saturating light intensity of 200 µmol PAR.m^{-2}.s^{-1}.

3.3.4 qE is enhanced in CO_2-limiting conditions

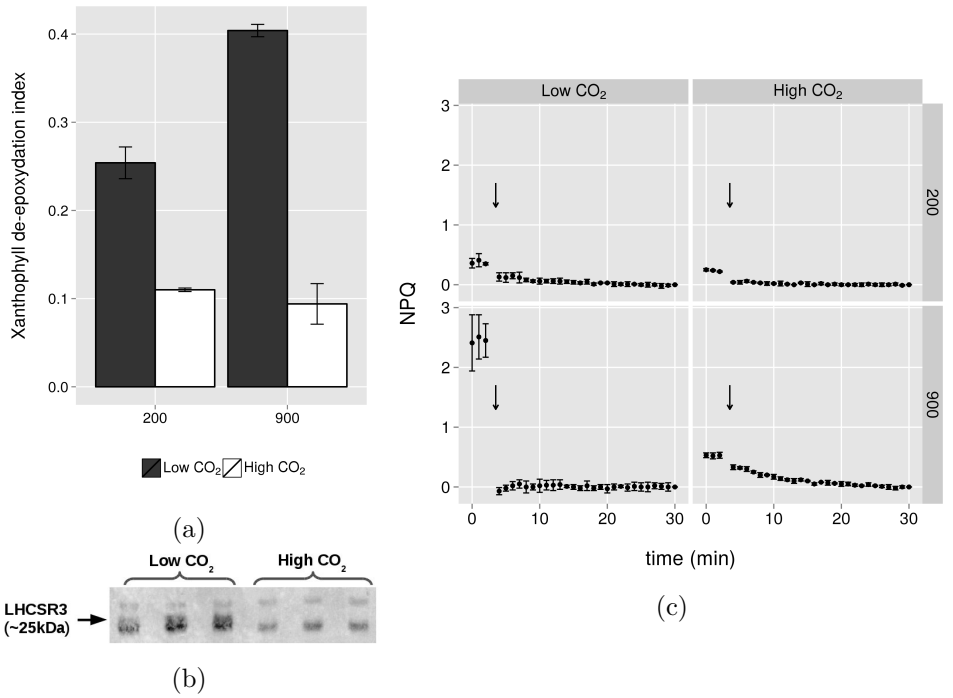

Figure 3.12: (a): Xanthophyll de-epoxydation index of cultures cultivated at 200 and 900 µmol PAR.m^{-2}.s^{-1} in high and low CO_2 conditions. (b): Western blot analysis of the LHCSR3 protein of cultures cultivated under 200 µmol PAR.m^{-2}.s^{-1} in high and low CO_2 conditions. (c): Non-photochemical quenching (NPQ) of cultures cultivated under 200 and 900 µmol PAR.m^{-2}.s^{-1} in high and low CO_2 conditions. NPQ was determined using PAM fluorimetry by submersing a fluorescence probe in the culture. The arrows indicate when the light is turned off. Saturating pulses were given every 60 seconds. Shown are means ± SD (n=3).

A decreased photochemical efficiency (ΦPSII) in condition of limitation in CO_2 has to be compensated by dissipative mechanisms such as increased heat dissipation in the antennas (or energy dependent quenching qE NPQ). qE has been shown to be associated with xanthophyll de-epoxidation (Förster *et al.*, 2001) as well as protonation and binding of LHCSR3 to PSII-LHCII supercomplexes (Bonente *et al.*, 2011b; Tokutsu and Minagawa, 2013b). We

first determined the xanthophyll de-epoxidation index by HPLC. Figure 3.12a shows that it increased with light intensity and was high in low CO_2 condition. In high CO_2 condition, the level of depoxidation was low and did not vary significantly with light intensity. The presence of the protonated form of the LHCSR3 protein was determined by immunoblot on cultures cultivated under 200 µmol PAR.m^{-2}.s^{-1} (fig 3.12b). The protonated form of LHCSR3 (corresponding to the middle band in the westernblot) was only detected in low CO_2 condition. These results suggest a stress and the development of the components associated with increased thermal dissipation of excitation energy in low CO_2 condition.

In order to determine if qE effectively develops in the cultures, we measured NPQ by submersing the probe of our fluorimeter directly in the cultures (fig 3.11a). The protocol consisted to measure the maximal fluorescence yield F'_M under the light of cultivation (200 and 900 µmol PAR.m^{-2}.s^{-1}) and to follow its increase after switching off the light as a result of NPQ relaxation. F_M after full relaxation was taken as the reference fluorescence yield for NPQ calculation. Figure 3.12c shows that under 200 µmol PAR.m^{-2}.s^{-1}, NPQ under illumination was low (0.36±0.08 and 0.25±0.02 for low and high CO_2 conditions, respectively). The immediate relaxation observed under darkness indicates that this NPQ was the high-energy state quenching qE form. The absence of a slow relaxing NPQ in both conditions indicates that state transitions were not engaged under this light intensity. Under 900 µmol PAR.m^{-2}.s^{-1}, NPQ was very high in the low CO_2 condition (2.41±0.47) and its immediate relaxation under darkness indicated that this NPQ was also qE. On the other hand, NPQ remained low in the high CO_2 condition (0.53±0.04) even under high light and the slow relaxation under darkness indicated that this NPQ was mainly dependent on state transitions (qT).

We then verified if the CO_2 limitation was responsible for the high NPQ observed in low CO_2 cultures under 900 µmol PAR.m^{-2}.s^{-1}. To this end, we measured again the NPQ by submersing the probe of our fluorimeter directly in the cultures and we followed the relaxation of this NPQ after $NaHCO_3$ 10mM addition. Figure 3.13 shows that the NPQ was high under 900 µmol PAR.m^{-2}.s^{-1}, in agreement with figure 3.12c. Directly after $NaHCO_3$ 10mM addition, a significant part of this NPQ quickly relaxed to a value very close to the value observed for high CO_2 cells grown under the same light intensity (fig 3.12c). This rapid relaxation indicated that it was a qE NPQ. After turning off the light, approximately half of the NPQ relaxed immediately, which is indicative of some qE remaining in the light after $NaHCO_3$ addition. The remaining part of NPQ relaxed more slowly, which indicates its dependence on state transitions.

The high value of qE NPQ obtained in the low CO_2 condition under 900

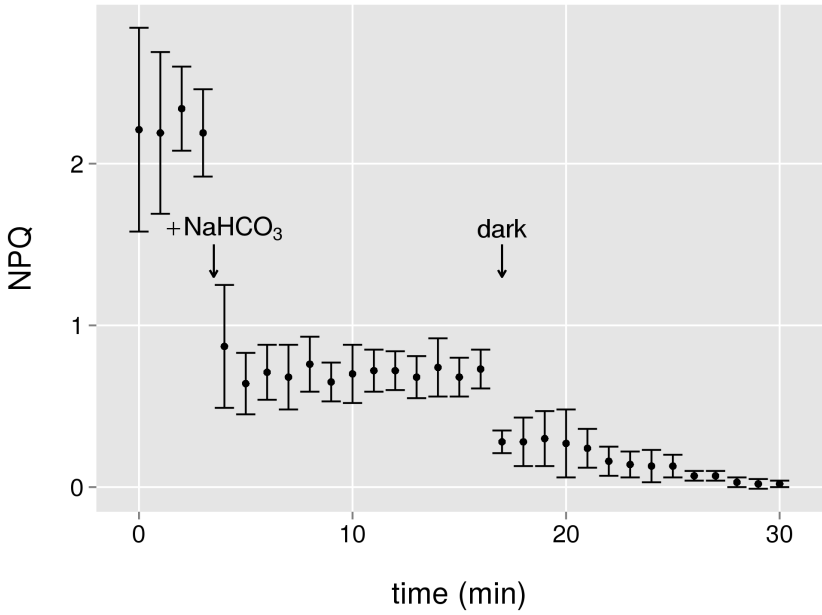

Figure 3.13: Evolution of the non-photochemical quenching (NPQ) following $NaHCO_3$ addition on low CO_2 cells cultivated under 900 µmol PAR.m^{-2}.s^{-1}. NPQ was determined using PAM fluorimetry by submersing a fluorescence probe in the culture. The first arrow indicates when $NaHCO_3$ 10mM is added and the second arrow indicates when the light is turned off. Saturating pulses were given every 60 seconds. Shown are means ± SD (n=3).

µmol PAR.m^{-2}.s^{-1} indicates that *Chlamydomonas reinhardtii* is capable of inducing a significant thermal dissipation of excitation energy and the extent of this process is influenced mainly by the CO_2 availability. NPQ remains weak in high light in the absence of CO_2 limitation. In previous studies, although NPQ was discussed as a high-light response, large NPQ values were always reported in experimental conditions which obviously led to CO_2 limitation (Peers *et al.*, 2009; Bonente *et al.*, 2011a). Here, we provide evidence that this photoprotective mechanism can rather be described as a response to electron transport chain saturation. This saturation being influenced by the balance between the conversion of light into chemical energy and its use for the absorption and reduction of carbon dioxide and nutrients in order to produce biomass.

3.3.5 A decreased PSII antenna size and a state 2 transition in high CO_2 conditions

Interestingly, the occurrence of a slow phase of NPQ relaxation in high CO_2 cells suggests that these cells are shifted towards state 2 under 900 µmol PAR.m^{-2}.s^{-1} (fig 3.12c). This is not expected if we assume that state 2 favors increased ATP production by enhancing PSI activity and cyclic electron flow around PSI (Vallon *et al.*, 1991; Finazzi *et al.*, 2002; Cardol *et al.*, 2009) because we may expect a lower ATP demand in high CO_2 conditions due to absence of the CCM. Moreover, the fact that the state transition is observed in high light (900 µmol PAR.m^{-2}.s^{-1}) is in contradiction with previous results which showed an inactivation of the kinase STT7 under high light intensity (Schuster *et al.*, 1986; Rintamäki *et al.*, 2000).

To confirm the fact that high CO_2 cells were more in state 2, we measured low temperature (77K) fluorescence spectra on cells grown under 200, 400 and 900 µmol PAR.m^{-2}.s^{-1} in high and low CO_2 conditions. At this

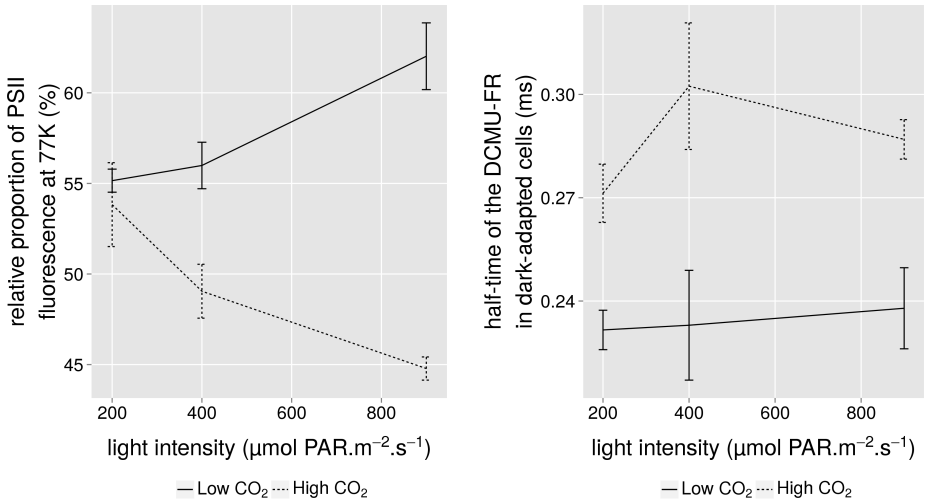

(a) (b)

Figure 3.14: (a): Variations in the relative proportion of PSII fluorescence at 77K in light-adapted high and low CO_2 cells and under 200, 400 and 900 µmol PAR.m^{-2}.s^{-1}. This proportion was calculated from the ratio F685/(F685+F715) measured at 77K. (b): Variation of the time when the normalized variable fluorescence level reaches 0.5 (halftime) in presence of DCMU 20µM in 30 min dark-adapted high and low CO_2 cells and under 200, 400 and 900 µmol PAR.m^{-2}.s^{-1}. Shown are means ± SD (n=3).

temperature, fluorescence emission by PSI and PSII can be distinguished. The 685 nm fluorescence is emitted by PSII while the 715 nm fluorescence is emitted by PSI. The relative proportion of PSII fluorescence can be calculated from the ratio F685/(F685+F715). Variation of this ratio indicates variation in distribution of excitation energy between PSI and PSII, which can result from state transitions or variation in photosystems antenna sizes and stoichiometry. Figure 3.14a shows that under 200 µmol PAR.m^{-2}.s^{-1}, about 55% of the fluorescence is emitted by PSII and this proportion is similar in both conditions. At higher light intensities, cultures behave differently with low CO_2 cells being characterized by a higher proportion of fluorescence emitted by PSII in contrast to high CO_2 cells which are characterized by a lower proportion of fluorescence emitted by PSII. These results indicate an increased proportion of energy absorbed by PSI in high CO_2 cells compared to low CO_2 cells.

A decreased PSII antenna size has been described in low CO_2 conditions compared to high CO_2 conditions in *Chlamydomonas reinhardtii* cultures grown in laboratory (Berger *et al.*, 2014). This phenomenon can be interpreted as an adaptation to avoid an over-reduction of the electron transport chain in condition of restricted DIC availability. We thus determined if the control culture had a reduced PSII antenna size compared to the CO_2 supplemented culture. For this, we measured the functional PSII antenna size by measuring the halftime of the time course of the DCMU fluorescence rise (DCMU-FR) under illumination. In presence of this inhibitor, the fluorescence rise represents the photochemical reduction of Q_A without influence of its reoxidation by plastoquinones. This parameter has proven to be a good indicator of the PSII antenna size in *Chlamydomonas reinhardtii* (de Marchin *et al.*, 2014). Measurements were performed on 30 min dark-adapted samples to permit the relaxation of other processes affecting the PSII antenna size such as state transitions. Figure 3.14b shows that the half-time of the DCMU-FR was higher in high CO_2 conditions than in low CO_2 conditions. This indicates that high CO_2 cells had a lower functional PSII antenna size than low CO_2 cells.

We thus conclude that CO_2 availability influences the energy distribution between PSI and PSII. In high light, high CO_2 cells were characterized by an increased proportion of energy absorbed by PSI. This observation can be explained by a decreased PSII antenna size and/or by a state 2 transition. Our conclusions are in apparent contradiction with previous studies which showed an increased PSII light-harvesting capacities in high CO_2 conditions compared to low CO_2 conditions (Berger *et al.*, 2014). State 2 transition and reduced PSII activity have been observed when cells acclimated to high CO_2 were transferred to low CO_2 concentrations (Palmqvist *et al.*, 1990; Falk and Palmqvist, 1992; Iwai *et al.*, 2007). However, these results were obtained

on short-term acclimated samples (i.e. high CO_2 cultures were subjected to CO_2 depletion during a few minutes or hours) in contrast to our study which was conducted on long-term acclimated samples (i.e. cultures were cultivated in high and low CO_2 for at least three days). In this respect, it was reported that the state 2 transition occurring during the first minutes to low CO_2 exposure relaxed after 120 min (Iwai *et al.*, 2007). It is thus clear that two acclimation phases can be described in response to CO_2 concentration variations: a short-term acclimation as evidenced in previous studies and a long-term acclimation as evidenced in this study.

In *Chlamydomonas reinhardtii*, state transitions have long been linked to increased CEF (Vallon *et al.*, 1991; Finazzi *et al.*, 2002; Cardol *et al.*, 2009). However, this theory has been recently challenged and it was proposed that CEF is regulated by the redox state of the chloroplast rather than by state transitions in *Chlamydomonas reinhardtii* (Takahashi *et al.*, 2013; Lucker and Kramer, 2013). We observed that high CO_2 cells were more in state 2 which would conduct to an increased CEF if this process was linked to state transition. Lower CEF in low CO_2 conditions compared to high CO_2 conditions is not expected since more ATP is needed to power the CCM in the former condition. In this respect, increased CEF has been shown in low CO_2 conditions (Lucker and Kramer, 2013). From these considerations, there appears to be no link between state 2 and increased CEF in the context of CO_2 limitation; rather, CEF seems better correlated with the more reducing context associated to this condition.

3.4 Conclusion

In this study, we developed a method to rationalize the relationship between the apparent quantum yields of oxygen evolution and of electron transport at PSII while taking into account the variations in the proportion of energy absorbed by PSII. This allowed us to evidence significant alternative photosynthetic electron transport to O_2 when cells had been cultivated in conditions of low availability in CO_2 (low CO_2 cells). We showed that this alternative electron transport represented up to 60% of the total electron transport in low CO_2 cells. In contrast, we could not show a significant alternative electron transport in cells cultivated under high CO_2 conditions (high CO_2 cells). We suggest that this alternative electron transport represents a structural adaptation for meeting the higher ATP costs for the concentration of CO_2. By using mutants and inhibitors, we ruled out the involvement of the cytochrome pathway, the alternative oxidase pathway and chlororespiration in this alternative electron transport.

Additionally, we showed a lower PSII efficiency and a higher qE NPQ

in the light under low CO_2 conditions. Our results indicate that *Chlamydomonas reinhardtii* is capable to induce an ample thermal dissipation of excitation energy and the extent of this process is influenced essentially by the CO_2 availability. In contrast with results obtained in previous studies, we showed that in high light, high CO_2 cells were characterised by a higher proportion of energy absorbed by PSI than for low CO_2 cells. Our results, considered with those of previous works on CO_2 limitation, are consistent with the idea that CEF is regulated by the redox state of the chloroplast rather than by state transitions.

Acknowledgements

Thomas de Marchin and Anthony Fratamico thank the F.R.I.A. for the award of a fellowship. Fabrice Franck is research director of the Fonds de la Recherche Scientifique F.R.S-FNRS. Many thanks are given to Dr P. Cardol for his helpful suggestions during this work and Prof R. Bassi and Dr C. Formighieri for the gift of the LHCSR3 antibody.

3.5 Annex

During this work, we conducted some additional experiments concerning:

1. The changes of the redox state of the PQ pool in darkness upon inhibition of oxidative phosphorylation in low and high CO_2 conditions.
2. The alternative electron transport to O_2 during photosynthesis induction.

These observations are not directly related to the main body of work on acclimation to high and low CO_2, but we found they were worth to be reported in this annex.

The rate of PQ pool reduction is increased in high CO_2 cells compared to low CO_2 cells upon inhibition of oxidative phosphorylation

State transitions are usually studied by manipulating the redox state of the plastoquinone (PQ) pool. State 2 transition is often triggered using the method described by Bulté *et al.* (1990), which consists of inhibiting mitochondrial oxidative phosphorylation either by using inhibitors/uncouplers of respiration, or by anoxia. Impairment of oxidative phosphorylation leads to a depletion of ATP and a non-photochemical reduction of the PQ pool by

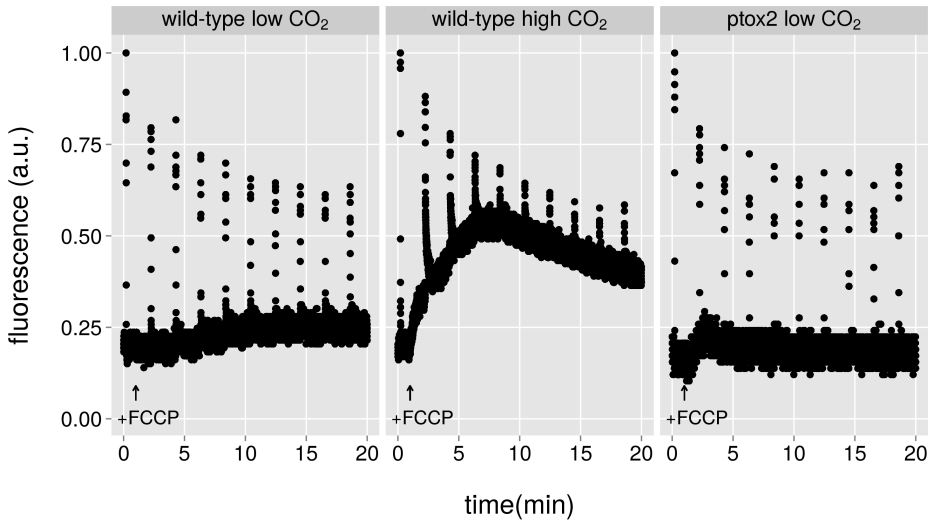

Figure 3.15: Fluorescence traces during the state 2 transition in darkness after addition of FCCP 1µM (arrow) in high and low CO_2 *wild-type* cells and in low CO_2 *ptox2* cells. Cultures were dark-adapted 30 min prior to measurements. Saturating pulses are given every 90 s to visualize the progressive decrease of F_M.

the NAD(P)H dehydrogenase NDA2, thus inducing a transition to state 2. It is possible to follow the changes in the redox state of the PQ pool and the transition to state 2 by monitoring chlorophyll fluorescence changes which follow addition of the inhibitor. The fluorescence level of PSII is measured under low analytic modulated light and is dependent on the redox state of Q_A in the reaction center of PSII which is itself dependent on the redox state of the PQ pool. Saturating light flashes allow to record the maximal fluorescence yield upon PSII closure, which reflects the antenna size of PSII.

Figure 3.15 shows the fluorescence changes upon addition of an uncoupler of respiration (FCCP 1µM) in darkness in high and low CO_2 conditions on 30 min dark-adapted *wild-type* cells. In high and low CO_2 condition, as expected, F_M level decreased gradually after FCCP addition, which indicates a state 2 transition. Noteworthy, F_O level increased gradually after FCCP addition in high CO_2 condition, which indicates an increase in the redox state of plastoquinones. In contrast, F_O level remained almost stable in low CO_2 cells although there was an active reduction of plastoquinones (as demonstrated by the state 2 transition).

In darkness, the redox state of the PQ pool is in equilibrium between its reduction by reductants via NDA2 and its oxidation by PTOX. It follows

that the higher reduced state of the PQ pool observed in high CO_2 cells could result either from a higher reduction rate by NDA2 or by a lower oxidation by PTOX. We thus verified if PTOX was involved in this process by following the effect of FCCP addition on the redox state of PQ on the chlororespiratory deficient strain *ptox2* cultivated in low CO_2 condition. F_O level remained stable after FCCP addition (except for a slight increase shortly after FCCP addition) as it did with the *wild-type* in the same condition. This indicates that PTOX is not involved in a higher oxidation of the PQ pool in darkness in the low CO_2 condition and thus, the higher PQ reduction state observed in the high CO_2 condition when oxidative phosphorylation is inhibited probably results from a higher reduction rate. This higher reduction rate could result from a higher availability of reductants and/or an increased expression of NDA2.

The alternative electron transport to O_2 during photosynthesis induction is not dependent on PTOX

In algae, reduction of O_2 can be the dominant electron transport pathway, such as during the induction of photosynthesis before the light-induced activation of the Calvin-Benson cycle (Radmer and Kok, 1976; Schreiber *et al.*, 1995; Franck and Houyoux, 2008). We investigated the effect of fast-O_2 removal on the induction of photosynthesis in the *wild-type Jex4* and the *ptox2* mutant with the method described by Franck and Houyoux (2008). In this approach, alternative electron transport to O_2 is evidenced by the effect of O_2 removal on the fluorescence induction curve recorded after a dark-to-light transition in the period of photosynthetic induction ($\pm$ 1 min). A saturating light flash is given a short time after the onset of actinic light in order to appreciate the efficiency of electron transport at PSII with or without O_2 in the medium. Removal of oxygen is obtained by addition of glucose oxidase, glucose and catalase a short time after exposure of the algae to actinic light. The short time lapse (30 s) between O_2 removal and recordings of light-induced fluorescence changes is essential in order not to promote a state transition.

Figure 3.16 shows that the photosynthetic electron transport chain of the *wild-type* and the *ptox2* mutant are completely saturated during the photosynthesis induction in absence of O_2, as shown by the absence of variable fluorescence during a saturating pulse (indicated by the arrows) in this condition. In contrast, the shape of the induction curve is completely different in presence of O_2. The presence of a large variable fluorescence during a saturating pulse indicates a significant electron transport rate. These results confirm previous observations concerning the importance of the alternative electron transport to O_2 during photosynthesis induction.

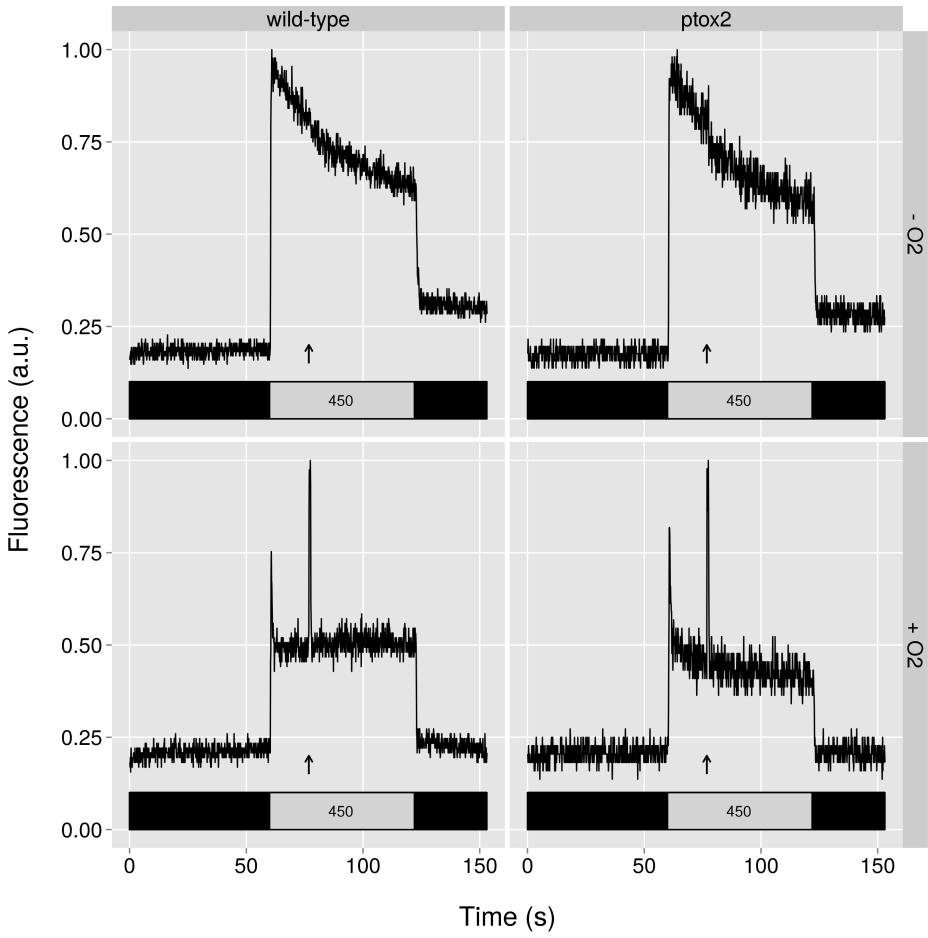

Figure 3.16: Effect of fast-O_2 removal on the fluorescence traces during the photosynthesis induction under actinic light of 450 µmol PAR.m^{-2}.s^{-1} in the *wild-type Jex4* and the *ptox2* mutant grown in low CO_2 conditions. Cultures were dark-adapted for 30 min prior to the measurements. The arrows indicate when a saturating pulse is applied in order to reveal the efficiency of electron transport.

The absence of difference between the wild-type and the *ptox2* mutant in presence of O_2 indicates that PTOX is not involved in the process evidenced here. On the other hand, Franck and Houyoux (2008) have shown that inhibitors of mitochondrial respiration (KCN + BHAM) had no significant effect either. Therefore, the efficient alternative electron transport at the beginning of photosynthetic induction must be of Mehler type.

Chapter 4

From CO_2 to biomass : photosynthetic adaptations to high and low CO_2 conditions in outdoor microalgae mass cultures of *Scenedesmus obliquus*

Contents

4.1 Introduction 114
4.2 Material and methods 116
4.3 Results and discussion 119
4.3.1 Productivity and photosynthetic efficiency of *Scenedesmus obliquus* in high and low CO_2 conditions 119
4.3.2 Characterisation of the photosynthetic apparatus in high and low CO_2 conditions 123
4.4 Conclusion 130
4.5 Appendix 131

Photosynthesis of *Scenedesmus obliquus* in outdoor open thin-layer cascade system in high and low CO_2 in Belgium

Thomas de Marchin[a], Michel Erpicum[b] and Fabrice Franck[a]

[a]Laboratory of Bioenergetics, B22, University of Liège, B-4000 Liège/Sart-Tilman, Belgium
[b]Laboratory of climatology and topoclimatology, B11, University of Liège, B-4000 Liège/Sart-Tilman, Belgium

Two outdoor open thin-layer cascade systems operated as batch cultures with the alga *Scenedesmus obliquus* were used to compare the productivity and photosynthetic adaptations in control and CO_2 supplemented cultures in relation with the outdoor light irradiance. We found that the culture productivity was limited by CO_2 availability. In the CO_2 supplemented culture, we obtained a productivity of up to 25 g dw.m^{-2}.day^{-1} and found a photosynthetic efficiency of 2.6%. Fluorescence and oxygen evolution measurements showed that ETR and oxygen evolution light saturation curves, as well as light-dependent O_2 uptake were similar in algal samples from both cultures when the CO_2 limitation was removed. In contrast, we found that CO_2 limitation conducted to a decreased PSII photochemical efficiency and an increased light-induced heat-dissipation in the control culture compared to the CO_2 supplemented culture. These features may contribute to the lower productivity observed in absence of CO_2 supplementation in outdoor mass cultures of *Scenedesmus obliquus*.

4.1 Introduction

Figure 4.1: Top-left: light exposed part of the thin-layer cascade system on the roof. Top-right: zoom on the overflow tank. Bottom-left: engine room located downstairs. Bottom-right: zoom on a tank.

Over the last decades, microalgae have been increasingly studied because of their potential applications in the industry. Because of their great biodiversity, microalgae can produce a lot of valuable compounds for biofuels, food and feed, pharmaceutical and cosmetic industry. Despite a growing interest in microalgae mass cultures, the majority of studies on microalgae have been carried out at the laboratory scale and only few studies have addressed the question of photosynthetic adaptations in mass cultures.

Different mass culture systems are used in the world to produce microalgae biomass. Although some industry use closed tubular photobioreactors, most of microalgae biomass production units rely on horizontal open raceways systems (Zittelli *et al.*, 2013). The advantage of raceways are a relatively low building cost as well as a simple design permitting a rapid development of the installation. The culture thickness of these systems is usually high (15-30 cm), implying a low biomass density because of the reduced penetration of light in the suspension. Another drawback of these systems is the relatively

poor mixing of the culture, which do not permit an efficient CO_2 and O_2 exchange with the atmosphere.

In this study, we used a thin-layer culture system similar to the one designed by Dr. Ivan Šetlík in the 1960s (Šetlík *et al.*, 1970). This system is characterised by an inclined surface exposed to sunlight in which the algal suspension flows by gravity (fig 4.1). At the end of the inclined surface, the suspension falls in a tank and is then pumped to the upper part of the inclined surface. Transverse laths are placed on the inclined surface in order to increase the mixing of the suspension, to ensure good gas exchange with the atmosphere and to favour fast light-dark cycle. The tank serves as a buffer to cushion the concentration effect of high evaporation during hot days as well as the dilution effect of heavy rainfalls. The productivity, the CO_2/O_2 exchange properties and the different variants of this system have been well characterised in the past using *Chlorella* and *Scenedesmus* species (Kajan *et al.*, 1994; Grobbelaar *et al.*, 1995; Doucha and Lívanský, 1995; Lívanský and Doucha, 1996; Doucha and Livansky, 1999; Livansky, 2000; Doucha *et al.*, 2005; Doucha and Lívanský, 2006; Doucha and Lívanský, 2009; Masojídek *et al.*, 2011; Jerez *et al.*, 2014). This system is currently used in a modified version for commercial production of *Spirulina* by the Biorigin farm in Ecuador.

Chlorophyll fluorescence has become one of the most common technique used to asses the photochemistry of photosynthetic organisms due to its non-invasiveness, sensitivity and to the wide availability of measuring instruments (Masojídek *et al.*, 2010). Chlorophyll fluorescence reflects the performance of PSII and is thus influenced by processes occurring downstream of PSII. One of the most used chlorophyll fluorescence approach is the saturation-pulse (PAM) method. With this method, fluorescence can be recorded continuously without being affected by ambient light and photochemical quenching and non-photochemical quenching can be easily separated (for a review, see Baker, 2008). Several parameters have been developed to account for the photosynthetic performances of sample. Maximal photochemical efficiency of PSII (F_V/F_M) is a parameter characterizing the proportion of absorbed light quanta which can be used by PSII to drive photosynthesis. The optimal value of this parameter is about 0.7-0.8, meaning that in optimal conditions, about 70 to 80% of the absorbed light quanta are used for photochemistry while the rest is wasted as heat and fluorescence. This parameter is determined after dark-adaptation as $(F_M - F_O)/F_M$ ($=F_V/F_M$), where F_M is the maximal fluorescence level determined by applying a saturating pulse and F_O is the basal fluorescence level. Another useful parameter is the PSII operating photochemical efficiency (ΦPSII) which is determined in the same way as F_V/F_M except that it is measured under actinic light. While F_V/F_M is a measure of the maximal photochemical capacity of PSII, ΦPSII is a measure

of the actual photochemical capacity of PSII when photosynthesis is active. This means that any stress affecting a component of the photosynthetic apparatus will be reflected by a decreased ΦPSII. Finally, non-photochemical quenching (NPQ) is a third parameter which is often calculated to determine if photoprotective mechanisms are activated to deal with excessive absorbed light energy. NPQ is reflected as a general decrease of the fluorescence level and it is calculated as $(F_M/F'_M) - 1$ where F'_M is the maximal fluorescence level obtained by applying a saturating pulse under a particular actinic light intensity and F_M is the maximal fluorescence level when photoprotective mechanisms are not active. NPQ is composed of three components: energy-dependent quenching qE, which reflects an increased heat dissipation in the antennas, state transition qT which reflects a dissociation of light-harvesting complexes from PSII and photoinhibition qI, which reflect photodamages to PSII. These different components have different relaxation times ranging from a few seconds (qE) to several minutes (qT and qI).

It is well known that CO_2 addition increases the growth rate of microalgae. For this reason, some mass microalgae cultures are CO_2 supplemented. However, it is not always the case. Among the studies on microalgae mass culture, as far as we know, none directly compared high CO_2 (CO_2 supplemented) and low CO_2 (non CO_2 supplemented) conditions. The aim of this study was to analyse the photosynthetic adaptations of the culture to the CO_2 addition by measuring chlorophyll fluorescence. For this, we performed two simultaneous microalgae cultures with or without CO_2 addition. Experiments were realised with *Scenedesmus obliquus*, which is known to have a high growth rate and a strong cell wall making it resistant for cultivation in various cultivation systems.

4.2 Material and methods

Organism and culture medium The *Scenedesmus obliquus 276.10* strain was used for cultivation (SAG culture collection). The medium was made of FloraGro and FloraMicro (GHE) diluted in tap water. FloraGro and FloraMicro were added in a ratio 1:1000 and 1:1000, respectively, for each 4kg of biomass accumulated. N content of the cultures was regularly checked to ensure that it was available and assimilated. This was taken as a indicator for the absence of nutrient limitation. FloraMicro and FloraGro composition can be found in Tocquin *et al.* (2012). In one culture, pH of the medium was stabilized to a value close to 7.5 by injecting pure CO_2 while in the other, pH was not stabilized.

Outdoor culture system The two outdoor open culture systems used for cultivation are similar to the one designed by Dr. Ivan Šetlík in the 1960s (Šetlík *et al.*, 1970). They consists of a 35m² inclined surface (inclination 2.5°) exposed to sunlight. The suspension flows on the surface due to the gravity before falling in a tank located downstairs. The suspension is then pumped to the roof by a hydraulic pump (1000 liters.h^{-1}) to ensure a continuous cycle. Transverse laths are placed on the inclined surface in order to increase the thickness and the mixing of the suspension. Layer thickness increases from 26mm behind the lath to 44mm in front of the next lath. The suspension volume was 4000l at the beginning of the culture. The volume on the inclined surface was 1900l while the volume in the tank varied around a value of 2100l, depending of evaporation and rain.

Supply of carbon dioxide In the CO_2 supplemented culture, pure CO_2 was added in the suction pipe of the circulation pump. CO_2 injection was regulated by a pH-meter to stabilize the pH at a value close to 7.5.

Outdoor light intensity measurement The light intensity was measured every 6 minutes by a brightness transmitter 7.1414.51.150 from Thies Clima (Göttingen, Germany). The light intensity was measured in lux and was converted to PAR (µmol PAR.m^{-2}.s^{-1}) by dividing lux by 54 (constant for sunlight spectrum, Thimijan and Heins, 1983).

Culture temperature The culture temperature was recorded every 20 minutes by an immersed probe DS1922L from Waranet solutions (Auch, France).

Analytical methods Biomass concentration (g.l^{-1}) was determined daily by measuring the optical density at 750nm (A750). After having established the relationship between A750 and dry weight ($dw[g.l^{-1}] = A750 * 0.35$, R^2 =0.99), total biomass in the suspension was calculated, taking into account the suspension volume variations due to evaporation and rain. Net algal productivity, including night biomass loss, was estimated from the difference between successive morning algal dry weights.

Chlorophyll concentration determination Pigments were extracted from whole cells in ethanol. Extracts were incubated 4 hours on a shaker in presence of small beads and debris were removed by centrifugation at 10,000g for 5 min. The Chl (a + b) concentration was determined according to Lichtenthaler, 1987 with a lambda 20 UV/Vis spectrophotometer (Perkin Elmer, Norwalk, CT).

Chlorophyll fluorescence and O_2 evolution measurements Chlorophyll fluorescence emission measurements were made using either a PAM (pulse amplitude modulated) chlorophyll fluorimeter FMS1 from Hansatech instruments (UK) or using an Aquapen AP-C 100 fluorimeter from PSI (Czech Republic).

For the dark-adapted measurements, we used the FMS1 fluorimeter. Cultures were dark-adapted for 30 minutes prior to each measurement and the chlorophyll concentration was adjusted to 8 µg.ml^{-1}. The analytical light was provided by light-emitting diodes with an emission maximum at 594 nm. The frequency of measuring flashes was 1500 per second and their integral light intensity was less than 0.1 µmol PAR.m^{-2}.s^{-1}. F_M and F'_M levels were obtained by applying a pulse of saturating light (6000 µmol PAR.m^{-2}.s^{-1}) provided by a halogen light source. rETR was determined by multiplying the photochemical efficiency of PSII by the light intensity and by 0.5 (assuming that light is equally absorbed by PSII and PSI).

Oxygen evolution was simultaneously recorded using a Clark electrode system from Hansatech (UK). The protocol consisted of 6 light periods of 150 sec with light intensities of 50, 160, 300, 550, 750 and 1000 µmol PAR.m^{-2}.s^{-1} during which we recorded net oxygen evolution. Because mitochondrial respiration is known to increase with light intensity, successive light periods were separated by dark periods of 120 sec during which we recorded the respiration rate. Gross oxygen evolution was defined as $P_{gross} = P_{net} - R_{dark}$. Light saturating pulses were given every 60 sec.

For the light-adapted measurements, we used the Aquapen fluorimeter. These measurements were always made at noon. Cultures were directly taken from the culture (dark-adaptation of $\approx$ 15 seconds) and diluted in the cell-free medium (obtained by centrifugation of the culture). Actinic light and saturating pulse were given at 455 nm. The protocol of NPQ and ΦPSII measurements was the LC2 protocol. It consisted of 6 different periods of 30 sec with light intensities of 0, 50, 100, 200, 450 and 750 µmol PAR.m^{-2}.s^{-1}. Saturating pulses were given at the end of each period. For the DCMU-fluorescence rise curves, DCMU was added at a final concentration of 20µM and the light intensity was 2000 µmol PAR.m^{-2}.s^{-1}.

pH measurement The pH of the control culture was recorded by a pH-meter BL931700 from Hanna instruments (USA). The pH of the CO_2 supplemented culture was regulated by a pH-meter Evolution deluxe from Dennerle (Germany).

4.3 Results and discussion

4.3.1 Productivity and photosynthetic efficiency of *Scenedesmus obliquus* in high and low CO_2 conditions

In outdoor conditions, irradiance and temperature vary continuously, depending on the weather. During cloudy days, the light intensity and the air temperature are lower than during sunny days. This has an impact on the growth of the culture. We thus continuously recorded irradiance and culture temperature during the whole experiment. A fist experiment was started in June 24 2014 at a density of 0.4 $g.l^{-1}$ and lasted 15 days. In order to obtain data from exponential-phase cultures, a second experiment was started in July 29 2014 at a lower density of 0.05 $g.l^{-1}$ and lasted 12 days. Figure 4.2 summarizes the irradiance, the culture temperature, the culture density and the pH during these two experiments.

Despite a starting density similar at the beginning of the experiments, it is clear that it increased faster in the CO_2 supplemented culture than in the control culture. This shows that CO_2 availability is the main limiting factor in microalgae mass cultures in open thin-layer cascade system.

The pH varied extensively in the control culture. It increased during the day because of carbon assimilation by photosynthesis. This is explained by the carbon dioxide equilibrium:

$$CO_2 + H_2O \rightleftharpoons H_2CO_3 \rightleftharpoons H^+ + HCO_3^- \rightleftharpoons CO_3^{2-} + 2H^+$$

When CO_2 is consumed by photosynthesis, H^+ is released in the medium, thus increasing the pH. During the night, photosynthesis is stopped and CO_2 concentration increases due to mitochondrial respiration and to equilibration with atmospheric CO_2, leading to a decrease of the pH. At low density (<0.2 $g.l^{-1}$), the pH shift during the day gradually increased with cell concentration whereas at higher density (>0.2 $g.l^{-1}$), the maximal pH attained during the day reached a plateau at a value of 11. The fact that the plateau of 11 was not reached at very low density implies that DIC availability was sufficient to drive photosynthesis and thus we can conclude that CO_2 supplementation is needed only at densities higher than 0.2 $g.l^{-1}$.

At pH higher than 9, it is known that there is virtually no CO_2 species and the totality of DIC is present in the form of HCO_3^- and CO_3^{2-} (Knud-Hansen *et al.*, 1998). The fact that *Scenedesmus obliquus* can grow at such high pH, in contrast with other species like *Chlamydomonas reinhardtii*, is probably due to the existence of an additional alkaline HCO_3^- pump in this species (Thielmann *et al.*, 1990). The ability of this species to grow at high pH is interesting because the majority of contaminants cannot grow and

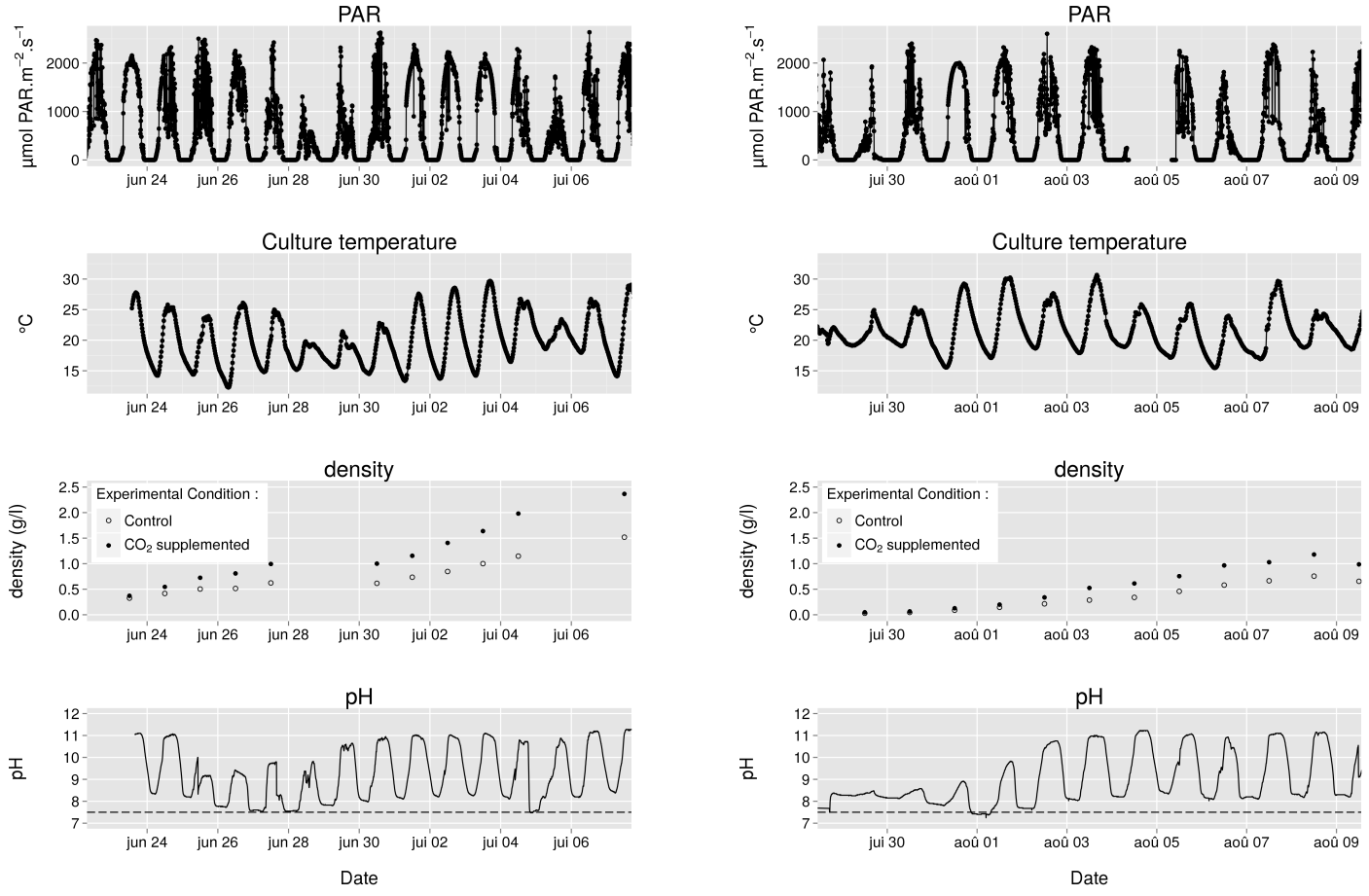

Figure 4.2: Summary of the data acquired during the two successive experiments. PAR: photosynthetic active radiation measurements from the weather station. The culture temperature was recorded using a probe immersed in the culture. The density of the culture was determined by dividing the total dry biomass by the volume of the culture. The pH of the control culture was recorded every 5 minutes. The pH of the CO_2 supplemented culture was not recorded but was set to 7.5 by injecting pure CO_2.

rapidly die at such high pH. The pH shift could then be used to control contamination in outdoor microalgae mass cultures.

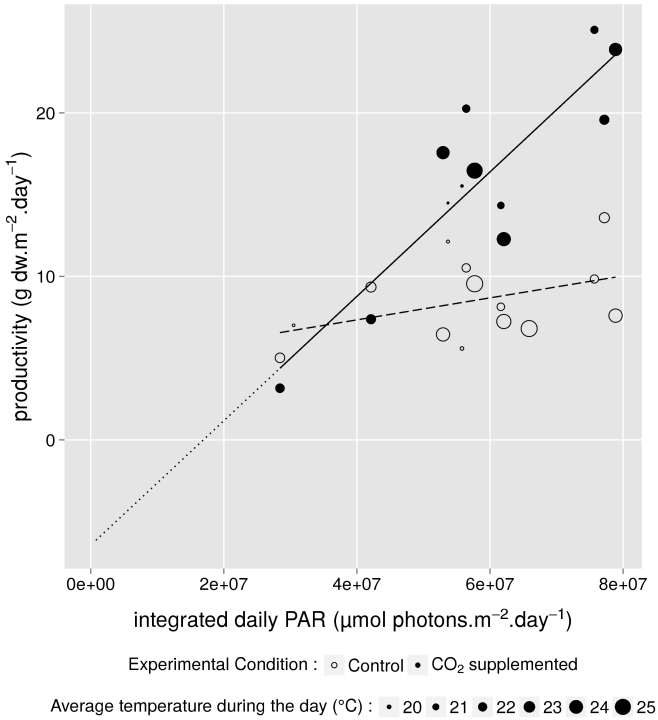

Figure 4.3: Correlation between productivity and daily integrated PAR for control and CO_2 supplemented conditions. The point size represents the average temperature during the day. Regression equation for control condition : y=4.60+6.73e(-08).x, R^2=0.18. Regression equation for CO_2 supplemented condition : y=-6.441+3.805e(-07).x, R^2=0.77.

In order to compare the growth of the control and CO_2 supplemented cultures, we made a correlation between daily areal productivity (g dry weight.m^{-2}.day^{-1}) and integrated daily photosynthetic active radiations (µmol PAR.m^{-2}.day^{-1}). Figure 4.3 shows that during cloudy days, at integrated daily PAR below about 4.10^7 µmol PAR.m^{-2}.day^{-1}, the productivity of both cultures is similar. This indicates that CO_2 supplementation is not necessary when light availability is that low. However, when light intensity increases, the productivity of the cultures differs with a near doubled productivity for the CO_2 supplemented culture during full sunny days (integrated daily PAR of about 8.10^7 µmol PAR.m^{-2}.day^{-1}). The correlations between productivity and integrated daily PAR were fitted with a linear equation.

The correlation coefficients were good for the CO_2 supplemented culture but not for the control culture (0.77 and 0.18, respectively). Two reasons may explain this fact. First, the relation is probably not linear in the control condition. The relation would probably be linear at low irradiance but would saturate at high irradiance due to limited DIC availability which would prevent an efficient photosynthesis. The second reason is the great variability observed in this condition (i.e. for the same irradiation, the productivity vary extensively). One explanation for this variability could have been the culture temperature as this parameter greatly influence the metabolic reactions of the cell. However, no relation between productivity variability and temperature (shown as the point size in figure 4.3) could be determined.

By extrapolation of the productivity/integrated PAR relationship of the CO_2 supplemented culture, the critical irradiance value for zero algal productivity was found to be 1.7e(07) µmol PAR.m^{-2}.day^{-1}. At this irradiance, a compensation point is reached at which an algal culture would not be productive due to a loss of biomass caused by respiration.

From the linear equation of the CO_2 supplemented culture, we could determine the photosynthetic efficiency (PE) of the culture. Zijffers *et al.* (2010) calculated the theoretical biomass yield based on the stoichiometric reaction equations for formation of biomass on carbon dioxide, water and the nitrogen source used for cultivation. They found a value of 1.5 g.mol photons^{-1} for *Chlorella* species when grown on nitrate media. In practice, this yield is never reached because it does not take into account: 1) The absorbed energy dissipated as heat due to exposure of algae to supersaturating light levels (typically at the surface of the culture). 2) Biomass loss due to respiration, especially during the night in outdoor condition. Night respiratory loss has been estimated to represent about 6% of biomass accumulated during the day with *Scenedesmus obliquus* (Hindersin *et al.*, 2014). In an extreme case, it attained up to 64% with a *Chlorella* species (Masojídek *et al.*, 2011)! 3) Light reflectance on the culture surface.

The PE calculation of Zijffers *et al.* is valid only for microalgae species having the same elemental composition as *Chlorella* species when grown on nitrate media. However, *Scenedesmus obliquus* elemental composition differs from *Chlorella* species (Zelibor *et al.*, 1988; Duboc *et al.*, 1999). Moreover, the nitrogen source of our medium is made of 4/5 of nitrate and 1/5 of ammonium. We thus recalculated the theoretical biomass yield for *Scenedesmus obliquus* for our medium composition (appendix). We obtained a theoretical biomass yield of 1.77 and 2.02 g.mol photons^{-1} when grown on nitrate and ammonium, respectively. These value are higher than the values obtained for *Chlorella* species, which imply that *Scenedesmus obliquus* is more efficient for biomass production than *Chlorella* species. Taking into

account the N composition of our medium, the maximum theoretical biomass yield in our culture condition was 1.82 g.mol photons^{-1}.

Using the maximal reference value and the effective value obtained in this study (0.38 g.mol photons^{-1}), we calculated a photosynthetic efficiency of 21% for the CO_2 supplemented culture. Determination of the photosynthetic efficiency of the control culture is difficult because it varies with light intensity (i.e. at low light intensity, the PE is good but at high light intensity, DIC limitations prevent an efficient light utilisation). In several studies, PE are expressed relative to the total energy of the total solar radiation, thus not including inevitable loss due to photosynthetic process whereas the calculation method of Zijffers *et al.* gives a result including these losses. In order to compare our result with those of literature, we recalculated the PE of our system by multiplying the value we obtained by the theoretical maximum PE based on the total solar radiation energy (12.4% according to Tredici, 2010), which gave a value of 2.58%. This value is in accordance with previous values obtained for such cultivation system with *Chlorella* sp. (2.88% in Trebon and 2.22% in Kalamata, see Zittelli *et al.*, 2013).

4.3.2 Characterisation of the photosynthetic apparatus in high and low CO_2 conditions

We then wanted to determine if the productivity differences were accompanied by adaptations of the photosynthetic apparatus to high and low CO_2 conditions. For this, we performed fluorescence measurements either on dark-adapted or on light-adapted samples. Dark-adapted samples were dark-adapted for 40 min to permit the relaxation of dissipation and photoprotective processes. Measurements were carried in presence of saturating DIC concentrations (10mM $NaHCO_3$) in order to measure the photosynthetic performances of the samples without limitations. In this manner, we characterised the structural adaptations of the photosynthetic apparatus. In order to characterise the photosynthetic apparatus of the cells as they were in the culture units, we also performed fluorescence measurements on light-adapted samples without $NaHCO_3$ addition. For this, samples were directly taken from the mass culture systems and submitted to the measurements. Due to the high sensitivity of the fluorimeter used for light-adapted measurements, samples had to be diluted. This was done in the cell-free medium obtained by centrifugation of the culture in order to keep the DIC concentration unchanged.

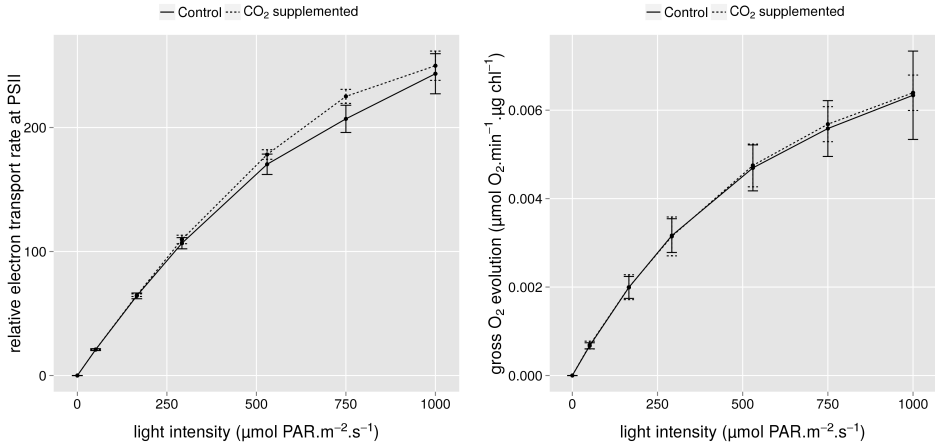

Figure 4.4: Light-response curves of the relative electron transport rate at PSII (rETR) and of the gross oxygen evolution under different light intensities in high and low CO_2 cells. Measurements were performed in presence of 10 mM $NaHCO_3$ after 40 min of dark-adaptation. Data are average of 5 measurements (±SD) obtained during the linear growth phase (beyond 0.2 g.l^{-1} biomass density) of the two experiments shown in figure 4.2.

Fluorescence and oxygen evolution measurements on dark-adapted samples

We began our analysis by determining if the two conditions led to differences in the light responses of the photosynthetic apparatus. For this, we established light-response curves for simultaneously measured relative electron transport rate at PSII (rETR) and gross oxygen evolution (VO_2) in presence of saturating DIC on 40 min dark-adapted samples. No differences in electron transport rate or gross oxygen evolution could be found between the control and the CO_2 supplemented cultures for samples taken during the linear growth phase (fig 4.4). This demonstrates that the capacity of high density cultures to realise photosynthesis was not different once the CO_2 availability limitation was removed. It is thus tempting to conclude that the structural organisation of the photosynthetic apparatus of *Scenedesmus obliquus* is not modified by CO_2 availability in our mass cultivation system.

It has been shown that ΦPSII (or ETR) measured in the light was linearly correlated to the quantum yield of oxygen or CO_2 uptake in C3 higher plants when photorespiration was avoided (Genty *et al.*, 1989; Krall and Edwards, 1990; Cornic and Ghashghaie, 1991; Genty and Meyer, 1995; Hymus *et al.*, 1999). This finding permitted the use of simple fluorescence measurements

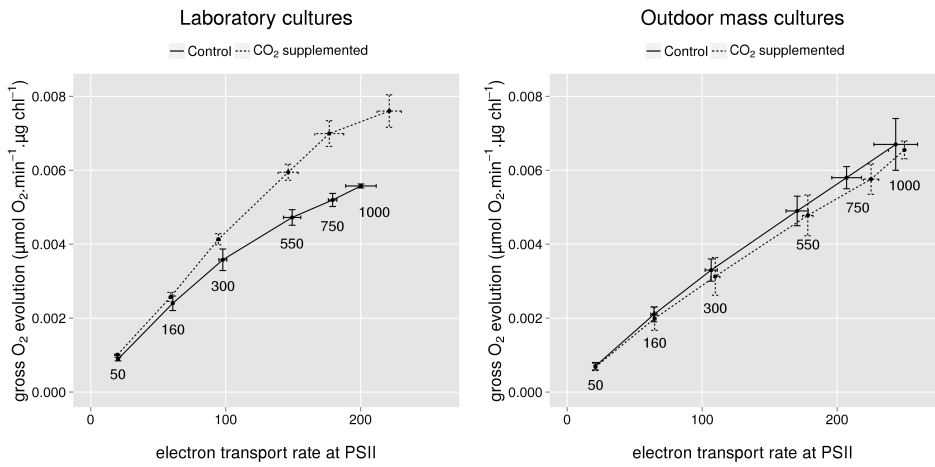

Figure 4.5: Relationship between relative electron transport rate and gross oxygen evolution measured at different light intensities. Left: Cultures grown in flasks in the laboratory under 200 µmol PAR.m^{-2}.s^{-1} continuous illumination in bold 3N medium. Cell were grown either with air or with CO_2 5% as sparging gas. Data are averages of 3 biological replicates (±SD). Right: Outdoor mass cultures. Data are average of 5 measurements (±SD) obtained during the linear growth phase of the cultures. Light intensities (µmol PAR.m^{-2}.s^{-1}) at which measurements were realised are indicated in the figure.

to estimate the CO_2 uptake and the productivity of plants.

However, the photosynthetic electron transport chain of microalgae is endowed with great flexibility, due to the existence of auxiliary electron transfer pathways (Peltier *et al.*, 2010), such as electron transfer to O_2 at PSI (known as the Mehler reaction) or through PTOX (the plastidial oxidase). Electron transfer to O_2 (most probably Mehler-type) has been found earlier to be very effective in the green microalga *Chlamydomonas reinhardtii* (Sueltemeyer *et al.*, 1986; Bassi *et al.*, 2012). In *Scenedesmus*, a significant light-dependent O_2 uptake has been shown to occur (Radmer and Kok, 1976; Radmer and Ollinger, 1980; Flameling and Kromkamp, 1998) although it was not always observed (Heinze *et al.*, 1996). The function of this O_2-dependent electron flux is not clear. It could be a way to dissipate reducing power in DIC-limited condition in order to prevent reactive oxygen species (ROS) production which would lead to damages. It could also be a way to produce the ATP needed to concentrate CO_2 when its availability is restricted. It follows that electron transport rate estimations, performed fluorimetrically (using ETR as a basis), should not necessarily match photosynthetic rate

but may include the rate of electron transport to O_2 as sink, even in the absence of significant photorespiration.

This was first investigated here in lab-grown *Scenedesmus obliquus* (grown in flasks at 200 µmol PAR.m^{-2}.s^{-1}) by plotting ETR and gross oxygen production measured at different light intensities. Measurements were carried out in presence of $NaHCO_3$ to avoid CO_2 limitations and photorespiration during the measurements. Figure 4.5 shows that the ETR/VO_2 relationship in the control and the CO_2 supplemented cultures was different, even though the CO_2 limitation was removed during measurements.

In both conditions, the relationship was characterized by a curvature which indicates that the flux of electrons is gradually redirected to O_2 with increasing irradiance. However, in CO_2 supplemented culture, the ETR/VO_2 ratio became higher than in the control culture as the light intensity increased. This indicates that the proportion of electron flux directed to O_2 is higher in low CO_2 than in high CO_2 cells. Absence of CO_2 limitation during the measurement indicates that this O_2-dependent electron flux is structurally active. It can be concluded that alternative electron flow to O_2 occurs in both conditions at high light intensity but is most active after growth in low CO_2 condition.

However, this was not the case for the outdoor mass cultures for which the ETR/VO_2 relationships were characterised by a straight line for both conditions. This observation indicates that, if we except the photorespiration which was not assessed in this study, alternative electron flow to O_2 probably either did not occur in outdoor mass culture or was independent of CO_2 supply.

The reason for the absence of differences in the ETR/VO_2 relationship for the outdoor mass culture compared to the cultures grown in the laboratory must be due to the culture conditions which were very different. While the culture grown in the laboratory was cultivated at a low density and under continuous illumination, the outdoor mass culture was characterised by a higher density, day/night cycles and light/dark cycles during the day.

Fluorescence measurements on shortly dark-adapted samples

We then measured the evolution of the PSII operating photochemical efficiency (ΦPSII) under different light intensities on light-adapted samples, i.e. after a dark period as short as 15 s which was necessary for transfer to the fluorimeter (fig 4.6). At low density during the first four days, there was no difference between the two cultures, suggesting that the control culture was not limited by DIC availability. This observation is confirmed by the small pH shift observed during the first four days (fig 4.2, second experiment). The fact that the maximal pH 11 was not attained at these days indicates

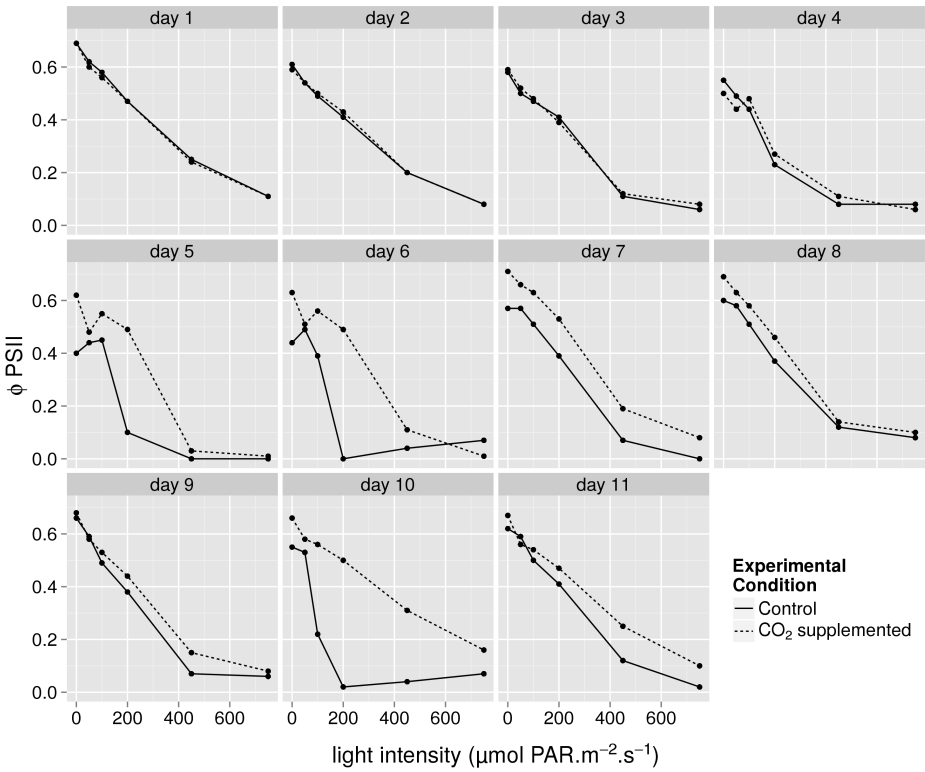

Figure 4.6: Evolution of the PSII photochemical efficiency (ΦPSII) under different light intensities during the course of the culture. Data shown are from experiment 2. A similar trend was observed for experiment 1.

that DIC availability was sufficient to sustain photosynthesis.

From day 5 to day 11, the general trend was that ΦPSII was always lower in the control culture than in the CO_2 supplemented culture, suggesting that DIC availability became too low to sustain an efficient photosynthesis in the former culture.

Noteworthy, figure 4.6 also shows that the maximal ΦPSII values (F_V/F_M obtained in the dark) became lower in the control culture compared to the CO_2-supplemented culture starting from day 5, with this difference varying from one day to another. Low F_V/F_M values in microalgae mass cultures are generally taken as indicating some degree of photoinhibition. Midday PSII photoinhibition of $\approx 30\%$ has been described in outdoor mass culture with *Arthrospira platensis* (Vonshak *et al.*, 1994; Vonshak *et al.*, 1996; Torzillo *et al.*, 1996; Torzillo *et al.*, 1998) and *Chlorella* (Masojídek *et al.*, 2011). Most photoinhibition studies conducted on *Scenedesmus obliquus* have been

performed on cultures grown in the laboratory (Flameling and Kromkamp, 1997; Yang and Gao, 2003). Here, we show that a decreased F_V/F_M also occurs in Scenedesmus obliquus grown in outdoor mass cultures and that this photoinhibition is influenced by DIC availability. It must be noted, however, that differences in F_V/F_M and ΦPSII found here in relation to CO_2 supply were suppressed after dark-adaptation (40 min) followed by $NaHCO_3$ addition in the measurement cuvette (see fig 4.4).

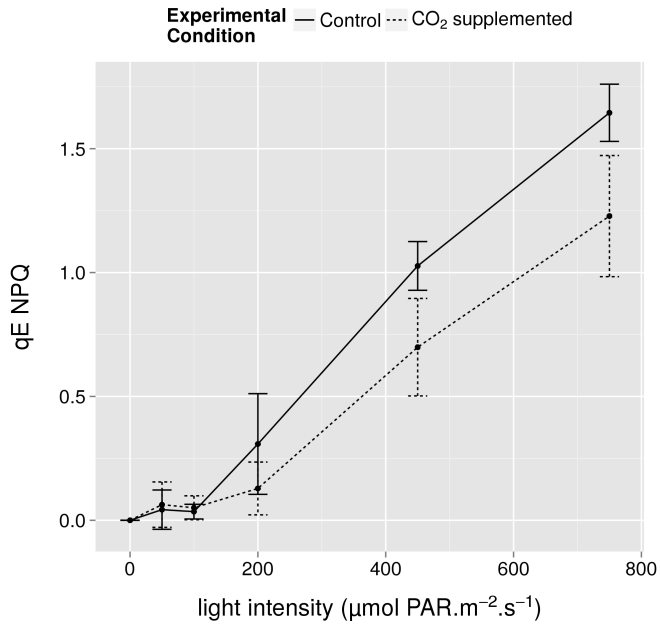

Figure 4.7: Evolution of the energy-dependent non-photochemical quenching (qE NPQ) under different light intensities showing a higher qE NPQ in the control culture than in the CO_2 supplemented culture at light intensities higher than 200 µmol PAR.m^{-2}.s^{-1}. Data are averages of 6 days (±SD) during the linear growth phase of the second culture, when DIC availability was limiting for the control culture.

A decreased photochemical efficiency (ΦPSII) in the control culture has to be compensated by dissipative mechanisms such as increased heat dissipation in the antennas (or energy dependent quenching qE NPQ). This process can be highlighted by monitoring the decrease of the F_M fluorescence level (NPQ) following illumination. We thus measured NPQ of samples directly taken from the cultures and exposed to different light intensities (fig 4.7). We checked that the fluorescence quenching observed here was relaxed in a few seconds, indicating that this quenching was due to qE NPQ and

not to photoinhibition or state transitions. Figure 4.7 shows that this NPQ was higher in the control culture than in the CO_2 supplemented culture. This demonstrates that a part of the absorbed light energy which could not be used for CO_2 assimilation due to its reduced availability in the control culture was dissipated as heat.

These measurements showed that heat dissipation for a particular light intensity is higher in the control culture compared to the CO_2 supplemented culture. However, although the cultures were inoculated at the same density, the density became different as the time elapses due to the different growth rates of the cultures (i.e. CO_2 supplemented culture density was higher than control culture density for each particular day). It follows that the average light intensity in the thickness of the cultivation system was higher in the control culture than for the CO_2 supplemented culture for the same incident light intensity and thus, differences in effective qE NPQ between the two culture must have been even higher than experimentally estimated on the basis of equal excitation.

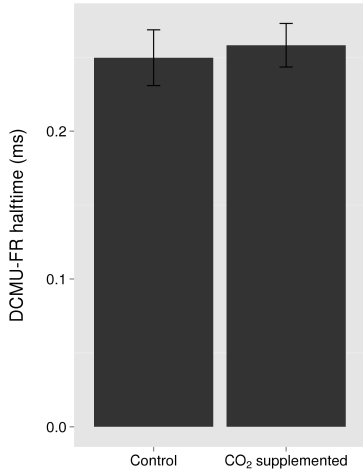

Figure 4.8: Average of the halftime of the DCMU-FR curve. The halftime is the time when the normalised variable fluorescence level reaches 0.5. Data are averages of 14 measurements (±SD) from experiments 1 and 2 during linear growth phase.

A decreased PSII antenna size has been described in low CO_2 condition compared to high CO_2 condition in *Chlamydomonas reinhardtii* cultures grown in laboratory (Berger *et al.*, 2014). This phenomenon can be interpreted as a way to avoid on over-reduction of the electron transport chain in condition of restricted DIC availability. We thus determined if the control

culture had a reduced PSII antenna size compared to the CO_2 supplemented culture. For this, we measured the functional PSII antenna size by measuring the halftime of the time course of the DCMU fluorescence rise. In presence of this inhibitor, the fluorescence rise represents the photochemical reduction of Q_A without influence of its reoxidation by plastoquinones. This measurement has been shown to be a good indicator of the PSII antenna size in *Chlamydomonas reinhardtii* (de Marchin *et al.*, 2014). We couldn't notice significant difference in the halftime between the control and the CO_2 supplemented culture during linear growth phase (fig 4.8). This indicates that the PSII functional antenna size is not modulated by CO_2 availability in *Scenedesmus obliquus* in outdoor mass culture conditions.

4.4 Conclusion

In this study, we showed that the productivity of outdoor mass cultures of *Scenedesmus obliquus* is limited by the CO_2 availability in open thin-layer cultivation systems when the light irradiance exceeds 4.10^7 µmol PAR.m^{-2}.day^{-1} for biomass densities higher than 0.25 g.l^{-1}. This limitation is suppressed by injecting carbon dioxide in the culture. In such condition, we obtained a productivity of up to 25 g dw.m^{-2}.day^{-1} and found a photosynthetic efficiency of 2.58% (value based on the total solar radiation energy). From fluorescence and oxygen evolution measurements on dark-adapted samples, we couldn't find significant differences in the ETR and oxygen evolution light saturation curves between high and low CO_2 cultures. In contrast to cultures grown in the laboratory under constant light, there was no difference in the ETR/VO_2 relationship between the two cultures. This suggests that light-dependent O_2 uptake is not enhanced by DIC limitation in outdoor mass cultures. We conclude that the structural organisation of the photosynthetic apparatus is not affected by the CO_2 availability in outdoor mass cultures in this species. From fluorescence measurements on light-adapted samples, we found a lowest PSII photosynthetic efficiency and a higher NPQ for the low CO_2 culture which could be explained by an increased heat-dissipation and photoinhibition in this culture. In contrast, we couldn't find any differences in the PSII antenna size between the two conditions. The lowest productivity of the low CO_2 culture is paralleled by a decreased PSII photochemical efficiency and an increased heat-dissipation. These results exemplify the fact that high density microalgae mass cultures should be CO_2 supplemented to ensure efficient light utilisation and biomass productivity.

Acknowledgements

Thomas de Marchin thanks the F.R.I.A. for the award of a fellowship. Fabrice Franck is research director of the Fonds de la Recherche Scientifique F.R.S-FNRS.

4.5 Appendix

The maximum theoretical biomass yield was calculated following Zijffers *et al.* (2010). Assuming an elemental composition of $CH_{1.64}O_{0.49}N_{0.10}$ for *Scenedesmus obliquus* (Zelibor *et al.*, 1988), the stoichiometric reaction equation for the formation of biomass on carbon dioxide, water and nitrogen source is the following:

- When grown on nitrate:

$$1\ CO_2(g) + 0.87\ H_2O(l) + 0.10\ NO_3^-(aq) \rightarrow CH_{1.64}O_{0.49}N_{0.10}(s) + 1.29\ O_2(g) + 0.10\ OH^-(aq) \quad (4.1)$$

- When grown on ammonium:

$$1\ CO_2(g) + 0.67\ H_2O(l) + 0.10\ NH_4^+(aq) \rightarrow CH_{1.64}O_{0.49}N_{0.10}(s) + 1.09\ O_2(g) + 0.10\ H^+(aq) \quad (4.2)$$

Assuming that the quantum yield of the light reactions is 0.1 mol O_2 evolved per mol of photons and that the molecular mass of a C-mol biomass of Scenedesmus obliquus is 22.88 g.mol^{-1}, 12.9 and 10.9 mol of photons are needed to produce one C-mol of biomass when grown on nitrate and ammonium, respectively. This leads to a theoretical biomass yield of 1.77 and 2.06 g.mol photons^{-1} when grown on nitrate and ammonium, respectively.

Chapter 5

General discussion

5.1 What chlorophyll fluorescence can and cannot do for you

Chlorophyll fluorescence has become one of the most convenient approaches to assess how absorbed light quanta are used or dissipated during photosynthesis. This is due to its sensitivity, its non-invasiveness and the wide availability of measuring instruments. The analysis of the fast chlorophyll fluorescence transient has been widely used to monitor the transition of PSII from the open to the closed state shortly after the transition from darkness to light. Because the yield of fluorescence emission is controlled by the Q_A reduction state, which is directly dependent of its light-induced reduction and its reoxydation by the plastoquinone pool, chlorophyll fluorescence gives insight into the functioning of PSII as well as processes occurring downstream of it. Using DCMU, it is possible to isolate the PSII from the electron transport chain and thereby isolate the photochemical phase of the fast chlorophyll *a* fluorescence transient. We used this method in chapter 2 to study the variations in PSII optical cross-section during a state transition. A detailed analysis of the kinetics of the fluorescence transient allowed us to show that state transitions can be explained by an inter-conversion of PSIIα and PSIIβ with constant kinetic characteristics. In our study, we only focussed on PSII regardless of the changes affecting PSI. While it is well accepted that the PSII optical cross-section decreases during a state 2 transition, conflicting views have been expressed on the fact that all the LHCII released from PSII may bind to PSI. The experimental evidences and the arguments in favor or against a complementary change in PSI and PSII optical cross-sections during state transitions are discussed in the annex.

The study of the photosynthetic apparatus using fluorimetry boomed in the eighties with the development of the PAM fluorimetry. In contrast to

the direct measurement of the fast chlorophyll fluorescence transient, this method allows to measure the fluorescence yield in the presence of additional continuous light required for the purposes of the experiment. A measurement *in-situ* can be made by simply pointing the fluorimeter fiber-optics at a photobioreactor or by submersing it into a suspension.

From an ecophysiological perspective, PAM fluorimetry development allowed to get a better understanding of the photosynthesis of diverse microalgae in their natural habitats. From a more applied perspective, it can be a valuable tool to monitor microalgae cultures (reviewed in Masojídek *et al.*, 2010). Since unfavorable environmental conditions often affect the functioning of PSII, chlorophyll fluorescence represents a useful monitoring tool in microalgal biotechnology. Its measurement gives a rapid evidence of stress affecting the photosynthetic activity of the culture such as nutrients limitations, non-optimal temperatures and/or high light exposure.

In this thesis, we used chlorophyll fluorescence together with O_2 evolution measurements to study the adaptations of the photosynthetic apparatus to high and low CO_2 conditions under different light intensities. These studies were conducted on *Chlamydomonas reinhardtii* cultures cultivated in photobioreactors and on *Scenedesmus obliquus* cultivated in an outdoor mass microalgae culture system.

The measurement of chlorophyll fluorescence in light-adapted cells showed a decreased PSII photochemical efficiency in cultures limited by CO_2 availability. This decreased light use efficiency was concomitant to a decreased growth rate and productivity. The light-induced heat-dissipation was also increased in low CO_2 conditions, especially under high light and we found that this process was greatly influenced by the CO_2 availability. While energy-dependent qE quenching is generally described as a response to high light exposure (Iwai *et al.*, 2007), we provide evidence that this photoprotective mechanism can rather be described as a response to electron transport chain saturation. This saturation being influenced by the balance between the conversion of light into chemical energy and its use for the absorption and reduction of carbon dioxide and nutrients in order to produce biomass.

Surprisingly, by measuring 77K fluorescence spectra, we observed that an increased proportion of energy was absorbed by PSI in high light in high CO_2 cells compared to low CO_2 cells in *Chlamydomonas reinhardtii*. This observation could be explained by a decreased PSII antenna size (as determined by DCMU fluorescence rise measurements) and by a state 2 transition in high CO_2 conditions. We thus concluded that CO_2 availability influences the energy distribution between PSI and PSII. Our conclusions are in apparent contradiction with previous studies which showed an increased PSII light-harvesting capacity in high CO_2 conditions compared to low CO_2 conditions (Berger *et al.*, 2014). Moreover, in some of these works, state 2

transition and reduced PSII activity have been observed when cells acclimated to high CO_2 where transferred to low CO_2 concentrations (Palmqvist *et al.*, 1990; Falk and Palmqvist, 1992; Iwai *et al.*, 2007). We ascribe these different results to the different acclimation times used in previous studies compared to the present one. While previous studies were conducted on short-term acclimated samples (i.e. high CO_2 cultures were subjected to CO_2 depletion during a few minutes or hours), our study was conducted on long-term acclimated samples (i.e. cultures were cultivated in high and low CO_2 for at least three days). In this respect, we propose that two acclimation phases can be described in response to a decrease in dissolved CO_2 concentration: a short-term acclimation as evidenced in previous studies and a long-term acclimation as evidenced in this study.

In contrast, no difference in PSII antenna size could be determined in *Scenedesmus obliquus* cultures grown in outdoor mass culture systems in high or low CO_2 conditions. This absence of difference, compared to laboratory grown *Chlamydomonas* cultures, could be explained either by the possible existence of different photoprotection mechanisms in the two species or by the culture conditions which were very different. While the cultures grown in the laboratory were cultivated at a low density and under continuous illumination, the outdoor mass cultures were characterized by a higher density, day/night cycles and light/dark cycles during the day.

Many attempts have been made to use fluorescence as a tool to estimate the quantum yield of photosynthesis. An important step in this respect was the demonstration of a linear relationship between ΦPSII and ΦCO_2 (the quantum yield of CO_2 fixation), when photorespiration was avoided, in higher plants (Genty *et al.*, 1989). This finding suggested that it would be possible to use simple fluorescence measurements to estimate the CO_2 uptake rate and hence the productivity of microalgae cultures. However, 25 years later, we are still not able to estimate culture productivities based on fluorescence signals. Two major explanations can be advanced:

Discrepancies between PSII electron transport rate and CO_2 fixation rate Other sinks than CO_2 reduction can lead to the uncoupling between ETR, O_2 evolution and CO_2 fixation. Among them, we find the assimilation of nutrients such as nitrogen. Indeed, the proportion of electrons diverted to nitrogen assimilation depends of the nitrogen form present in the medium (NH_4^+, NO_3^- or urea) and is thus dependent of the culture conditions (Turpin, 1991). The photosynthetic electron transport chain of microalgae is also endowed with great flexibility due to the existence of auxiliary electron transfer pathways such as electron transfer to O_2 via photorespiration, chlororespiration and/or the Mehler-type reactions (re-

viewed in Peltier *et al.*, 2010). Therefore, electron transport rate estimations performed fluorimetrically (using ETR as a basis) should not necessarily match photosynthetic rate but may include the rate of electron transport to O_2 as sink. Although the study of such discrepancies may be interesting to answer complex physiological questions, from a more applied perspective, it means that accurate determination of CO_2 fixation is not possible with fluorescence measurements, unless complemented by other measurements.

Electron transport to O_2 can be evidenced by simultaneously measuring the electron transport rate at PSII (ETR derived from fluorescence measurements) and the gross oxygen evolution rate. Because the electron transport rate measured at PSII reflects the total linear electron flux while oxygen evolution is the balance of the oxygen evolved by PSII and the oxygen consumed by other pathways, a difference between these two measurements should reflect a light-dependent O_2 uptake.

Concomitant measurements of fluorescence-based electron transport rate and of polarographically-measured O_2 exchanges have already been used to show a deviation between ΦO_2 and ΦPSII in a variety of microalgae species. This deviation was mainly ascribed to the existence of an alternative electron transport to O_2 (Rees *et al.*, 1992; Flameling and Kromkamp, 1998; Franck and Houyoux, 2008) although it could also be explained by a cyclic electron transport around PSII (Falkowski *et al.*, 1986). However, a light-dependent O_2 uptake has clearly been evidenced by mass spectrometry approaches (Radmer and Kok, 1976; Radmer and Ollinger, 1980; Peltier and Thibault, 1985; Sueltemeyer *et al.*, 1986; Sültemeyer *et al.*, 1993). Moreover, a recent study of Roberty *et al.* (2014) on the dinoflagellate *Symbiodinium* sp. evidenced a significant alternative electron transport to O_2 and a perfect relationship between the electron transport rates measured at PSII and at PSI. This rules out the possibility of an electron leak at PSII due to a cyclic electron transport around PSII. Altogether, the available data favor the idea that the deviation between ΦO_2 and ΦPSII is due to an alternative electron transport to O_2.

However, the expression of fluorescence results in terms of relative ETR values (rETR) does not allow quantitative comparisons with VO_2 values, which makes it impossible to derive the rates of electron transport to O_2. This problem was carefully investigated in chapter 3 in *Chlamydomonas reinhardtii* laboratory grown cultures. We developed a method to rationalize the relationship between the apparent quantum yields of oxygen evolution and of electron transport at PSII while taking into account the variations in the proportion of energy absorbed by PSII. This relationship allowed us to derive quantitative parameters such as the quantum yield of the alternative electron transport measured at PSII and the ratio of the rate of this electron transport to the total linear electron transport rate. Using this approach we

demonstrated the importance of alternative electron transport to O_2 in low CO_2 cells. We showed that this alternative electron transport represented up to 60% of the total electron transport in low CO_2 acclimated cells even when the CO_2 limitation had been removed by bicarbonate addition. In contrast, no significant alternative electron transport was detected in high CO_2 acclimated cells. We thus suggest that the alternative electron transport to O_2 observed in low CO_2 cells represents an adaptation that could help to meet the higher ATP demand for the concentration of CO_2 by the CCM. In contrast, in high CO_2 conditions, the absence of the CCM would reduce the need for ATP and thus the need for electron transport to O_2. Altogether, our results suggest that the alternative electron transport to O_2 evidenced here could be driven by a Mehler-type reaction.

In contrast to laboratory grown cultures, we could not evidence any difference in the alternative electron flow to O_2 in outdoor mass cultures of *Scenedesmus obliquus* based on ETR/VO_2 relationships (chapter 4). Again, this difference compared to laboratory grown cultures is certainly to be found in the different culture conditions. While the cultures grown in the laboratory were cultivated at a low density, the outdoor mass cultures were cultivated at a higher density. At high density, local irradiance is reduced due to light absorption by the successive layers of the suspension. As a result, the photosynthesis and CO_2 fixation rates decrease. It is thus possible that the CCM may be less active at high density compared to low density. In this case, the decreased activity of the CCM would reduce the need for ATP and thus the need for a highly efficient light-dependent O_2 uptake.

Despite the growing number of studies showing the occurrence of alternative electron transport to O_2 in microalgae, only few studies have directly compared simultaneous measurements of chlorophyll fluorescence and O_2 evolution. We believe that this approach should be used more often in order to understand the underlying nature of the variable relationships between rates of electron transport, O_2 evolution and CO_2 fixation.

The fluorescence signal alone cannot be used to calculate the quantitative (absolute) electron transport rate PAM fluorimetry is used to estimate the quantum yield of photosystem II (ΦPSII). This value represents the average quantum yield of the PSII population and is often multiplied by the light intensity to obtain a relative estimate of the electron transfer rate through PSII (rETR): $\mathrm{rETR} = \Phi\mathrm{PSII} * \mathrm{PFD} * 0.5$. However, there are a number of assumptions in this calculation, most notably that excitation energy is equally absorbed by PSI and PSII. This is often not true since it is well known that the optical cross-sections of both photosystems can vary in different culture conditions due to state transitions and PSII

antenna size variations.

For many ecological and industrial applications, absolute rates of photosynthetic electron transport are highly desirable. Translating a rETR value to an absolute ETR requires the quantification of the light absorption specific to PSII. A more robust equation to calculate a true ETR in order to compare samples with different light absorption characteristics has been derived: $\mathrm{ETR} = \Phi\mathrm{PSII} * \mathrm{PFD} * \sigma_{\mathrm{PSII}} * [\mathrm{PSII}]$, where σ_{PSII} is the optical cross-section of PSII and [PSII] is the concentration in PSII reaction centres. σ_{PSII} can be directly derived with particular fluorimetry techniques such as the pump and probe (Kolber and Falkowski, 1993), the Fast Repetition Rate fluorescence (Kolber *et al.*, 1998), or as we did in chapter 3 by monitoring the decrease of F'_M due to state transitions. The concentration in PSII reaction centers [PSII], however, has to be determined by independent methods, which can be complex and time-consuming. Therefore, fluorescence measurements alone cannot be used to calculate an absolute ETR and derive a biomass productivity.

5.2 Perspectives

5.2.1 Determination of the cell redox state in high and low CO_2 conditions

In chapter 3, we showed the occurrence of significant alternative photosynthetic electron transport in low CO_2 *C. reinhardtii* cells that we ascribe to a Mehler-type electron transport to O_2. We suggest that this alternative electron flow represents an adaptation that could help to meet the higher ATP demand for the concentration of CO_2 by the CCM. We also observed a higher qE NPQ under low CO_2 which implies that there is a significant ΔpH across the thylakoid membrane in this condition. It is surprising that a ΔpH is maintained in low CO_2 conditions though there is a significant ATP consumption by the CCM. On the other hand, one could imagine that the alternative electron transport to O_2 is not enhanced by the ATP demand from the CCM but rather due to a limitation in the pool of electron acceptor $NADP^+$ in case of low CO_2 availability. In this case, the ATP produced by the alternative electron transport to O_2 could exceed the ATP demand of the CCM, thus conducting to a significant ΔpH across the thylakoid membrane which would ultimately lead to the development of qE NPQ. We think that it would be interesting to assess the redox and phosphate potential states of the cells in high and low CO_2 conditions and under different light intensities, for example by performing ADP/ATP and $NADP^+$/NADPH measurements. This would permit to have a better understanding of the metabolic changes that occur in response to CO_2 limitation.

5.2.2 What is the relative contribution of light-dependent O_2 uptake and CEF?

Cyclic electron transport around PSI (CEF) has long been thought to be the mechanism responsible for the adjustment of the ATP/NADPH ratio (Spalding *et al.*, 1984; Miyachi *et al.*, 2003). In this respect, Lucker and Kramer (2013) recently observed a 33% increase of CEF/LEF in low CO_2 *Chlamydomonas* cells compared to high CO_2 cells at steady-state and in physiological conditions. They suggested that CEF could provide sufficient energy in the form of ATP to power the CCM. However, this was recently challenged by Dang *et al.* (2014) who showed that the growth rate of the CEF mutant *pgrl1* was similar to the *wild-type* under a wide range of illuminations and CO_2 concentrations and that a combination of mitochondrial cooperation and oxygen photoreduction downstream of PSI (Mehler reactions) may provide the ATP needed to supply the CCM. We think that it may not be relevant to consider one of the pathways (i.e. alternative electron transport to O_2 and CEF) to be more important than the other for the generation of ATP. Taking into account that for efficient CEF operation, the PQ and NADPH pool must be partly oxidized (Allen, 2003), CEF would be impaired by a lack of electron acceptors when the availability of CO_2 is severely restricted. In this condition, light-dependent O_2 uptake could be the main mechanism able to generate the supplemental ATP needed by the CCM. Clearly, it would be really interesting to quantify the relative contribution of alternative electron transport to O_2 and CEF on the synthesis of the extra ATP needed by the CCM in different conditions.

5.2.3 Measuring O_2 evolution in physiological conditions

Measurements of photosynthetic O_2 evolution are usually performed with a Clark electrode in a closed chamber. The problem is that the DIC concentration in the chamber rapidly decreases due to photosynthesis. In a similar manner, O_2 concentration increases. To avoid any CO_2 depletion during the measurement, which could reduce the photosynthetic rate significantly, $NaHCO_3$ is added at a saturating concentration. However, by doing so, the photosynthetic measurements are realized in conditions which significantly differ from the culture conditions and cells may not behave as they would in the culture system. For example, at high DIC concentration, photorespiration is inhibited. In other words, the enclosure of a sample in a closed chamber necessarily alters the environmental conditions to which it has been previously exposed.

We think that it would be interesting to rely on another approach to measure the O_2 evolution without changing the conditions. It is possible to

do this using an open flow gas exchange system. In such system, the cell suspension is placed in a semi-closed photobioreactor through which gas is flushed at a measured flow rate and then vented to atmosphere. Differences in O_2 and CO_2 concentrations between the gas entering the system (reference gas) and that leaving the system (sample gas) are multiplied by the flow rate to obtain rates of gas exchange (Hunt, 2003). This approach has two major advantages over the more often used closed systems: (1) it is easier to control environmental conditions in a flushed chamber than in one that is sealed, and (2) the analysis is non-invasive so that the same culture may be measured at different stages of development, or at different times after the imposition of a treatment.

5.2.4 Determining the light-dependent O_2 uptake pathway in physiological conditions

In chapter 3, we suggested that the alternative electron transport found in low CO_2 acclimated cells could be mediated by a Mehler-type reaction. For this, we took care to inhibit photorespiration (by addition of $NaHCO_3$) and we found that this electron transport persisted or was even enhanced when other O_2 consuming pathways were inhibited by using inhibitors or in appropriate mutants. The problem when using inhibitors is that they lead to dramatic changes of the metabolism, which can conduct to an increase or a decrease of the investigated pathways. Similarly, mutants may have acclimated to their mutation by adapting their metabolism. Therefore, care should be taken when generalizing observations obtained with mutants and/or inhibitors to a *wild-type*. Further development of non-invasive techniques which allow to measure these fluxes in a *wild-type* in physiological conditions would be highly desirable.

By applying an oxygen isotope discrimination technique, it is possible to discriminate between the O_2 uptake pathways *in vivo* without using inhibitors (Guy *et al.*, 1989). The starting point of this method is that O_2 originating from PSII is produced without isotopic fractionation while the different O_2 uptake pathways discriminate differentially against oxygen isotopes. Knowing the discriminations end points of the different pathways against O^{18} (Cyt pathway $\approx$ 18 ‰, AOX pathway $\approx$ 28 ‰, Mehler $\approx$ 15 ‰, photorespiration $\approx$ 22 ‰, see Angert *et al.*, 2003), it should be theoretically possible to estimate the electron fluxes of these different pathways by determining the enrichment in O^{18}. This method has already been used to discriminate the dark respiration between the Cyt and AOX pathways (McDonald *et al.*, 2002). However, isotopic discrimination in the light is complicated due to the existence of at least five different pathways which can occur simultaneously. To our knowledge, such method has never been used to study the importance

of the different O_2 uptake pathways in the light and it would be challenging to investigate it.

5.2.5 Why measuring chlorophyll fluorescence on microalgae mass cultures is not an easy task

In contrast to the determination of O_2 evolution with a Clark electrode, fluorescence measurements can be performed directly in the culture conditions by submersing the probe of a fiber-optics PAM fluorimeter in the photobioreactor. However, in order to characterize the photosynthetic performances of the whole culture, the culture must be homogeneous and its density must be low to reduce self-shading. This was the case for cultures grown in photobioreactor (chapter 3), which allowed us to show a decreased PSII photochemical yield and an increased NPQ in CO_2-limiting condition.

In our outdoor open thin-layer cascade mass culture system (chapter 4), however, cultures were highly concentrated and we noticed the appearance of algae flocks. In high densities cultures, fluorescence measurements are derived mainly from the surface layer of the suspension closest to the excitation light and as such, they can not be considered representative of the entire sample. To circumvent this problem, we performed our light-adapted fluorescence measurements by diluting our samples in the cell-free medium (thus keeping the DIC concentration unchanged) in a cuvette and subsequently submitting them to an illumination protocol in a portable device. If these measurements were really helpful to evidence differences in PSII photochemical efficiency and light-induced heat-dissipation between the control and the CO_2 supplemented cultures at the light intensities given by the portable device, it would be really interesting to obtain a picture of the photosynthetic performances of the entire culture in the given culture conditions. One approach to study photosynthesis in microalgae mass cultures is based on the modelling of light and dissolved gas profiles taking into account the thickness of the suspension and the microalgae concentration (reviewed in Béchet *et al.*, 2013). Together with the development of better adapted chlorophyll fluorescence imaging systems, this could open new perspectives to the study of photosynthesis in microalgae mass cultures.

Chapter 6

Annex

Conflicting views concerning the complementary change in PSI and PSII optical cross-sections during state transitions

Conflicting views have been expressed on the complementary decrease and increase in PSII and PSI optical cross-sections during a state transition in *Chlamydomonas reinhardtii*. The original model of Delosme *et al.* (1996) proposes that all the LHCII released from PSII during a transition to state 2 bind to PSI. However, this model has been recently challenged by several studies. In higher plants, conflicting views have also been expressed on the complementary decrease and increase in PSII and PSI optical cross-sections (see Allen, 1992 for an extensive review). In the following section, we discuss the arguments in favor and against a complementary change in PSI and PSII optical cross-sections during state transitions in *Chlamydomonas reinhardtii*, an organism which is known to be characterised by extensive state transitions, in contrast to higher plants.

Studies against a complementary change in PSI and PSII optical cross-sections during state transitions

Unlu *et al.* (2014): Recently, these authors proposed that, in *Chlamydomonas reinhardtii*, only 10% of the LHCII released from PSII binds to PSI in State 2 and the rest is quenched. Their conclusion was based on two observations: (1) The 77K fluorescence intensity of PSI was only slightly higher in state 2 than in state 1 whereas it was significantly decreased for PSII. (2) Time-resolved fluorescence decay kinetics can be fitted with different components associated with PSI or PSII. The authors did not observe an increase in the relative amplitude component associated with PSI when

cells were in state 2.

In our opinion, 77K fluorescence can only be used to indicate variations in the relative antenna size of the two photosystems. Absolute determination of variations in the photosystems optical cross-sections between different samples is very difficult for two main reasons: (1) during a state transition, there is a change in the thylakoid structure conducting to changes in light dispersion in the sample, and (2) because of the low temperatures conditions, ice can accumulate around the sample and the absorbed and emitted lights can differ depending of the amount of ice. Concerning fluorescence lifetime studies, it requires a mathematical treatment implying a fitting procedure. As we used fitting procedures in chapter 2, we know that the choice of the number of components in the fit as well as the constrains affected to this fit can be somewhat subjective. In other words, identical data mathematically treated by two different persons could give different results. It should be pointed out that Wlodarczyk *et al.* (2015) showed very recently a significantly higher increase in the PSI optical cross-section in state 2 than previously described by Unlu *et al.* (2014) although they also performed 77K fluorescence and time-resolved fluorescence measurements. This emphasizes the fact that conclusions obtained using such measurements must be taken with care.

Iwai *et al.* (2009): In their study, the fluorescence lifetime in live *Chlamydomonas reinhardtii* cells was monitored under a fluorescence microscope during a transition from State 1 to 2. Initially, the average lifetime of fluorescence emitted between 680 and 700 nm was 170 ps, which was largely due to the PSII-bound LHCII, but it shifted to 250 ps when the cells were in transition to State 2 after 5min. Because a mutant lacking both photosystems but having retained free LHCII shows the same fluorescence lifetime, this 250 ps component was ascribed to dissociated and free LHCII. Further biochemical analyses indicated that dissociated phospho-LHCII formed a large aggregated structure, whereas unphosphorylated LHCII did not (Minagawa, 2011a). This indicates that a part of LHCII released from PSII do not effectively bind to PSI but aggregates and are in energy-dissipative form, which has previously been suggested (Tokutsu *et al.*, 2009).

Nagy *et al.* (2014): Using absorption spectroscopy and fluorescence measurements, the authors reveal that the enhancement of PSI antenna size during state 1 to state 2 transition (≈20%) is not commensurate to the decrease in PSII antenna size (≈70%), leading to the possibility that a large part of the phosphorylated LHCIIs do not bind to PSI in state 2, but instead form energetically quenched complexes. They obtained the state 2 transition by incubating cells in anoxia. The problem, when PSI antenna

size is measured from P700 oxidation kinetics, is that the pool of NADPH becomes highly reduced under anoxia and little or no $NADP^+$ acceptors are available to oxidize the PSI. This can lead to an underestimation of the size of the PSI antenna in state 2 because less absorbed photons are used for charge separations. This problem could perhaps be overcome using the method we developed in chapter 2 to obtain a state 2 with an oxidised electron transport chain.

Studies in favor of a complementary change in PSI and PSII optical cross-sections upon state transitions

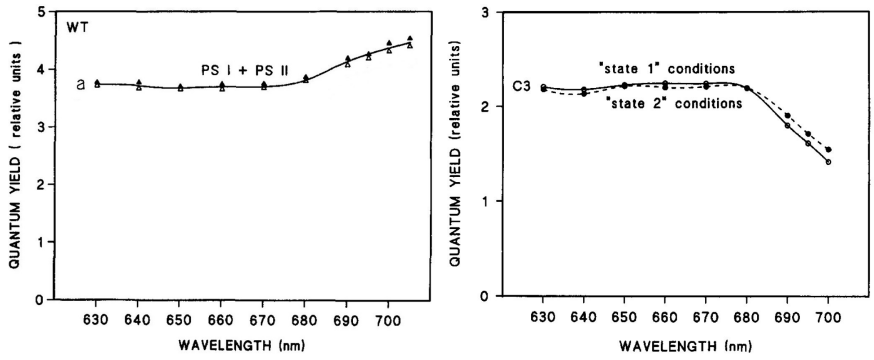

(a) (b)

Figure 6.1: (a): Spectral dependence of the quantum yield in *Chlamydomonas reinhardtii*. Solid symbols, state 2 conditions; open symbols, cells fixed in state 1. (b): Spectral dependence of the quantum yield in a PSI deficient strain. Solid symbols, state 2 conditions; open symbols, state 1 conditions. Figures modified from Delosme *et al.*, 1996.

Delosme *et al.* (1996): The authors investigated the changes in light energy distribution to the reaction centres of PSI and PSII upon state transitions *in Chlamydomonas reinhardtii* by a photoacoustic method. The principle of this method is to detect the volume changes occurring in a thin layer of photosynthetic suspension during the first microsecond following a monochromatic laser flash with a piezoelectric ceramic. These volume changes result from two components of opposite signs: (1) thermal expansion due to the release of heat by dissipation processes in the medium, and (2) contraction occurring in the neighbourhood of the charged photoproducts. Under weak flash excitation, the difference between the amounts of heat released by an active and an inactive sample measures the energy stored by the photoreactions. As the two components of the signal are linearly related to the number of flash-induced charge separations, the overall volume

change, when compared between the active and inactive states of the sample, gives a relative measure of the quantum yield of charge separations (Delosme *et al.*, 1994). Figure 6.1a shows the spectral dependence of the quantum yield of charge separations (including both photosystems) in *Chlamydomonas reinhardtii* in state 1 and state 2. The similarity of the two spectra indicates that, in both states, the same number of absorbed light quanta are converted to chemical energy, regardless of the light energy distribution among the two types of reaction centre. If a part of LHCII released from PSII in state 2 would not bind to PSI, the quantum yield in state 2 should be lower than in state 1. Figure 6.1b shows the spectral dependence of the quantum yield of PSII in state 1 and 2 in a mutant strain deficient in PSI. The spectrum is practically the same in both situations, and indicates that the whole PS II antenna remains efficiently connected to the PS II reaction centres, under both state 1 and state 2 conditions. If LHCII could aggregate and be in a quenched state in state 2, the quantum yield in state 2 should be lower than in state 1. Taken together, these results indicate that all the LHCII released from PSII in state 2 bind to PSI. In our opinion, these results cannot be easily contradicted since they did not result from a complex mathematical treatment but result from a direct measure of the photosystems quantum yield.

Conclusion

Based on the fact that the observations of Delosme *et al.* (1996) are the only ones which do not involve a complex interpretation or mathematical treatment (if we except the work of Nagy *et al.* (2014), who probably underestimated the optical cross-section of PSI in state 2), we favor the view that there is a complementary change in PSI and PSII optical cross-sections during a state transition. It remains that the results of Unlu *et al.* (2014) are intriguing though the relevance of their conclusions could be questioned in regard with the contradictory results obtained by Wlodarczyk *et al.* (2015) who used a similar experimental approach. Obviously, the observation of Iwai *et al.* (2009) concerning a pool of aggregated and quenched LHCII in state 2 cannot be excluded. Clearly, more studies would be needed in order to definitely choose between a complementary and a non-complementary change in PSI and PSII optical cross-sections during state transitions.

List of Figures

1.1 Simplified carbon cycle 18
1.2 Representation of a *Chlamydomonas* cell 19
1.3 Mitochondrion structure 21
1.4 Mitochondrial electron transport chain 22
1.5 Chloroplast structure 24
1.6 Chloroplastic electron transport chain 25
1.7 The Calvin cycle 27
1.8 Model of the CCM of Chlamydomonas reinhardtii. 30
1.9 Fate of excited chlorophyll. 38
1.10 Fast chlorophyll *a* fluorescence transient 40
1.11 Typical chlorophyll fluorescence measurement with a PAM fluorimeter. 42
1.12 Representation of oxygen electrode reactions. 44

2.1 Time course of the DCMU-FR and value of the rate constant of photochemistry of PSIIα and PSIIβ measured at different light intensities on the *wt* strain *1690*. 60
2.2 Correlation between $\frac{1}{\tau}$ and the proportions of PSIIα and PSIIβ. 62
2.3 Determination of changes in the redox status of PQ pool and state transitions by PAM fluorimetry. 65
2.4 Variations in the 77K ratio, $1/\tau$ and proportions of PSIIα during a transition from state 2 to state 1. 67
2.5 Residuals of the fits for models 1, 2 and 3. 71
2.6 DCMU-FR of *wt* strain 1690 in state 1 and in state 2 and residuals for the fits. 71

3.1 Light-response curves of the relative electron transport rate at PSII and of the gross oxygen evolution in high and low CO_2 conditions. 85
3.2 Relationship between relative electron transport rate and gross oxygen evolution in high and low CO_2 conditions. . . . 86

3.3 Comparison of the $\Phi O_2(r)/\Phi PSII$ relationship in cells cultivated under high and low CO_2 conditions. 91
3.4 Φ_{PSII}^{ALT} and ETR^{ALT}/ETR light-response curves for cells grown in high and low CO_2 conditions under 900 µmol $PAR.m^{-2}.s^{-1}$. 92
3.5 Φ_{PSII}^{ALT} and ETR^{ALT}/ETR light-response curves for cells grown in high and low CO_2 conditions under 200 and 400 µmol $PAR.m^{-2}.s^{-1}$. 94
3.6 Φ_{PSII}^{ALT} and ETR^{ALT}/ETR light-response curves for the *wild-type* and the *dum22* mutant grown under low CO_2. 95
3.7 Φ_{PSII}^{ALT} and ETR^{ALT}/ETR light-response curves for the *wild-type* and the *wild-type* in presence of SHAM 2mM grown under low CO_2. 95
3.8 Φ_{PSII}^{ALT} and ETR^{ALT}/ETR light-response curves for the *wild-type Jex4* and the *ptox2* mutant grown under low CO_2. . . . 96
3.9 Western blot analysis of FlvA abundance in low and high CO_2 conditions. 97
3.10 H_2O_2 production after 90 min of incubation in high and low CO_2 conditions and in the dark or under illumination. 98
3.11 PSII operating photochemical efficiency in cultures grown in high and low CO_2 conditions. 99
3.12 (a): Xanthophyll de-epoxydation index of cultures cultivated in high and low CO_2 conditions. (b): Western blot analysis of the LHCSR3 protein in high and low CO_2 conditions. (c): NPQ of cultures cultivated in high and low CO_2 conditions. . 100
3.13 Evolution of the NPQ following $NaHCO_3$ addition on low CO_2 cells. 102
3.14 (a): Variations in the relative proportion of PSII fluorescence at 77K in light-adapted high and low CO_2 cells. (b): Variation of the halftime of the DCMU-FR in 30 min dark-adapted high and low CO_2 cells. 103
3.15 Fluorescence traces during the state 2 transition in darkness after addition of FCCP 1µM in high and low CO_2 *wild-type* cells and in low CO_2 *ptox2* cells. 107
3.16 Effect of fast-O_2 removal on the fluorescence traces during the photosynthesis induction under actinic light in the *wild-type Jex4* and the *ptox2* mutant grown in low CO_2 conditions. . . 109

4.1 Pictures of the outdoor open thin-layer cascade system. . . . 114
4.2 Summary of the data acquired during the two successive experiments. 120
4.3 Correlation between productivity and daily integrated PAR. . 121

4.4 Light-response curves of the relative electron transport rate at PSII (rETR) and of the gross oxygen evolution under different light intensities. 124
4.5 Relationship between relative electron transport rate and gross oxygen evolution measured at different light intensities. 125
4.6 Evolution of the PSII photochemical efficiency (ΦPSII) under different light intensities during the course of the culture. . . 127
4.7 Evolution of the energy-dependent non-photochemical quenching (qE NPQ) under different light intensities. 128
4.8 Average of the halftime of the DCMU-FR curve. 129

6.1 Spectral dependence of the quantum yield of charge separations in *Chlamydomonas reinhardtii* determined by photoacoustic. 145

Bibliography

Akaike, H. (1974). "A new look at the statistical model identification". In: *IEEE Trans. Autom. Control* 19.6, pp. 716–723.

Allen, J. (1992). "Protein phosphorylation in regulation of photosynthesis". In: *BBA* 1098.1098, pp. 275–335.

Allen, J. F. (2003). "Cyclic, pseudocyclic and noncyclic photophosphorylation: new links in the chain". In: *Trends in plant science* 8.1, pp. 15–19.

Allorent, G., Tokutsu, R., Roach, T., Peers, G., Cardol, P., Girard-Bascou, J., Seigneurin-Berny, D., Petroutsos, D., Kuntz, M., Breyton, C., Franck, F., Wollman, F.-A., Niyogi, K. K., Krieger-Liszkay, A., Minagawa, J., and Finazzi, G. (2013). "A Dual Strategy to Cope with High Light in Chlamydomonas reinhardtii". In: *The Plant Cell* 25.2, pp. 545–557.

Alric, J. (2010). "Cyclic electron flow around photosystem I in unicellular green algae". In: *Photosynthesis research* 106.1-2, pp. 47–56.

Alric, J. (2014). "Redox and ATP control of photosynthetic cyclic electron flow in Chlamydomonas reinhardtii". In: *Biochimica et Biophysica Acta (BBA) - Bioenergetics* 1837.6, pp. 825–834.

Anderson, J. M. (1986). "Photoregulation of the composition, function, and structure of thylakoid membranes". In: *Annu. Rev. Plant. Physiol.* 37.1, pp. 93–136.

Anderson, J. M. and Melis, A. (1983). "Localization of different photosystems in separate regions of chloroplast membranes". In: *PNAS* 80.3, p. 745.

Angert, A., Rachmilevitch, S., Barkan, E., and Luz, B. (2003). "Effects of photorespiration, the cytochrome pathway, and the alternative pathway on the triple isotopic composition of atmospheric O2". In: *Global Biogeochemical Cycles* 17.1.

Arnon, D. I. and Chain, R. K. (1975). "Regulation of ferredoxin-catalyzed photosynthetic phosphorylations". In: *PNAS* 72.12, pp. 4961–4965.

Arnon, D. I., Tsujimoto, H. Y., and Mcswain, B. D. (1967). "Ferredoxin and Photosynthetic Phosphorylation". In: *Nature* 214.5088, pp. 562–566.

Aro, E.-M. (2004). "Dynamics of photosystem II: a proteomic approach to thylakoid protein complexes". In: *Journal of Experimental Botany* 56.411, pp. 347–356.

Aro, E.-M., Virgin, I., and Andersson, B. (1993). "Photoinhibition of Photosystem II. Inactivation, protein damage and turnover". In: *Biochimica et Biophysica Acta (BBA) - Bioenergetics* 1143.2, pp. 113–134.

Asada, K. (1999). "The water-water cycle in chloroplasts: scavenging of active oxygens and dissipation of excess photons." In: *Annual review of plant physiology and plant molecular biology.* 1999. v. 50 p. 601-639.

Asada, K., Kiso, K., and Yoshikawa, K. (1974). "Univalent reduction of molecular oxygen by spinach chloroplasts on illumination". In: *Journal of Biological Chemistry* 249.7, pp. 2175–2181.

Badger, M. R., Caemmerer, S. von, Ruuska, S., and Nakano, H. (2000). "Electron flow to oxygen in higher plants and algae: rates and control of direct photoreduction (Mehler reaction) and rubisco oxygenase". In: *Philosophical Transactions of the Royal Society B: Biological Sciences* 355.1402, pp. 1433–1446.

Bailey, S., Melis, A., Mackey, K. R., Cardol, P., Finazzi, G., Dijken, G. van, Berg, G. M., Arrigo, K., Shrager, J., and Grossman, A. (2008). "Alternative photosynthetic electron flow to oxygen in marine Synechococcus". In: *Biochimica et Biophysica Acta (BBA) - Bioenergetics* 1777.3, pp. 269–276.

Baker, N. R. (2008). "Chlorophyll fluorescence: a probe of photosynthesis in vivo". In: *Annu. Rev. Plant Biol.* 59, pp. 89–113.

Barthélemy, X., Popovic, R., and Franck, F. (1997). "Studies on the O-J-I-P transient of chlorophyll fluorescence in relation to photosystem II assembly and heterogeneity in plastids of greening barley". In: *J. Photochem. Photobiol. B* 39.3, pp. 213–218.

Bassi, R., Cardol, P., Choquet, Y., De Marchin, T., Economou, C., Franck, F., Goldschmidt-Clermont, M., Jacobi, A., Loizeau, K., Mathy, G., Plancke, C., Posten, C., Purton, S., Remacle, C., Vejrazka, C., Wei, L., and Wollman, F.-A. (2012). "13 Finding the bottleneck: A research strategy for improved biomass production". In: *Microalgal Biotechnology: Integration and Economy.* Ed. by C. Posten and C. Walter. Berlin, Boston: DE, pp. 227–252.

Baurain, D., Dinant, M., Coosemans, N., and Matagne, R. F. (2003). "Regulation of the alternative oxidase Aox1 gene in Chlamydomonas reinhardtii. Role of the nitrogen source on the expression of a reporter gene under the control of the Aox1 promoter". In: *Plant physiology* 131.3, p. 1418.

Béchet, Q., Shilton, A., and Guieysse, B. (2013). "Modeling the effects of light and temperature on algae growth: State of the art and critical assessment for productivity prediction during outdoor cultivation". In: *Biotechnology Advances* 31.8, pp. 1648–1663.

Bell, D. H. and Hipkins, M. F. (1985). "Analysis of fluorescence induction curves from pea chloroplasts: Photosystem II reaction centre heterogeneity". In: *BBA-Bioenergetics* 807.3, pp. 255–262.

Bennoun, P. (1982). "Evidence for a respiratory chain in the chloroplast". In: *Proceedings of the National Academy of Sciences of the United States of America* 79.14, pp. 4352–4356.

Bennoun, P. and Li, Y.-s. (1973). "New results on the mode of action of 3,-(3,4-dichlorophenyl)-1,1-dimethylurea in spinach chloroplasts". In: *BBA-Bioenergetics* 292.1, pp. 162–168.

Berger, H., Blifernez-Klassen, O., Ballottari, M., Bassi, R., Wobbe, L., and Kruse, O. (2014). "Integration of Carbon Assimilation Modes with Photosynthetic Light Capture in the Green Alga Chlamydomonas reinhardtii". In: *Molecular Plant* 7.10, pp. 1545–1559.

Bilger, W. and Bjorkman, O. (1994). "Relationships among violaxanthin deepoxidation, thylakoid membrane conformation, and nonphotochemical chlorophyll fluorescence quenching in leaves of cotton (Gossypium hirsutum L.)" In: *Planta* 193.2, pp. 238–246.

Black, M. T., Brearley, T. H., and Horton, P. (1986a). "Heterogeneity in chloroplast photosystem II". In: *Photosynth. Res.* 8.3, pp. 193–207.

Black, M. T., Lee, P., and Horton, P. (1986b). "Changes in topography and function of thylakoid membranes following membrane protein phosphorylation". In: *Planta* 168.3, pp. 330–336.

Boekema, E. J., Breemen, J. F. van, Roon, H. van, and Dekker, J. P. (2000). "Arrangement of photosystem II supercomplexes in crystalline macrodomains within the thylakoid membrane of green plant chloroplasts". In: *J. Mol. Biol.* 301.5, pp. 1123–1133.

Bonaventura, C. and Myers, J. (1969). "Fluorescence and oxygen evolution from Chlorella pyrenoidosa". In: *BBA-Bioenergetics* 189.3, pp. 366–383.

Bonente, G., Pippa, S., Castellano, S., Bassi, R., and Ballottari, M. (2011a). "Acclimation of Chlamydomonas reinhardtii to Different Growth Irradiances". In: *Journal of Biological Chemistry* 287.8, pp. 5833–5847.

Bonente, G., Ballottari, M., Truong, T. B., Morosinotto, T., Ahn, T. K., Fleming, G. R., Niyogi, K. K., and Bassi, R. (2011b). "Analysis of LhcSR3, a Protein Essential for Feedback De-Excitation in the Green Alga Chlamydomonas reinhardtii". In: *PLoS Biology* 9.1. Ed. by T. Shikanai, e1000577.

Briantais, J.-M., Vernotte, C., Picaud, M., and Krause, G. H. (1979). "A quantitative study of the slow decline of chlorophyll a fluorescence in isolated chloroplasts". In: *Biochimica et Biophysica Acta (BBA) - Bioenergetics* 548.1, pp. 128–138.

Bukhov, N. G. and Carpentier, R. (2000). "Heterogeneity of photosystem II reaction centers as influenced by heat treatment of barley leaves". In: *Physiol. Plant.* 110.2, pp. 279–285.

Bulté, L. and Wollman, F. (1990). "Stabilization of states I and II by p-benzoquinone treatment of intact cells of Chlamydomonas reinhardtii". In: *BBA-Bioenergetics* 1016.2, pp. 253–258.

Bulté, L., Gans, P., Rebéillé, F., and Wollman, F. (1990). "ATP control on state transitions in vivo in Chlamydomonas reinhardtii". In: *BBA-Bioenergetics* 1020.1, pp. 72–80.

Burnham, K. P. and Anderson, D. R. (2002). *Model Selection and Multimodel Inference: A Practical Information-theoretic Approach*. Springer.

Cadoret, J.-C., Demoulière, R., Lavaud, J., Gorkom, H. J. van, Houmard, J., and Etienne, A.-L. (2004). "Dissipation of excess energy triggered by blue light in cyanobacteria with CP43 (isiA)". In: *BBA-Bioenergetics* 1659.1, pp. 100–104.

Cardol, P., Gloire, G., Havaux, M., Remacle, C., Matagne, R., and Franck, F. (2003). "Photosynthesis and State Transitions in Mitochondrial Mutants of Chlamydomonas reinhardtii Affected in Respiration 1". In: *Plant Physiology* 133.4, pp. 2010–2020.

Cardol, P., Alric, J., Girard-Bascou, J., Franck, F., Wollman, F.-A., and Finazzi, G. (2009). "Impaired respiration discloses the physiological significance of state transitions in Chlamydomonas". In: *Proceedings of the National Academy of Sciences* 106.37, pp. 15979–15984.

Cardol, P. and Remacle, C. (2008). In: *The Chlamydomonas Sourcebook: Organellar and metabolic processes*. Ed. by D. Stern and E. H. Harris. Academic Press.

Cardol, P., Bailleul, B., Rappaport, F., Derelle, E., Béal, D., Breyton, C., Bailey, S., Wollman, F. A., Grossman, A., Moreau, H., *et al.* (2008). "An original adaptation of photosynthesis in the marine green alga Ostreococcus". In: *Proceedings of the National Academy of Sciences* 105.22, p. 7881.

Carol, P., Stevenson, D., Bisanz, C., Breitenbach, J., Sandmann, G., Mache, R., Coupland, G., and Kuntz, M. (1999). "Mutations in the Arabidopsis gene IMMUTANS cause a variegated phenotype by inactivating a chloroplast terminal oxidase associated with phytoene desaturation". In: *The Plant Cell Online* 11.1, pp. 57–68.

Chow, W. S. (1994). "Photoprotection and Photoinhibitory Damage". In: *Advances in Molecular and Cell Biology*. Ed. by E. Edward Bittar and J. Barber. Vol. Volume 10. Molecular Processes of Photosynthesis. Elsevier, pp. 151–196.

Clark Jr, L. (1956). "Monitor and control of blood and tissue oxygen tensions". In: *ASAIO Journal* 2.1, pp. 41–48.

Cornic, G. and Ghashghaie, J. (1991). "Effect of temperature on net CO2 assimilation and photosystem II quantum yield of electron transfer of French bean (Phaseolus vulgaris L.) leaves during drought stress". In: *Planta* 185.2, pp. 255–260.

Crofts, A. R. and Yerkes, C. T. (1994). "A molecular mechanism for qE-quenching". In: *FEBS Letters* 352.3, pp. 265–270.

DalCorso, G., Pesaresi, P., Masiero, S., Aseeva, E., Schünemann, D., Finazzi, G., Joliot, P., Barbato, R., and Leister, D. (2008). "A Complex Containing PGRL1 and PGR5 Is Involved in the Switch between Linear and Cyclic Electron Flow in Arabidopsis". In: *Cell* 132.2, pp. 273–285.

Dall'Osto, L., Lico, C., Alric, J., Giuliano, G., Havaux, M., and Bassi, R. (2006). "Lutein is needed for efficient chlorophyll triplet quenching in the major LHCII antenna complex of higher plants and effective photoprotection in vivo under strong light". In: *BMC Plant. Biol.* 6.1, p. 32.

Dang, K.-V., Plet, J., Tolleter, D., Jokel, M., Cuine, S., Carrier, P., Auroy, P., Richaud, P., Johnson, X., Alric, J., Allahverdiyeva, Y., and Peltier, G. (2014). "Combined Increases in Mitochondrial Cooperation and Oxygen Photoreduction Compensate for Deficiency in Cyclic Electron Flow in Chlamydomonas reinhardtii". In: *The Plant Cell* 26.7, pp. 3036–3050.

Davies, D. R. and Plaskitt, A. (1971). "Genetical and Structural Analyses of Cell-Wall Formation in Chlamydomonas Reinhardi". In: *Genet. Res.* 17.01, pp. 33–43.

de Marchin, T., Ghysels, B., Nicolay, S., and Franck, F. (2014). "Analysis of PSII antenna size heterogeneity of Chlamydomonas reinhardtii during state transitions". In: *Biochimica et Biophysica Acta (BBA) - Bioenergetics* 1837.1, pp. 121–130.

Delosme, R., Olive, J., and Wollman, F. A. (1996). "Changes in light energy distribution upon state transitions: an in vivo photoacoustic study of the wild type and photosynthesis mutants from Chlamydomonas reinhardtii". In: *BBA-Bioenergetics* 1273.2, pp. 150–158.

Delosme, R. (1967). "Etude de l'induction de fluorescence des algues vertes et des chloroplastes au debut d'une illumination intense". In: *Biochimica et Biophysica Acta (BBA) - Bioenergetics* 143.1, pp. 108–128.

Delosme, R., Béal, D., and Joliot, P. (1994). "Photoacoustic detection of flash-induced charge separation in photosynthetic systems. Spectral dependence of the quantum yield". In: *Biochimica et Biophysica Acta (BBA) - Bioenergetics* 1185.1, pp. 56–64.

Demmig-Adams, B. (1990). "Carotenoids and photoprotection in plants: A role for the xanthophyll zeaxanthin". In: *Biochimica et Biophysica Acta (BBA) - Bioenergetics* 1020.1, pp. 1–24.

Depege, N., Bellafiore, S., and Rochaix, J. (2003). "Role of Chloroplast Protein Kinase Stt7 in LHCII Phosphorylation and State Transition in Chlamydomonas". In: *Science* 299.5612, pp. 1572–1575.

Dietzel, L., Brautigam, K., Steiner, S., Schuffler, K., Lepetit, B., Grimm, B., Schottler, M. A., and Pfannschmidt, T. (2011). "Photosystem II Supercomplex Remodeling Serves as an Entry Mechanism for State Transitions in Arabidopsis". In: *Plant Cell* 23.8, pp. 2964–2977.

Doschek, W. W. and Kok, B. (1972). "Photon Trapping in Photosystem II of Photosynthesis: The Fluorescence Rise Curve in the Presence of 3-(3,4-Dichlorophenyl)-1,1-dimethylurea". In: *Biophys. J.* 12.7, pp. 832–838.

Doucha, J. and Lívanský, K. (2006). "Productivity, CO2/O2 exchange and hydraulics in outdoor open high density microalgal (Chlorella sp.) photobioreactors operated in a Middle and Southern European climate". en. In: *Journal of Applied Phycology* 18.6, pp. 811–826.

Doucha, J. and Lívanský, K. (2009). "Outdoor open thin-layer microalgal photobioreactor: potential productivity". In: *Journal of applied phycology* 21.1, pp. 111–117.

Doucha, J. and Livansky, K. (1999). *Process of outdoor thin-layer cultivation of microalgae and blue-green algae and bioreactor for performing the process*. US Patent 5,981,271. Google Patents.

Doucha, J. and Lívanský, K. (1995). "Novel outdoor thin-layer high density microalgal culture system: Productivity and operational parameters". In: *A1golog. Stud., Stuttgart* 76, pp. 129–147.

Doucha, J., Straka, F., and Lívanský, K. (2005). "Utilization of flue gas for cultivation of microalgae Chlorella (sp.) in an outdoor open thin-layer photobioreactor". en. In: *Journal of Applied Phycology* 17.5, pp. 403–412.

Duboc, P., Marison, I., Von Stockar, U., and Kemp, R. (1999). "Handbook of thermal analysis and calorimetry". In: *Elsevier*, pp. 267–365.

Duysens, L. and Sweers, H. (1963a). "Mechanism of two photochemical reactions in algae as studied by means of fluorescence". In: *Studies on microalgae and photosynthetic bacteria*, pp. 353–372.

Duysens, L. and Sweers, H. (1963b). "Studies on microalgae and photosynthetic bacteria". In: *Jap. Soc. Plant Physiol.* University of Tokyo Press Tokyo, pp. 353–372.

Ellis, R. J. (1979). "The most abundant protein in the world". In: *Trends in Biochemical Sciences* 4.11, pp. 241–244.

Falk, S. and Palmqvist, K. (1992). "Photosynthetic light utilization efficiency, photosystem II heterogeneity, and fluorescence quenching in Chlamydomonas reinhardtii during the induction of the CO2-concentrating mechanism". In: *Plant physiology* 100.2, pp. 685–691.

Falkowski, P. G., Fujita, Y., Ley, A., and Mauzerall, D. (1986). "Evidence for cyclic electron flow around photosystem II in Chlorella pyrenoidosa". In: *Plant physiology* 81.1, pp. 310–312.

Feild, T. S., Nedbal, L., and Ort, D. R. (1998). "Nonphotochemical reduction of the plastoquinone pool in sunflower leaves originates from chlororespiration". In: *Plant Physiology* 116.4, pp. 1209–1218.

Field, C. B., Behrenfeld, M. J., Randerson, J. T., and Falkowski, P. (1998). "Primary Production of the Biosphere: Integrating Terrestrial and Oceanic Components". In: *Science* 281.5374, pp. 237–240.

Finazzi, G. (2005). "The central role of the green alga Chlamydomonas reinhardtii in revealing the mechanism of state transitions". In: *Journal of experimental botany* 56.411, p. 383.

Finazzi, G., Furia, A., Barbagallo, R. P., and Forti, G. (1999). "State transitions, cyclic and linear electron transport and photophosphorylation in Chlamydomonas reinhardtii". In: *BBA-Bioenergetics* 1413.3, pp. 117–129.

Finazzi, G. and Forti, G. (2004). "Metabolic flexibility of the green alga Chlamydomonas reinhardtii as revealed by the link between state transitions and cyclic electron flow". In: *Photosynthesis research* 82.3, pp. 327–338.

Finazzi, G., Johnson, G. N., Dall'Osto, L., Zito, F., Bonente, G., Bassi, R., and Wollman, F.-A. (2006). "Nonphotochemical Quenching of Chlorophyll Fluorescence in *Chlamydomonas reinhardtii*". In: *Biochemistry* 45.5, pp. 1490–1498.

Finazzi, G., Rappaport, F., Furia, A., Fleischmann, M., Rochaix, J.-D., Zito, F., and Forti, G. (2002). "Involvement of state transitions in the switch between linear and cyclic electron flow in Chlamydomonas reinhardtii". In: *EMBO reports* 3.3, pp. 280–285.

Flameling, I. A. and Kromkamp, J. (1998). "Light dependence of quantum yields for PSII charge separation and oxygen evolution in eucaryotic algae". In: *Limnology and oceanography* 43, pp. 284–297.

Flameling, I. A. and Kromkamp, J. (1997). "Photoacclimation of Scenedesmus protuberans (Chlorophyceae) to fluctuating irradiances simulating vertical mixing". In: *Journal of plankton research* 19.8, pp. 1011–1024.

Fleischmann, M. M., Ravanel, S., Delosme, R., Olive, J., Zito, F., Wollman, F. A., and Rochaix, J. D. (1999). "Isolation and Characterization of Photoautotrophic Mutants of Chlamydomonas reinhardtii Deficient in State Transition". In: *J. Biol. Chem.* 274.43, pp. 30987–30994.

Förster, B., Osmond, C. B., and Boynton, J. E. (2001). "Very high light resistant mutants of Chlamydomonas reinhardtii: responses of photosystem II, nonphotochemical quenching and xanthophyll pigments to light and CO2". In: *Photosynthesis research* 67.1, pp. 5–15.

Franck, F. and Houyoux, P. A. (2008). "The Mehler Reaction in Chlamydomonas During Photosynthetic Induction and Steady-State Photosynthesis in Wild-Type and in a Mitochondrial Mutant". In: *Photosynthesis. Energy from the Sun*, pp. 581–584.

Frank, H. A., Cua, A., Chynwat, V., Young, A., Gosztola, D., and Wasielewski, M. R. (1994). "Photophysics of the carotenoids associated with the xanthophyll cycle in photosynthesis". In: *Photosynthesis Research* 41.3, pp. 389–395.

Furbank, R. T. and Badger, M. R. (1983). "Oxygen exchange associated with electron transport and photophosphorylation in spinach thylakoids". In: *Biochimica et Biophysica Acta (BBA) - Bioenergetics* 723.3, pp. 400–409.

García-Cerdán, J., Kovács, L., Tóth, T., Kereïche, S., Aseeva, E., Boekema, E., Mamedov, F., Funk, C., and Schröder, W. (2011). "The PsbW protein stabilizes the supramolecular organization of photosystem II in higher plants". In: *Plant J.* 65.3, pp. 368–381.

Genty, B., Briantais, J.-M., and Baker, N. R. (1989). "The relationship between the quantum yield of photosynthetic electron transport and quenching of chlorophyll fluorescence". In: *Biochimica et Biophysica Acta (BBA) - General Subjects* 990.1, pp. 87–92.

Genty, B. and Meyer, S. (1995). "Quantitative mapping of leaf photosynthesis using chlorophyll fluorescence imaging". In: *Functional Plant Biology* 22.2, pp. 277–284.

Gorman, D. S. and Levine, R. P. (1965). "Cytochrome f and plastocyanin: their sequence in the photosynthetic electron transport chain". In: *PNAS* 54.6, p. 1665.

Govindjee, R., Rabinowitch, E., and Govindjee (1968). "Maximum quantum yield and action spectrum of photosynthesis and fluorescence in chlorella". In: *Biochimica et Biophysica Acta (BBA) - Bioenergetics* 162.4, pp. 539–544.

Grobbelaar, J. U. (2010). "Microalgal biomass production: challenges and realities". In: *Photosynthesis Research*.

Grobbelaar, J. U., Nedbal, L., Tichy, L., and Setlik, L. (1995). "Variation in some photosynthetic characteristics of microalgae cultured in outdoor thin-layered sloping reactors". In: *Journal of applied phycology* 7.2, pp. 175–184.

Guiry, M. D. (2012). "How many species of algae are there?" In: *Journal of phycology* 48.5, pp. 1057–1063.

Guy, R. D., Berry, J. A., Fogel, M. L., and Hoering, T. C. (1989). "Differential fractionation of oxygen isotopes by cyanide-resistant and cyanide-sensitive respiration in plants". In: *Planta* 177.4, pp. 483–491.

Harris, E. H. (1989). *The Chlamydomonas Sourcebook: A Comprehensive Guide to Biology and Laboratory Use*. Academic Press Inc.

Harris, E. H. (2001). "Chlamydomonas as a model organism". In: *Annual Review of Plant Physiology and Plant Molecular Biology* 52.1, pp. 363–406.

Havaux, M. and Tardy, F. (1999). "Loss of chlorophyll with limited reduction of photosynthesis as an adaptive response of Syrian barley landraces to high-light and heat stress". In: *Aust. J. Plant Physiol.* 26.6, pp. 569–578.

Heinze, I., Dau, H., and Senger, H. (1996). "The relation between the photochemical yield and variable fluorescence of photosystem II in the green alga Scenedesmus obliquus". In: *Journal of Photochemistry and Photobiology B: Biology* 32.1, pp. 89–95.

Helman, Y., Tchernov, D., Reinhold, L., Shibata, M., Ogawa, T., Schwarz, R., Ohad, I., and Kaplan, A. (2003). "Genes Encoding A-Type Flavoproteins Are Essential for Photoreduction of O2 in Cyanobacteria". In: *Current biology* 13.3, pp. 230–235.

Hertle, A. P., Blunder, T., Wunder, T., Pesaresi, P., Pribil, M., Armbruster, U., and Leister, D. (2013). "PGRL1 Is the Elusive Ferredoxin-Plastoquinone Reductase in Photosynthetic Cyclic Electron Flow". In: *Molecular Cell* 49.3, pp. 511–523.

Hindersin, S., Leupold, M., Kerner, M., and Hanelt, D. (2014). "Key parameters for outdoor biomass production of Scenedesmus obliquus in solar tracked photobioreactors". In: *Journal of Applied Phycology* 26.6, pp. 2315–2325.

Hoefnagel, M. H., Atkin, O. K., and Wiskich, J. T. (1998). "Interdependence between chloroplasts and mitochondria in the light and in the dark". In: *Biochimica et Biophysica Acta (BBA) - Bioenergetics* 1366, pp. 235–255.

Horton, P., Ruban, A. V., and Walters, R. G. (1996). "Regulation of Light Harvesting in Green Plants". In: *Annual Review of Plant Physiology and Plant Molecular Biology* 47.1, pp. 655–684.

Horton, P. and Black, M. T. (1981). "Light-dependent quenching of chlorophyll fluorescence in pea chloroplasts induced by adenosine 5'-triphosphate". In: *BBA-Bioenergetics* 635.1, pp. 53–62.

Horton, P. and Black, M. T. (1983). "A comparison between cation and protein phosphorylation effects on the fluorescence induction curve in chloroplasts treated with 3-(3,4-dichlorophenyl)-1,1-dimethylurea". In: *BBA-Bioenergetics* 722.1, pp. 214–218.

Houille-Vernes, L., Rappaport, F., Wollman, F.-A., Alric, J., and Johnson, X. (2011a). "Plastid terminal oxidase 2 (PTOX2) is the major oxidase involved in chlororespiration in Chlamydomonas". In: *Proceedings of the National Academy of Sciences* 108.51, pp. 20820–20825.

Houille-Vernes, L., Rappaport, F., Wollman, F.-A., Alric, J., and Johnson, X. (2011b). "Plastid terminal oxidase 2 (PTOX2) is the major oxidase

involved in chlororespiration in Chlamydomonas". In: *Proceedings of the National Academy of Sciences* 108.51, pp. 20820–20825.

Hsu, B. and Lee, J. (1991). "A study on the fluorescence induction curve of the DCMU-poisoned chloroplast". In: *BBA-Bioenergetics* 1056.3, pp. 285–292.

Hsu, B., Lee, Y., and Jang, Y. (1989). "A method for analysis of fluorescence induction curve from DCMU-poisoned chloroplasts". In: *BBA-Bioenergetics* 975.1, pp. 44–49.

Hunt, S. (2003). "Measurements of photosynthesis and respiration in plants". In: *Physiologia Plantarum* 117.3, pp. 314–325.

Hymus, G. J., Ellsworth, D. S., Baker, N. R., and Long, S. P. (1999). "Does Free-Air Carbon Dioxide Enrichment Affect Photochemical Energy Use by Evergreen Trees in Different Seasons? A Chlorophyll Fluorescence Study of Mature Loblolly Pine". In: *Plant Physiology* 120.4, pp. 1183–1192.

Iwai, M., Takahashi, Y., and Minagawa, J. (2008). "Molecular remodeling of photosystem II during state transitions in Chlamydomonas reinhardtii". In: *Plant Cell* 20.8, p. 2177.

Iwai, M., Yokono, M., Inada, N., and Minagawa, J. (2009). "Live-cell imaging of photosystem II antenna dissociation during state transitions". In: *Proceedings of the National Academy of Sciences* 107.5, pp. 2337–2342.

Iwai, M., Kato, N., and Minagawa, J. (2007). "Distinct physiological responses to a high light and low CO2 environment revealed by fluorescence quenching in photoautotrophically grown Chlamydomonas reinhardtii". In: *Photosynthesis Research* 94.2, pp. 307–314.

Iwai, M., Takizawa, K., Tokutsu, R., Okamuro, A., Takahashi, Y., and Minagawa, J. (2010). "Isolation of the elusive supercomplex that drives cyclic electron flow in photosynthesis". In: *Nature* 464.7292, pp. 1210–1213.

Jans, F., Mignolet, E., Houyoux, P. A., Cardol, P., Ghysels, B., Cuiné, S., Cournac, L., Peltier, G., Remacle, C., and Franck, F. (2008). "A type II NAD (P) H dehydrogenase mediates light-independent plastoquinone reduction in the chloroplast of Chlamydomonas". In: *Proceedings of the National Academy of Sciences* 105.51, p. 20546.

Jassby, A. D. and Platt, T. (1976). "Mathematical formulation of the relationship between photosynthesis and light for phytoplankton". In: *Limnology and oceanography* 21.4, pp. 540–547.

Jerez, C., Navarro, E., Malpartida, I., Rico, R., Masojídek, J., Abdala, R., and Figueroa, F. (2014). "Hydrodynamics and photosynthesis performance of Chlorella fusca (Chlorophyta) grown in a thin-layer cascade (TLC) system". In: *Aquatic Biology* 22, pp. 111–122.

Johnson, M. P., Brain, A. P. R., and Ruban, A. V. (2011). "Changes in thylakoid membrane thickness associated with the reorganization of photosystem II light harvesting complexes during photoprotective energy dissipation". In: *Plant Signaling & Behavior* 6.9, pp. 1386–1390.

Johnson, M. L. and Faunt, L. M. (1992). "[1] Parameter estimation by least-squares methods". In: *Methods in enzymology* 210, pp. 1–37.

Johnson, X., Steinbeck, J., Dent, R. M., Takahashi, H., Richaud, P., Ozawa, S.-I., Houille-Vernes, L., Petroutsos, D., Rappaport, F., Grossman, A. R., *et al.* (2014). "Proton Gradient Regulation 5-Mediated Cyclic Electron Flow under ATP-or Redox-Limited Conditions: A Study of ATPase pgr5 and rbcL pgr5 Mutants in the Green Alga Chlamydomonas reinhardtii". In: *Plant physiology* 165.1, pp. 438–452.

Joliot, P. and Joliot, A. (1964). "Etude cinétique de la réaction photochimique libérant de l'oxygène au cours de la photosynthèse". In: *CR Acad. Sci. Paris* 258, pp. 4622–4625.

Joliot, P. and Joliot, A. (1977). "Evidence for a double hit process in Photosystem II based on fluorescence studies". In: *BBA-Bioenergetics* 462.3, pp. 559–574.

Joliot, P. and Joliot, A. (2002). "Cyclic electron transfer in plant leaf". In: *PNAS* 99.15, pp. 10209–10214.

Joliot, P., Béal, D., and Delosme, R. (2004). "In vivo Measurements of Photosynthetic Activity: Methods". In: *The Molecular Biology of Chloroplasts and Mitochondria in Chlamydomonas*. Ed. by Govindjee, J. Rochaix, M. Goldschmidt-Clermont, and S. Merchant. Vol. 7. Advances in Photosynthesis and Respiration. 10.1007/0-306-48204-5_22. Springer Netherlands, pp. 433–449.

Kajan, M., Tichý, V., and Simmer, J. (1994). "Productivity of algae in different culture systems". en. In: *Algological Studies/Archiv für Hydrobiologie, Supplement Volumes*, pp. 111–117.

Kautsky, H. and Hirsch, A. (1931). "Neue Versuche zur Kohlensäureassimilation". In: *Naturwissenschaften* 19.48, p. 964.

Knud-Hansen, C. F., McElwee, K., Baker, J., and Clair, D. (1998). *Pond fertilization: ecological approach and practical application*. Pond Dynamics/Aquaculture Collaborative Research Support Program, Oregon State University Corvallis, Oregon.

Kolber, Z. S., Prášil, O., and Falkowski, P. G. (1998). "Measurements of variable chlorophyll fluorescence using fast repetition rate techniques: defining methodology and experimental protocols". In: *Biochimica et Biophysica Acta (BBA) - Bioenergetics* 1367.

Kolber, Z. and Falkowski, P. G. (1993). "Use of active fluorescence to estimate phytoplankton photosynthesis in situ". In: *Limnology and Oceanography* 38.8, pp. 1646–1665.

Kouřil, R., Dekker, J. P., and Boekema, E. J. (2012). "Supramolecular organization of photosystem II in green plants". In: *Biochimica et Biophysica Acta (BBA)-Bioenergetics* 1817.1, pp. 2–12.

Krall, J. P. and Edwards, G. E. (1990). "Quantum yields of photosystem II electron transport and carbon dioxide fixation in C4 plants". In: *Functional Plant Biology* 17.5, pp. 579–588.

Kyle, D. J., Haworth, P., and Arntzen, C. J. (1982). "Thylakoid membrane protein phosphorylation leads to a decrease in connectivity between photosystem II reaction centers". In: *BBA-Bioenergetics* 680.3, pp. 336–342.

Kyle, D., Staehelin, L., and Arntzen, C. (1983). "Lateral mobility of the light-harvesting complex in chloroplast membranes controls excitation energy distribution in higher plants". In: *Arch. Biochem. Biophys.* 222.2, pp. 527–541.

Larsson, U. K., Jergil, B., and Andersson, B. (1983). "Changes in the lateral distribution of the light-harvesting chlorophyll-a/b—protein complex induced by its phosphorylation". In: *Eur. J. Biochem.* 136.1, pp. 25–29.

Lavaud, J., Rousseau, B., Van Gorkom, H. J., and Etienne, A. L. (2002). "Influence of the diadinoxanthin pool size on photoprotection in the marine planktonic diatom Phaeodactylum tricornutum". In: *Plant Physiol.* 129.3, pp. 1398–1406.

Lavergne, J. and Trissl, H. (1995). "Theory of fluorescence induction in photosystem II: derivation of analytical expressions in a model including exciton-radical-pair equilibrium and restricted energy transfer between photosynthetic units". In: *Biophys. J.* 68.6, pp. 2474–2492.

Lavergne, J. and Briantais, J.-M. (2004). "Photosystem II heterogeneity". In: *Oxygenic photosynthesis: The light reactions*. Springer, pp. 265–287.

Lavergne, J. and Rappaport, F. (1998). "Stabilization of charge separation and photochemical misses in photosystem II". In: *Biochemistry-US* 37.21, pp. 7899–7906.

Lazár, D. (2006). "The polyphasic chlorophyll a fluorescence rise measured under high intensity of exciting light". In: *Funct. Plant Biol.* 33.1, pp. 9–30.

Lazár, D., Tomek, P., Ilik, P., and Nauš, J. (2001). "Determination of the antenna heterogeneity of Photosystem II by direct simultaneous fitting of several fluorescence rise curves measured with DCMU at different light intensities". In: *Photosynth. Res.* 68.3, pp. 247–257.

Lennon, A. M., Prommeenate, P., and Nixon, P. J. (2003). "Location, expression and orientation of the putative chlororespiratory enzymes, Ndh and IMMUTANS, in higher-plant plastids". In: *Planta* 218.2, pp. 254–260.

Ley, A. C. and Mauzerall, D. C. (1982). "Absolute absorption cross-sections for Photosystem II and the minimum quantum requirement for photosyn-

thesis in Chlorella vulgaris". In: *Biochimica et Biophysica Acta (BBA) - Bioenergetics* 680.1, pp. 95–106.

Lichtenthaler (1987). "Chlorophylls and carotenoids: pigment of photosynthetic biomembranes." In: *Methods Enzymol.* 148.148, pp. 350–382.

Livansky, K. (2000). "Comparison of continuous and stepwise control of CO2 supply into outdoor open thin-layer algal culture units". eng. In: *Archiv für Hydrobiologie. Supplementband, Algological studies* 131, pp. 119–129.

Lívanský, K. and Doucha, J. (1996). "CO2 and O2 gas exchange in outdoor thin-layer high density microalgal cultures". In: *Journal of Applied Phycology* 8.4-5, pp. 353–358.

Lucker, B. and Kramer, D. M. (2013). "Regulation of cyclic electron flow in Chlamydomonas reinhardtii under fluctuating carbon availability". In: *Photosynthesis Research*.

Malkin, S. and Kok, B. (1966). "Fluorescence induction studies in isolated chloroplasts. I. Number of components involved in the reaction and quantum yields." In: *BBA* 126.3, p. 413.

Masojídek, J., Vonshak, A., and Torzillo, G. (2010). "Chlorophyll fluorescence applications in microalgal mass cultures". In: *Chlorophyll a Fluorescence in Aquatic Sciences: Methods and Applications*, pp. 277–292.

Masojídek, J., Kopecký, J., Giannelli, L., and Torzillo, G. (2011). "Productivity correlated to photobiochemical performance of Chlorella mass cultures grown outdoors in thin-layer cascades". In: *Journal of industrial microbiology & biotechnology* 38.2, pp. 307–317.

Mathur, S., Allakhverdiev, S., and Jajoo, A. (2011). "Analysis of high temperature stress on the dynamics of antenna size and reducing side heterogeneity of Photosystem II in wheat leaves Triticum aestivum". In: *BBA-Bioenergetics* 1807.1, pp. 22–29.

Mathy, G., Cardol, P., Dinant, M., Blomme, A., Gérin, S., Cloes, M., Ghysels, B., DePauw, E., Leprince, P., Remacle, C., Sluse-Goffart, C., Franck, F., Matagne, R. F., and Sluse, F. E. (2010). "Proteomic and Functional Characterization of a *Chlamydomonas reinhardtii* Mutant Lacking the Mitochondrial Alternative Oxidase 1". In: *Journal of Proteome Research* 9.6, pp. 2825–2838.

McDonald, A. E., Ivanov, A. G., Bode, R., Maxwell, D. P., Rodermel, S. R., and Hüner, N. P. (2011). "Flexibility in photosynthetic electron transport: The physiological role of plastoquinol terminal oxidase (PTOX)". In: *Biochimica et Biophysica Acta (BBA) - Bioenergetics* 1807.8, pp. 954–967.

McDonald, A. E., Sieger, S. M., and Vanlerberghe, G. C. (2002). "Methods and approaches to study plant mitochondrial alternative oxidase". In: *Physiologia Plantarum* 116.2, pp. 135–143.

Mehler, A. H. (1951). "Studies on reactions of illuminated chloroplasts: I. Mechanism of the reduction of oxygen and other hill reagents". In: *Archives of Biochemistry and Biophysics* 33.1, pp. 65–77.

Melis, A. and Akoyunoglou, G. (1977). "Development of the two heterogeneous Photosystem II units in etiolated bean leaves". In: *Plant Physiol.* 59.6, p. 1156.

Melis, A. and Duysens, L. N. M. (1979). "Biphasic Energy Conversion Kinetics and Absorbance Difference Spectra of Photosystem II of Chloroplasts. Evidence for Two Different Photosystem II Reaction Centers". en. In: *Photochem. Photobiol.* 29.2, pp. 373–382.

Melis, A. and Homann, P. H. (1976). "Heterogeneity of the photochemical centers in system II of chloroplasts". In: *Photochem. Photobiol.* 23.5, pp. 343–350.

Melis, A. and Anderson, J. M. (1983). "Structural and functional organization of the photosystems in spinach chloroplasts. Antenna size, relative electron-transport capacity, and chlorophyll composition". In: *BBA-Bioenergetics* 724.3, pp. 473–484.

Melis, A. and Homann, P. H. (1975). "Kinetic analysis of the fluorescence induction in 3-(3,4-dichlorophenyl)-1,1-dimethylurea poisoned chloroplasts". In: *Photochem. Photobiol.* 21.6, pp. 431–437.

Minagawa, J. (2011a). "State Transitions–the molecular remodeling of photosynthetic supercomplexes that controls energy flow in the chloroplast". In: *Biochimica et Biophysica Acta (BBA)-Bioenergetics*.

Minagawa, J. (2011b). "State Transitions–the molecular remodeling of photosynthetic supercomplexes that controls energy flow in the chloroplast". In: *BBA-Bioenergetics* 1807.8, pp. 897–905.

Miyachi, S., Iwasaki, I., and Shiraiwa, Y. (2003). "Historical perspective on microalgal and cyanobacterial acclimation to low- and extremely high-CO2 conditions". In: *Photosynthesis Research* 77.2, pp. 139–153.

Moise, N. and Moya, I. (2004a). "Correlation between lifetime heterogeneity and kinetics heterogeneity during chlorophyll fluorescence induction in leaves:: 1. Mono-frequency phase and modulation analysis reveals a conformational change of a PSII pigment complex during the IP thermal phase". In: *BBA-Bioenergetics* 1657.1, pp. 33–46.

Moise, N. and Moya, I. (2004b). "Correlation between lifetime heterogeneity and kinetics heterogeneity during chlorophyll fluorescence induction in leaves: 2. Multi-frequency phase and modulation analysis evidences a loosely connected PSII pigment–protein complex". In: *BBA-Bioenergetics* 1657.1, pp. 47–60.

Molen, T. A., Rosso, D., Piercy, S., and Maxwell, D. P. (2006). "Characterization of the alternative oxidase of Chlamydomonas reinhardtii in

response to oxidative stress and a shift in nitrogen source". In: *Physiologia Plantarum* 127.1, pp. 74–86.

Moore, A. L. and Siedow, J. N. (1991). "The regulation and nature of the cyanide-resistant alternative oxidase of plant mitochondria". In: *Biochimica et Biophysica Acta (BBA) - Bioenergetics* 1059.2, pp. 121–140.

Moroney, J. V. and Ynalvez, R. A. (2007). "Proposed Carbon Dioxide Concentrating Mechanism in Chlamydomonas reinhardtii". In: *Eukaryotic Cell* 6.8, pp. 1251–1259.

Moroney, J. V., Jungnick, N., DiMario, R. J., and Longstreth, D. J. (2013). "Photorespiration and carbon concentrating mechanisms: two adaptations to high O2, low CO2 conditions". In: *Photosynthesis Research* 117.1, pp. 121–131.

Moroney, J. V., Ma, Y., Frey, W. D., Fusilier, K. A., Pham, T. T., Simms, T. A., DiMario, R. J., Yang, J., and Mukherjee, B. (2011). "The carbonic anhydrase isoforms of Chlamydomonas reinhardtii: intracellular location, expression, and physiological roles". In: *Photosynthesis Research* 109, pp. 133–149.

Morosinotto, T. and Bassi, R. (2014). "Molecular Mechanisms for Activation of Non-Photochemical Fluorescence Quenching: From Unicellular Algae to Mosses and Higher Plants". In: *Non-Photochemical Quenching and Energy Dissipation in Plants, Algae and Cyanobacteria*. Ed. by B. Demmig-Adams, G. Garab, W. Adams III, and Govindjee. Vol. 40. Dordrecht: Springer Netherlands, pp. 315–331.

Muller, P., Li, X. P., and Niyogi, K. K. (2001). "Non-photochemical quenching. A response to excess light energy". In: *Plant Physiology* 125.4, p. 1558.

Munekage, Y., Hashimoto, M., Miyake, C., Tomizawa, K.-I., Endo, T., Tasaka, M., and Shikanai, T. (2004). "Cyclic electron flow around photosystem I is essential for photosynthesis". In: *Nature* 429.6991, pp. 579–582.

Murata, N. (1969). "Control of excitation transfer in photosynthesis I. Light-induced change of chlorophyll a fluoresence in Porphyridium cruentum". In: *BBA-Bioenergetics* 172.2, pp. 242–251.

Murata, N., Nishimura, M., and Takamiya, A. (1966). "Fluorescence of chlorophyll in photosynthetic systems II. Induction of fluorescence in isolated spinach chloroplasts". In: *BBA - Biophys. incl. Photos.* 120.1, pp. 23–33.

Murata, N., Takahashi, S., Nishiyama, Y., and Allakhverdiev, S. I. (2007). "Photoinhibition of photosystem II under environmental stress". In: *Biochimica et Biophysica Acta (BBA) - Bioenergetics*. Structure and Function of Photosystems 1767.6, pp. 414–421.

Nagy, G., Unnep, R., Zsiros, O., Tokutsu, R., Takizawa, K., Porcar, L., Moyet, L., Petroutsos, D., Garab, G., Finazzi, G., and Minagawa, J. (2014). "Chloroplast remodeling during state transitions in Chlamydomonas reinhardtii as revealed by noninvasive techniques in vivo". In: *Proceedings of the National Academy of Sciences*.

Nedbal, L., Trtílek, M., and Kaftan, D. (1999). "Flash fluorescence induction: a novel method to study regulation of Photosystem II". In: *J. Photochem. Photobiol. B* 48.2-3, pp. 154–157.

Neubauer, C. and Schreiber, U. (1987). "The polyphasic rise of chlorophyll fluorescence upon onset of strong continuous illumination: I. Saturation characteristics and partial control by the photosystem II acceptor side". In: *Z Naturforsch 42c* 12461254.

Nield, J., Redding, K., and Hippler, M. (2004). "Remodeling of light-harvesting protein complexes in Chlamydomonas in response to environmental changes". In: *Eukaryot. Cell* 3.6, pp. 1370–1380.

Nishiyama, Y., Allakhverdiev, S. I., and Murata, N. (2005). "Inhibition of the repair of Photosystem II by oxidative stress in cyanobacteria". In: *Photosynthesis Research* 84.1, pp. 1–7.

Nishiyama, Y., Allakhverdiev, S. I., and Murata, N. (2006). "A new paradigm for the action of reactive oxygen species in the photoinhibition of photosystem II". In: *Biochimica et Biophysica Acta (BBA) - Bioenergetics* 1757.7, pp. 742–749.

Niyogi, K. K. (2000). "Safety valves for photosynthesis". In: *Current Opinion in Plant Biology* 3.6, pp. 455–460.

Palmqvist, K., Sundblad, L.-G., Wingsle, G., and Samuelsson, G. (1990). "Acclimation of photosynthetic light reactions during induction of inorganic carbon accumulation in the green alga Chlamydomonas reinhardtii". In: *Plant physiology* 94.1, pp. 357–366.

Peers, G., Truong, T. B., Ostendorf, E., Busch, A., Elrad, D., Grossman, A. R., Hippler, M., and Niyogi, K. K. (2009). "An ancient light-harvesting protein is critical for the regulation of algal photosynthesis". In: *Nature* 462.7272, pp. 518–521.

Peltier, G. and Thibault, P. (1985). "O2 uptake in the light in Chlamydomonas: evidence for persistent mitochondrial respiration". In: *Plant physiology* 79.1, p. 225.

Peltier, G., Tolleter, D., Billon, E., and Cournac, L. (2010). "Auxiliary electron transport pathways in chloroplasts of microalgae". In: *Photosynthesis Research* 106.1, pp. 19–31.

Pinheiro, J., Bates, D., DebRoy, S., Sarkar, D., and Team, R. D. C. (2011). *nlme: Linear and Nonlinear Mixed Effects Models*. R package version 3.1-102.

Prasil, O., Adir, N., and Ohad, I. (1992). "Dynamics of photosystem II : mechanism of photoinhibition and recovery process". In: *Topics in photosynthesis*. The Netherlands: Elsevier, vol. 2, pp. 295–348.

Pribil, M., Pesaresi, P., Hertle, A., Barbato, R., and Leister, D. (2010). "Role of Plastid Protein Phosphatase TAP38 in LHCII Dephosphorylation and Thylakoid Electron Flow". In: *PLoS Biol.* 8.1. Ed. by J. Chory, e1000288.

Purvis, A. C. (1997). "Role of the alternative oxidase in limiting superoxide production by plant mitochondria". In: *Physiologia Plantarum* 100.1.

Quick, W. and Horton, P. (1984). "Studies on the induction of chlorophyll fluorescenec in barley protoplasts. i. factors affecting the observation of oscillations in the yield of chlorophyll fluorescence and the rate of oxygen evolution". In: *Proceedings of the Royal society of London. Series B. Biological sciences* 220.1220, pp. 361–370.

Radmer, R. J. and Kok, B. (1976). "Photoreduction of O2 primes and replaces CO2 assimilation". In: *Plant physiology* 58.3, pp. 336–340.

Radmer, R. and Ollinger, O. (1980). "Light-driven uptake of oxygen, carbon dioxide, and bicarbonate by the green alga Scenedesmus". In: *Plant physiology* 65.4, pp. 723–729.

Rees, D., Lee, C. B., Gilmour, D. J., and Horton, P. (1992). "Mechanisms for controlling balance between light input and utilisation in the salt tolerant alga Dunaliella C9AA". In: *Photosynthesis research* 32.3, pp. 181–191.

Rintamäki, E., Martinsuo, P., Pursiheimo, S., and Aro, E. M. (2000). "Cooperative regulation of light-harvesting complex II phosphorylation via the plastoquinol and ferredoxin-thioredoxin system in chloroplasts". In: *PNAS* 97.21, p. 11644.

Roberty, S., Bailleul, B., Berne, N., Franck, F., and Cardol, P. (2014). "PSI Mehler reaction is the main alternative photosynthetic electron pathway in *Symbiodinium* sp., symbiotic dinoflagellates of cnidarians". In: *New Phytologist* 204.1, pp. 81–91.

Roelofs, T. A., Lee, C.-H., and Holzwarth, A. R. (1992). "Global target analysis of picosecond chlorophyll fluorescence kinetics from pea chloroplasts: A new approach to the characterization of the primary processes in photosystem II α- and β-units". In: *Biophys. J.* 61.5, pp. 1147–1163.

Ruban, A. V., Berera, R., Ilioaia, C., Stokkum, I. H. M. van, Kennis, J. T. M., Pascal, A. A., Amerongen, H. van, Robert, B., Horton, P., and Grondelle, R. van (2007). "Identification of a mechanism of photoprotective energy dissipation in higher plants". In: *Nature* 450.7169, pp. 575–578.

Ruban, A. V. and Johnson, M. P. (2008). "Dynamics of higher plant photosystem cross-section associated with state transitions". In: *Photosynth. Res.* 99, pp. 173–183.

Saradadevi, K. and Raghavendra, A. S. (1992). "Dark respiration protects photosynthesis against photoinhibition in mesophyll protoplasts of pea (Pisum sativum)". In: *Plant Physiology* 99.3, pp. 1232–1237.

Schansker, G., Tóth, S. Z., Kovács, L., Holzwarth, A. R., and Garab, G. (2011). "Evidence for a fluorescence yield change driven by a light-induced conformational change within photosystem II during the fast chlorophyll a fluorescence rise". In: *BBA-Bioenergetics* 1807.9, pp. 1032–1043.

Scheibe, R. (1987). "NADP+-malate dehydrogenase in C3-plants: Regulation and role of a light-activated enzyme". In: *Physiologia Plantarum* 71.3, pp. 393–400.

Schreiber, U. and Pfister, K. (1982). "Kinetic analysis of the light-induced chlorophyll fluorescence rise curve in the presence of dichlorophenyldimethylurea: Dependence of the slow-rise component on the degree of chloroplast intactness". In: *BBA-Bioenergetics* 680.1, pp. 60–68.

Schreiber, U., Endo, T., Mi, H., and Asada, K. (1995). "Quenching Analysis of Chlorophyll Fluorescence by the Saturation Pulse Method: Particular Aspects Relating to the Study of Eukaryotic Algae and Cyanobacteria". In: *Plant and Cell Physiology* 36.5, pp. 873–882.

Schuster, G., Dewit, M., Staehelin, L. A., and Ohad, I. (1986). "Transient inactivation of the thylakoid photosystem II light-harvesting protein kinase system and concomitant changes in intramembrane particle size during photoinhibition of Chlamydomonas reinhardtii." In: *The Journal of cell biology* 103.1, pp. 71–80.

Šetlík, I., Šust, V., and Málek, I. (1970). "Dual Purpose Open Circulation Units for Large Scale Culture of Algae in Temperate Zones. I. Basic Design Considerations and Scheme of a Pilot Plant". en. In: *Algological Studies/Archiv für Hydrobiologie, Supplement Volumes*, pp. 111–164.

Shapiguzov, A., Ingelsson, B., Samol, I., Andres, C., Kessler, F., Rochaix, J., Vener, A. V., and Goldschmidt-Clermont, M. (2010). "The PPH1 phosphatase is specifically involved in LHCII dephosphorylation and state transitions in Arabidopsis". In: *PNAS* 107.10, pp. 4782–4787.

Sinclair, J. and Spence, S. M. (1990). "Heterogeneous photosystem 2 activity in isolated spinach chloroplasts". In: *Photosynth. Res.* 24.3, pp. 209–220.

Sonoike, K. (2011). "Photoinhibition of photosystem I". In: *Physiologia Plantarum* 142.1, pp. 56–64.

Spalding, M. H., Critchley, C., and Orgren, W. L. (1984). "Influence of carbon dioxide concentration during growth on fluorescence induction characteristics of the green alga Chlamydomonas reinhardii". In: *Photosynthesis research* 5.2, pp. 169–176.

Spalding, M. H. and Portis Jr, A. R. (1985). "A model of carbon dioxide assimilation in Chlamydomonas reinhardii". In: *Planta* 164.3, pp. 308–320.

Stirbet, A. *et al.* (2012). "Chlorophyll a fluorescence induction: a personal perspective of the thermal phase, the J–I–P rise". In: *Photosynth. Res.* 113.1-3, pp. 15–61.

Stirbet, A. and Govindjee (2012). "Chlorophyll a fluorescence induction: a personal perspective of the thermal phase, the J–I–P rise". In: *Photosynthesis Research* 113.1, pp. 15–61.

Strand, D. D., Livingston, A. K., and Kramer, D. M. (2013). "Do State Transitions Control CEF1 in Higher Plants?" In: *Photosynthesis Research for Food, Fuel and the Future*. Springer, pp. 286–289.

Strasser, R. J., Srivastava, A., and Govindjee (1995). "Polyphasic chlorophyll a fluorescence transient in plants and cyanobacteria". In: *Photochemistry and Photobiology* 61.1, pp. 32–42.

Sueltemeyer, D., Klug, K., and Fock, H. (1986). "Effect of photon fluence rate on oxygen evolution and uptake by Chlamydomonas reinhardtii suspensions grown in ambient and CO2-enriched air". In: *Plant physiology* 81.2, p. 372.

Sültemeyer, D., Biehler, K., and Fock, H. P. (1993). "Evidence for the contribution of pseudocyclic photophosphorylation to the energy requirement of the mechanism for concentrating inorganic carbon in Chlamydomonas". In: *Planta* 189.2, pp. 235–242.

Takahashi, H., Clowez, S., Wollman, F.-A., Vallon, O., and Rappaport, F. (2013). "Cyclic electron flow is redox-controlled but independent of state transition". In: *Nature Communications* 4.

Takahashi, H., Iwai, M., Takahashi, Y., and Minagawa, J. (2006). "Identification of the mobile light-harvesting complex II polypeptides for state transitions in Chlamydomonas reinhardtii". In: *PNAS* 103.2, pp. 477–482.

Team, R. D. C. (2011). *R: A Language and Environment for Statistical Computing*. ISBN 3-900051-07-0. Vienna, Austria.

Thielen, A. and Gorkom, H. van (1981). "Quantum efficiency and antenna size of Photosystems IIα, IIβ and I in tobacco chloroplasts". In: *BBA-Bioenergetics* 635.1, pp. 111–120.

Thielmann, J., Tolbert, N., Goyal, A., and Senger, H. (1990). "Two systems for concentrating CO2 and bicarbonate during photosynthesis by Scenedesmus". In: *Plant physiology* 92.3, p. 622.

Thimijan, R. W. and Heins, R. D. (1983). "Photometric, radiometric, and quantum light units of measure: a review of procedures for interconversion". In: *HortScience* 18.6, pp. 818–822.

Tocquin, P., Fratamico, A., and Franck, F. (2012). "Screening for a low-cost Haematococcus pluvialis medium reveals an unexpected impact of a low N/P ratio on vegetative growth". In: *Journal of Applied Phycology* 24.3, pp. 365–373.

Tokutsu, R., Iwai, M., and Minagawa, J. (2009). "CP29, a Monomeric Light-harvesting Complex II Protein, Is Essential for State Transitions in Chlamydomonas reinhardtii". In: *J. Biol. Chem.* 284.12, pp. 7777–7782.

Tokutsu, R. and Minagawa, J. (2013a). "Energy-dissipative supercomplex of photosystem II associated with LHCSR3 in Chlamydomonas reinhardtii". In: *Proceedings of the National Academy of Sciences* 110.24, pp. 10016–10021.

Tokutsu, R. and Minagawa, J. (2013b). "Energy-dissipative supercomplex of photosystem II associated with LHCSR3 in Chlamydomonas reinhardtii". In: *Proceedings of the National Academy of Sciences* 110.24, pp. 10016–10021.

Tolleter, D., Ghysels, B., Alric, J., Petroutsos, D., Tolstygina, I., Krawietz, D., Happe, T., Auroy, P., Adriano, J.-M., Beyly, A., *et al.* (2011). "Control of hydrogen photoproduction by the proton gradient generated by cyclic electron flow in Chlamydomonas reinhardtii". In: *The Plant Cell Online* 23.7, pp. 2619–2630.

Torzillo, G., Accolla, P., Pinzani, E., and Masojidek, J. (1996). "In situ monitoring of chlorophyll fluorescence to assess the synergistic effect of low temperature and high irradiance stresses in Spirulina cultures grown outdoors in photobioreactors". In: *Journal of Applied Phycology* 8.4, pp. 283–291.

Torzillo, G., Bernardini, P., and Masojídek, J. (1998). "on-line monitoring of chlorophyll fluorescence to assess the extent of photoinhibition of photosynthesis induced by high oxygen concentration and low temperature and its effect on the productivity of outdoor cultures of spirulina platensis (cyanobacteria)". In: *Journal of phycology* 34.3, pp. 504–510.

Tredici, M. R. (2010). "Photobiology of microalgae mass cultures: understanding the tools for the next green revolution". In: *Biofuels* 1.1, pp. 143–162.

Trissl, H. and Lavergne, J. (1995). "Fluorescence induction from photosystem II: analytical equations for the yields of photochemistry and fluorescence derived from analysis of a model including exciton-radical pair equilibrium and restricted energy transfer between photosynthetic units". In: *Aust. J. Plant Physiol.* 22.2, pp. 183–193.

Turpin, D. H. (1991). "Effects of Inorganic N Availability on Algal Photosynthesis and Carbon Metabolism". In: *Journal of Phycology* 27.1, pp. 14–20.

Unlu, C., Drop, B., Croce, R., and Amerongen, H. van (2014). "State transitions in Chlamydomonas reinhardtii strongly modulate the functional size of photosystem II but not of photosystem I". In: *Proceedings of the National Academy of Sciences* 111.9, pp. 3460–3465.

Vallon, O., Bulte, L., Dainese, P., Olive, J., Bassi, R., and Wollman, F. A. (1991). "Lateral redistribution of cytochrome b6/f complexes along thylakoid membranes upon state transitions". In: *Proceedings of the National Academy of Sciences* 88.18, pp. 8262–8266.

Vallon, O., Wollman, F., and Olive, J. (1986). "Lateral distribution of the main protein complexes of the photosynthetic apparatus in Chlamydomonas reinhardtii and in spinach: an immunocytochemical study using intact thylakoid membranes and a PSII enriched membrane preparation". In: *Photobiochem. Photobiophys* 12, pp. 203–220.

Vander-Meulen, D. L. and Govindjee (1973). "Is there a triplet state in photosynthesis?" In: *Journal of scientific and industrial research* 32.2, pp. 62–69.

Velthuys, B. and Amesz, J. (1974). "Charge accumulation at the reducing side of system 2 of photosynthesis". In: *BBA-Bioenergetics* 333.1, pp. 85–94.

Vener, A. V., Van Kan, P. J., Rich, P. R., Ohad, I., and Andersson, B. (1997). "Plastoquinol at the quinol oxidation site of reduced cytochrome bf mediates signal transduction between light and protein phosphorylation: thylakoid protein kinase deactivation by a single-turnover flash". In: *PNAS* 94.4, pp. 1585–1590.

Vicente, J. B., Gomes, C. M., Wasserfallen, A., and Teixeira, M. (2002). "Module fusion in an A-type flavoprotein from the cyanobacterium Synechocystis condenses a multiple-component pathway in a single polypeptide chain". In: *Biochemical and biophysical research communications* 294.1, pp. 82–87.

Vonshak, A., Torzillo, G., Accolla, P., and Tomaselli, L. (1996). "Light and oxygen stress in Spirulina platensis (cyanobacteria) grown outdoors in tubular reactors". In: *Physiologia Plantarum* 97.1, pp. 175–179.

Vonshak, A., Torzillo, G., and Tomaseli, L. (1994). "Use of chlorophyll fluorescence to estimate the effect of photoinhibition in outdoor cultures of Spirulina platensis". In: *Journal of applied phycology* 6.1, pp. 31–34.

Walker, D. and Walker, R. (1987). "The use of the oxygen electrode and fluorescence probes in simple measurements of photosynthesis". In:

Wlodarczyk, L. M., Snellenburg, J. J., Ihalainen, J. A., Grondelle, R. van, Stokkum, I. H. van, and Dekker, J. P. (2015). "Functional Rearrangement of the Light-Harvesting Antenna upon State Transitions in a Green Alga". In: *Biophysical Journal* 108.2, pp. 261–271.

Wollman, F. A. (2001). "State transitions reveal the dynamics and flexibility of the photosynthetic apparatus". In: *EMBO J.* 20.14, pp. 3623–3630.

Wraight, C. A. and Crofts, A. R. (1970). "Energy-Dependent Quenching of Chlorophyll a Fluorescence in Isolated Chloroplasts". In: *European Journal of Biochemistry* 17.2, pp. 319–327.

Wu, D., Wright, D. A., Wetzel, C., Voytas, D. F., and Rodermel, S. (1999). "The IMMUTANS variegation locus of Arabidopsis defines a mitochondrial alternative oxidase homolog that functions during early chloroplast biogenesis". In: *The Plant Cell Online* 11.1, pp. 43–55.

Xue, X., Gauthier, D. A., Turpin, D. H., and Weger, H. G. (1996). "Interactions between photosynthesis and respiration in the green alga Chlamydomonas reinhardtii (characterization of light-enhanced dark respiration)". In: *Plant Physiology* 112.3, pp. 1005–1014.

Yang, Y. and Gao, K. (2003). "Effects of CO2 concentrations on the freshwater microalgae, Chlamydomonas reinhardtii, Chlorella pyrenoidosa and Scenedesmus obliquus (Chlorophyta)". In: *Journal of Applied Phycology* 15.5, pp. 379–389.

Yoshida, K. and Noguchi, K. (2011). "Interaction Between Chloroplasts and Mitochondria: Activity, Function, and Regulation of the Mitochondrial Respiratory System during Photosynthesis". In: *Plant Mitochondria*. Ed. by F. Kempken. New York, NY: Springer New York, pp. 383–409.

Zelibor, J. L., Romankiw, L., Hatcher, P. G., and Colwell, R. R. (1988). "Comparative analysis of the chemical composition of mixed and pure cultures of green algae and their decomposed residues by 13C nuclear magnetic resonance spectroscopy". In: *Applied and environmental microbiology* 54.4, pp. 1051–1060.

Zhang, P., Allahverdiyeva, Y., Eisenhut, M., and Aro, E.-M. (2009). "Flavodiiron Proteins in Oxygenic Photosynthetic Organisms: Photoprotection of Photosystem II by Flv2 and Flv4 in Synechocystis sp. PCC 6803". In: *PLoS ONE* 4.4. Ed. by Z. Finkel, e5331.

Zijffers, J.-W. F., Schippers, K. J., Zheng, K., Janssen, M., Tramper, J., and Wijffels, R. H. (2010). "Maximum Photosynthetic Yield of Green Microalgae in Photobioreactors". In: *Marine Biotechnology* 12.6, pp. 708–718.

Zito, F., Finazzi, G., Delosme, R., Nitschke, W., Picot, D., and Wollman, F.-A. (1999). "The Qo site of cytochrome b6f complexes controls the activation of the LHCII kinase". In: *EMBO J.* 18.11, pp. 2961–2969.

Zittelli, G. C., Biondi, N., Rodolfi, L., and Tredici, M. R. (2013). "Photobioreactors for Mass Production of Microalgae". In: *Handbook of Microalgal Culture*. Ed. by A. R. P. D. Emeritus and Q. H. Ph.D. John Wiley & Sons, Ltd, pp. 225–266.